Some aspects of the magnetic properties of rare earth- iron group laves phase intermetallic compounds

Piercy, A. R.

Some Aspects of the Magnetic Properties of Rare Earth - Iron Group Laves Phase Intermetallic Compounds

by

A. R. Piercy, B.Sc.

Presented in candidature for the degree of

Doctor of Philosophy

October 1968

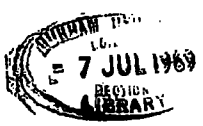

ABSTRACT

Measurements are presented of the structural and magnetic properties of several series of pseudo-binary compounds formed between the (heavy) Rare Earth metals, or Yttrium, and the 3d transitional metals, in the Laves phase structure. This work has been undertaken in an attempt to obtain a better understanding of the nature of the moments and coupling mechanisms in these compounds, RX_2.

The magnetic results are discussed on the basis of a rigid band model for the 3d electrons in these compounds and this model is shown to provide a unified account of the properties of all the RX_2 compounds. An elementary density of states histogram for the 3d band associated with the X component is presented.

The C 36 phase is found to coexist with the C 15 terminal phase at intermediate compositions in some of the series. For the C 15 phases the lattice parameters show a positive deviation from Vegard's Law and these results are discussed in relation to the magnetic properties.

Nomenclature

B	Constant
E	Energy
E_F	Fermi Energy
H	Magnetic Field
H_D	Demagnetising Field
H_i	Internal Field
Hm	Molecular Field
$\mathcal{H}$	Hamiltonian
I_σ	Current in Magnetometer D.C. coil
J	Total Angular Momentum Quantum Number
$\mathcal{J}$	Exchange Integral
K	Wave Vector
K_F	Fermi Vector
k	Boltzmann constant
M	Magnetisation (per unit vol.)
m_J	Magnetic Quantum Number
N	Number of Atoms/unit vol.
N_D	Demagnetisation Constant
N(E)	Density of States
n	Number of electrons

N	Avagadro's Number
P	Magneton Number
S	Ion Spin
T	Temperature
T_c	Ferromagnetic Curie Temperature
T_K	Compensation Temperature
U	Coulomb Correlation Energy
u,v,x	Concentrations
V	Potential
W_A	Atomic or Molecular Weight
W	Exchange Energy/pair of electrons
w	Mass of sample
$\sigma_{H,T}$	Magnetisation (per unit mass) - in applied field H, and at temperature T
λ_m	Molecular Field Constant
θ_p	Paramagnetic Curie Temperature
μ_B	Bohr Magneton
ϵ	Conduction Electron Spin
Γ	Exchange Coupling Constant
Λ	Magnetometer Calibration Constant
Δ	Half-width of Virtual Bound State

List of Figures

List of Tables

Chapter I INTRODUCTION

The Rare Earths have been available in pure form in quantity for little more than a decade but experimental and theoretical interest in them has been so great that they are now very well understood. It is one of the many ironies of physics that these materials should be understood so quickly while the theoretical problems of the iron group metals have proved intractable, even though, experimentally, their basic magnetic properties have been known for so long. Interest is now turning away from the pure Rare Earth metals to their alloys and compounds. In particular the intermetallic compounds formed between them and the transition metals may be helpful in elucidating problems associated with the parent metals. These compounds are also likely to provide a rich variety of properties which may be technologically useful.

The intermetallic compounds between the Rare Earths and the iron group metals have received considerable attention and several difficulties have been encountered in accounting for their properties. Again these have been mostly associated with the transition metal component. This present work is aimed at elucidating some of these problems through the study of some pseudo-binary series of alloys of compounds of the type RX_2. Here R represents a Rare Earth metal or yttrium, X is iron, cobalt, or nickel, and the compounds form in the cubic Laves

phase. Compounds of this particular type were chosen since they have received the greatest attention so that there exists a quantity of background experimental information and the problems are fairly well established.

Chapter II THEORETICAL BASIS

We recall that the absolute value of the total angular momentum for an isolated atom is $\hbar \left[J(J+1) \right]^{\frac{1}{2}}$ and the maximum measurable component is $\hbar J$ in any direction. The associated total magnetic moment is $g \left[J(J+1) \right]^{\frac{1}{2}} \mu_B$, where g is the spectroscopic splitting factor or gyromagnetic ratio (actually the inverse of the latter) which in Russel-Saunders coupling is given by the Landé g factor $g_J = 1 + \frac{J(J+1) + S(S+1) - L(L+1)}{2 J(J+1)}$ and μ_B is the Bohr magneton $\frac{e\hbar}{2mc}$. In a paramagnetic material it is possible to determine from the susceptibility the effective number of Bohr magnetons $p_{eff.} = g \left[J(J+1) \right]^{\frac{1}{2}}$. In a ferromagnet the atomic moments are coupled by an exchange interaction and when they are all aligned (at absolute zero) the measured moment may be expressed as the magneton number, p, per atom or molecule. For free atoms p is obviously given by $p = gJ$.

A polycrystalline specimen of a ferromagnetic material, in the absence of any applied magnetic field consists of an aggregate of magnetised domains oriented at random. The magnetisation $\sigma_{H,T}$ (referred to unit mass) within the domains is a fundamental property of the material related to the magneton number. The magnetisation when there is no applied field, $\sigma_{0,T}$ is termed the spontaneous magnetisation and the spontaneous magnetisation at the absolute zero, $\sigma_{0,0}$ is

termed the absolute saturation magnetisation. It is evident that the magneton number is related to the absolute saturation magnetisation through the relation

$$P = \frac{\sigma_{o,o} \cdot W_A}{\mathcal{N} \mu_B} \qquad (2.1)$$

where W_A is the effective atomic or molecular weight and $\mathcal{N}$ is Avagadro's Number.

II.1 Molecular Field Theory of Ferromagnetism

In general the spontaneous magnetisation will decrease when the temperature is raised above the absolute zero, as the effect of the exchange coupling is counteracted by the thermal energy, and will become zero at some definite temperature known as the Curie temperature.

An expression for the variation of spontaneous magnetisation with temperature was first given by Weiss (Ref. 2.1) who developed a phenomological theory in which the exchange interaction is considered as equivalent to an internal magnetic field. This Molecular Field, Hm, is taken as proportional to the magnetisation M, so that

$$Hm = \lambda_m M$$

where λ_m is called the molecular field constant. If we assume that all the atoms in the solid have a total angular momentum quantum number J then the atomic moment can have

components $m_J g\mu_B$ in the field direction $\left[m_J = J, (J-1), \ldots -(J-1), -J\right]$. The potential energy of this dipole in the field is thus $-m_J\, g\, \mu_B\, Hm$ and then, according to statistical mechanics the average moment is

$$\bar{\mu} = \frac{\sum_{-J}^{+J} m_J g \mu_B e^{m_J y}}{\sum_{-J}^{+J} e^{m_J y}}$$

where

$$y = \frac{g\mu_B H_m}{kT} = \frac{g\mu_B \lambda_m M}{kT}$$

Then we have for the magnetisation,

$$M = N\bar{\mu} = Ng\mu_B J B_J(x) \quad \ldots\ldots \text{(Eqn. 2.2)}$$

where N is the number of atoms per unit volume,

$$x = gJ\mu_B \lambda\, mM/k\, T \qquad \text{(Eqn. 2.3)}$$

and $$B_J(x) = \frac{2J+1}{2J} \coth \frac{2J+1}{2J} x - \frac{1}{2J} \coth \frac{x}{2J}$$

which is called the Brillouin Function.

Equations (2.2) and (2.3) may be solved for each value of T. It is found that there is a critical temperature above which

---

2.1 Weiss, P., J. Phys. 6 667, (1907)

the only solution is $M(T) = 0$. This is to be identified as the ferromagnetic Curie temperature, Tc. For temperatures below Tc a plot of $M(T)/M_o$ versus T/Tc yields a universal curve for a given value of J ; M_o is the saturation value corresponding to T = 0, given by

$$M_o = Ng\mu_B J$$

It is found that the Brillouin curve for $J = \frac{1}{2}$ represents the general shape of the experimental variation well but that it is incorrect in several details. For low temperatures, expansion of the Brillouim function yields (for $J = \frac{1}{2}$, $g = 2$) $M(T)/M_o = (1 - 2e^{-2x})$ while the best fit with the experimental data is given by $(1 - \text{const } T^{3/2})$ for $0<T/Tc < 0.3$.

For temperatures above Tc there is no spontaneous magnetisation, but the application of a magnetic field H will produce a magnetisation given again by eqn.(2.2) but with $x = gJ\mu_B (H + \lambda_m M)/k T$. If H is not too large we may use the expression

$$B_J(x) = \frac{J+1}{3J} \cdot x$$

when we have,

$$\chi = \frac{M}{H} = \frac{C}{T - \theta_p} \qquad \text{(Eqn. 2.4)}$$

where

$$C = \frac{N g^2 \mu_B^2 J(J+1)}{3k} \qquad \text{and} \qquad \theta_p = \lambda_m C.$$

Eqn.(2.4) is known as the Curie-Weiss law and within the Weiss theory θ_p is identical with Tc.

Experimentally it is found that, from a few degrees above Tc, $1/\chi$ is linear with T so that the data are in excellent agreement with the Curie-Weiss law. Near Tc however the curves are concave upards so that Tc lies a few degrees below θ_p which is termed the paramagnetic curie temperature.

II.2 Improvements on the Molecular Field Model

As was indicated in the last section the Molecular Field approximation is inaccurate in several details. Its failure is a result of the effective assumption that the field at any one ion is influenced equally by all others, so that nearest neighbour ions have no more effect than those many lattice spacings distant. At low temperatures the few reversed spins will give rise to spin waves as Bloch first showed (Ref. 2.2). To the first approximation in this theory, the magnetisation varies with temperature as $M = M_o - A_o T^{3/2} - A_1 T^{5/2}$ (Ref. 2.3). At higher temperatures near the Curie point, the few parallel spins will give rise to " clusters " (Ref. 2.4). This effect results in a susceptibility variation with temperature just above the Curie point which is concave upwards, and a difference between the paramagnetic and ferromagnetic Curie temperatures.

II.3 Ferrimagnetism

A Ferrimagnetic material is one in which a spontaneous magnetisation exists, below a critical temperature, while at the absolute zero there is a nonparallel arrangement of the strongly coupled atomic dipoles. This may result from an antiparallel alignment

---

2.2 F. Bloch, Z. Phys. 61, 206, (1930)

2.3 For review see T.G. Phillips and H.M. Rosenberg, Repts. Prog. Phys. 24, 285 (1966)

2.4 P.R. Weiss, Phys. Rev. 74, 1493 (1948)

of sublattices with differing magnetisations or from a canted alignment of sublattices with either equal or non-equal magnetisations. The separate sublattices will in general consist of different numbers of different atomic species. We shall consider the simplest case of two sublattices, first treated by Neel (Ref. 2.5), in the molecular field approximation.

Denoting the two sublattices by A and B we have for the molecular fields

$$H_{mA} = \lambda_{AA} M_A + \lambda_{AB} M_B$$

$$H_{mB} = \lambda_{AB} M_A + \lambda_{BB} M_B$$

where λ_{AB}, at least, must be negative for ferrimagnetism. It is common to relate the molecular field constants by the equations.

$$\lambda_{AA} = \alpha \lambda_{AB} \text{ and } \lambda_{BB} = \beta \lambda_{AB}$$

As in the ferromagnetic case the sublattice magnetisations are given by

$$M_A(T) = M_A(0) \; B_{J_A}(x_A) \text{ and } M_B(T) = M_B(0) \; B_{J_B}(x_B)$$

where $M_A(0) = N_A g_A \mu_B J_A$,

and $x_A = \dfrac{J_A g_A \mu_B}{kT} \text{ Hm A}$

2.5 L. Neel, Ann. phys. (Paris) 3, 137, (1948)

and similarly for $M_B(0)$ and x_B

If we assume that the sublattices are aligned antiparallel then the resultant spontaneous magnetisation is given by

$$M(T) = \left| M_A(T) - M_B(T) \right|$$

Clearly the variation of M with T depends on the actual values of $M_A(0)/M_B(0)$, α and β, and may be conveniently discussed either as a function of α and β with $M_A(0)/M_B(0)$ kept constant, or the converse. Fig. 2.1 shows how unusually shaped M versus T curves may be formed; in (a) $\alpha > \beta$ and in (b) $\beta > \alpha$. For the latter case the spontaneous magnetisation undergoes a reversal in direction and the temperature at which this occurs is called the compensation point, T_K. Since in practice the " saturation" magnetisation is measured (see section IV.4) the measured curve would follow the dashed line shown.

Various M vs. T curves that may occur when α and β are fixed but $M_A(0)/M_B(0)$ is varied are shown in Fig. 2.1(c). The curves (3) and (5) are similar to those shown in Fig. 2.2 (a) and (b) respectively; curve (4) is the limiting case between these where $M_A(0) = M_B(0)$; curve (2) is the limiting case between the " normal" type curve 1 (or 7) and the curve (3) and corresponds (Ref. 2.6) to the composition $M_A(0)/M_B(0) = \{\lambda_{AB} + \lambda_{AA}\}/\{\lambda_{AB} + \lambda_{BB}\}$ where $|H_{MA}| = |H_{MB}|$; curve (6) separates the " normal" curves from those with a compensation

FIGURE 2.1 Ferrimagnetic Magnetisation/Temperature Curves.

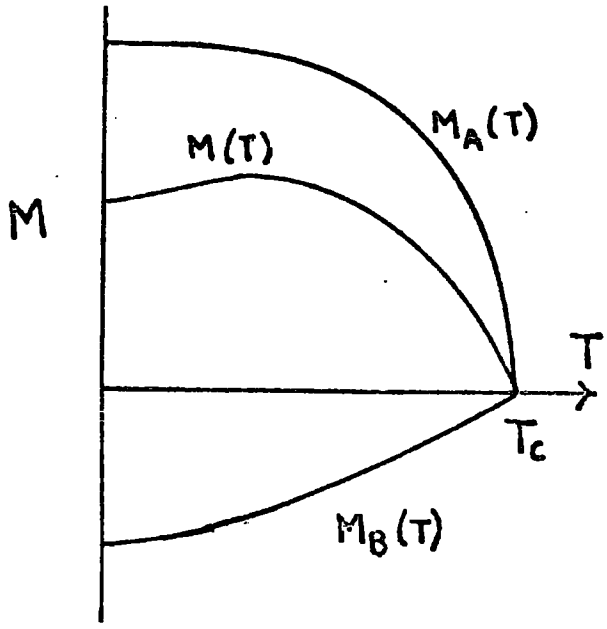

(a)

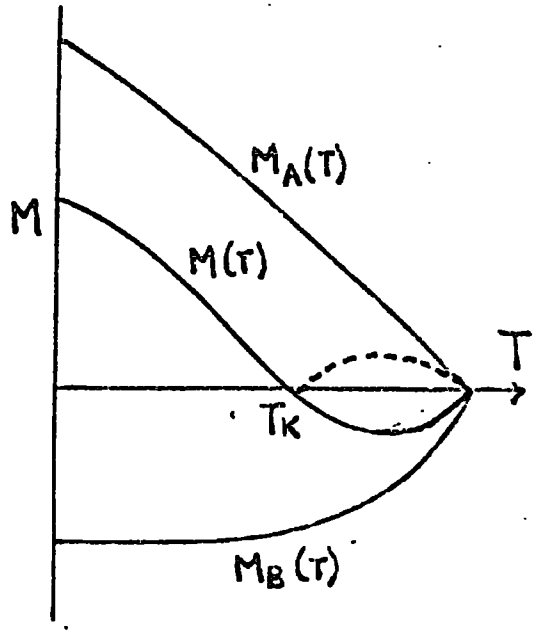

(b)

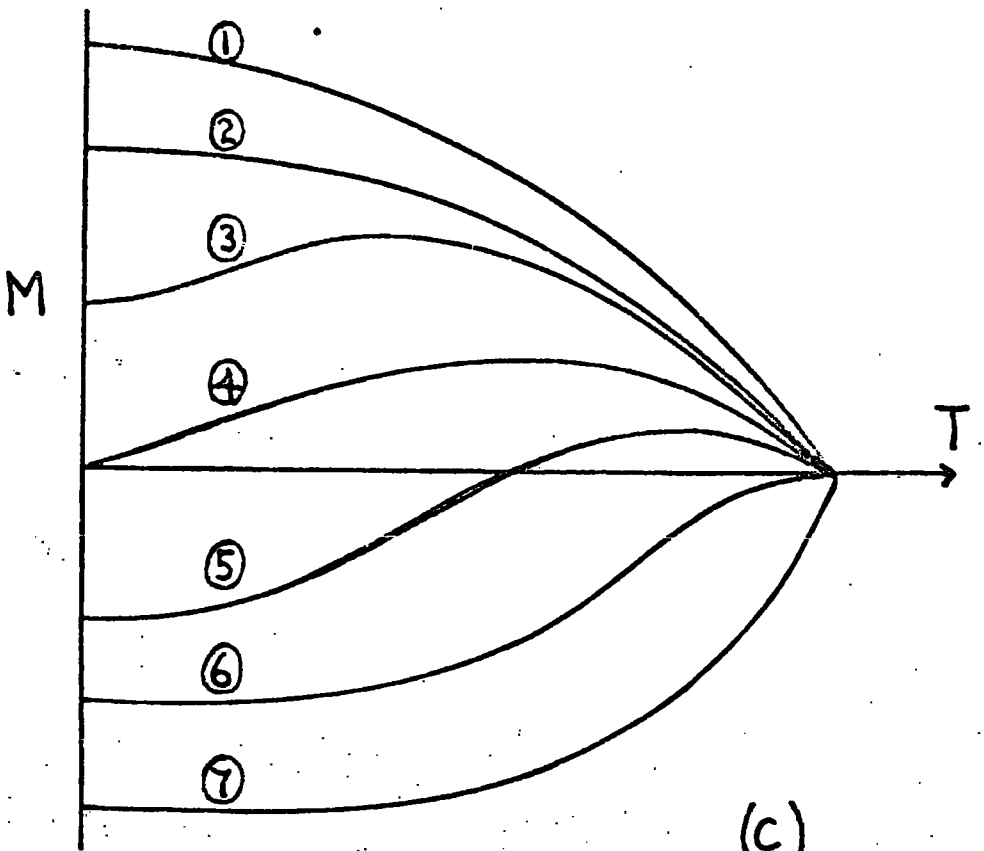

(c)

point and here $M_A(0)/M_B(0) = (\lambda_{AB} - \lambda_{AA})/(\lambda_{AB} - \lambda_{BB})$ which is the condition $dM/dT \rightarrow 0$ as $T \rightarrow Tc$.

It was assumed in the foregoing discussion that the sublattices were antiparallel which means effectively λ_{AB} is negative and $|\lambda_{AB}| \gg |\lambda_{AA}|, |\lambda_{BB}|$ or that $\lambda_{AA}, \lambda_{BB}$ are positive (ferromagnetic). In the usual ferrimagnetic insulators the molecular field constants have their origin in an indirect exchange interaction of the magnetic ions via intermediate non-magnetic ions and since this interaction is always antiferromagnetic (λ -ve) the above condition may not always hold. Under the conditions $\lambda_{AB} \sim \lambda_{AA}, \lambda_{BB}$ the spin configuration will be non-colinear. One possible spin configuration is the triangular arrangement where one sublattice splits into two further sublattices which align at an angle to each other and the second lattice. In general the sublattice magnetisations are different and vary with temperature so that transitions may occur in the spin configuration. These conditions have been treated by Lotgering (Ref. 2.7). Further complications are obviously possible involving more than three sublattices in

---

2.6 See, for example, A.H. Morrish, "The Physical Principles of Magnetism", Wiley, (1956) Chapter 9.

2.7 F. K. Lotgering, Phillips Res. Rept. 11, 190 (1956)

canted arrangements.

In metallic ferrimagnetics, such as are investigated in this report, the situation is different since the exchange interactions are not the same as in the insulating case and are not necessarily antiferromagnetic. Where ferromagnetic interactions occur within a sublattice, the spin configuration will tend towards the simple antiparallel arrangement. However, since the interactions within and between sublattices may be different, the critical temperatures (Curie points) for individual sublattices and for the coupling between them will not necessarily be the same and more complicated magnetisation - temperature curves may result. There is no molecular field treatment of this case in the literature.

The molecular field theory of ferrimagnetism as outlined above is subject to the same objections as the ferromagnetic case (Section II.2) and the various improvements outlined there have been applied also to the present situation (see, e.g. Ref. 2.6). Since in this case the sublattice magnetisations are not required to follow the Brillouin functions, yet further complications are introduced into the resultant magnetisation.

II. 4 Exchange Interactions

The origin of the Weiss molecular field was obscure until the advent of quantum mechanics when Heisenberg showed (1928)

that it resulted from the exchange interaction. Consider, for example, two atoms (a and b) and two electrons (1 and 2) then the interaction potential is of the form

$$V_{12} = \frac{e^2}{r_{ab}} + \frac{e^2}{r_{12}} - \frac{e^2}{r_{1b}} - \frac{e^2}{r_{2a}}$$

and there are additional energies of the system in the operator form $E = \mathcal{U}_{12} - \frac{1}{2}\mathcal{J}_{12} - 2\mathcal{J}_{12}\,\epsilon_1 - \epsilon_2$

where ϵ_1 and ϵ_2 are the electron spins (see, for example Ref. 2.6 Ch. 6). Here $\mathcal{U}_{12}$ is called the Coulomb correlation energy and $\mathcal{J}_{12}$, the exchange integral and they are given by

$$\mathcal{U}_{12} = \left\langle \phi_a(1)\,\phi_b(2) \,\middle|\, V_{12} \,\middle|\, \phi_a(1)\,\phi_b(2) \right\rangle$$

and $$\mathcal{J}_{12} = \left\langle \phi_a(1)\,\phi_b(2) \,\middle|\, V_{12} \,\middle|\, \phi_a(2)\,\phi_b(1) \right\rangle$$

If we consider only the spin dependent part of the operator we have the Hamiltonian $\mathcal{H} = -2\mathcal{J}_{ij}\,\epsilon_i \cdot \epsilon_j$ and when this is generalised to the entire crystal we have the Heisenberg Hamiltonian $\mathcal{H} = -2\sum_{ij}\mathcal{J}_{ij}\,S_i \cdot S_j$ where Si is the total spin of atom i.

Three types of exchange are usually distinguished in the

metallic state; direct exchange, itinerant exchange, and indirect exchange. These have been reviewed at considerable length in the " Magnetism" series (Refs. 2.8, 2.9 and 2.10 respectively). Direct exchange is the coupling of spins of atoms which are well enough separated to have almost free ~~electron~~ atom characteristics. The Heisenberg theory is based on concepts which have a clear meaning only in this limiting case. It has long been realized however that the d electrons in transition metals are likely to form a relatively wide energy band and hence that exchange couplings between itinerant electrons are important. This subject will be treated in section II.5. In these first two mechanisms it is the d-d coupling which is of prime importance and the effect of the conduction electrons is considered as a secondary effect. In the third type of exchange however the s-d (or f) interaction is considered explicitly; i.e. indirect exchange is the coupling of inner shells via their interaction with the conduction electrons. This mechanism is most clearly applicable to the Rare Earth metals

---

2.8 Herring, C., in " Magnetism", ed. Rado and Suhl, Academic Press, Ch. a Vol. IIb (1966)

2.9 Herring, C., ibid, Vol. IV (1966)

2.10 Kasuya, T., ibid, Vol. IIb Ch. 3

and will be considered in section II. 6.

II.5 Itinerant Electron Model

The correct description of the moments in the transitional metals is probably the greatest problem in theoretical magnetism. As is often the case in physics, two opposite extreme models have been extensively developed and there is still considerable uncertainty over which is more nearly correct. The problem of itinerant versus localised - spin models has been reviewed by Herring (Ref. 2.9 Chapter 6) and we will cite just a few instances. The itinerant model is favoured by the fractional saturation moments in the ferromagnetic state, by the electronic specific heat and by band calculations and fermi surface measurements. The localised model however appears to be more appropriate for the description of neutron scattering form factors, the magnetic entropy and the behaviour of dilute alloys. It appears that the true nature of these moments must lie intermediate between these two extreme models and a recent approach which lies between them is outlined later in this section. Firstly some of the important aspects of the itinerant model which seem likely to be retained by future models will be outlined.

II.5.a Origin of Ferromagnetism

The origin of the coupling in transition metals is at the heart of the various models. The main problem is the uncertainty

of the magnitude of the correlation energy U defined in section II.4. In the atomic case this energy is considerably larger than the intra-atomic exchange energy but, as discussed in the reviews (Ref. 2.9), (Ref. 2.11) and (Ref. 2.12) it is reduced, in the metallic state, due to screening by the S conduction electrons. Some authors assume that it is not large enough to prevent two carriers (electrons, holes) from coming onto the same atom so that the origin of ferromagnetism is the intra-atomic exchange coupling responsible for Hund's rule. The opposite point of view (i.e. strong correlation) has also been taken and here the origin of ferromagnetism is the strong repulsive energy between electrons with anti-parallel spins.

Other possible coupling mechanisms are the inter-atomic exchange (direct exchange) and the s-d exchange to be dealt with in Section II.6. It is shown in Ref. 2.9 that the former is about two orders of magnitude too low to account for the Curie points but that the latter, while also too low to account alone for the ferromagnetism, may be an important addition to other mechanisms.

The condition for ferromagnetism in the band model (Ref.2.13) is derived as follows. We start with equally populated half bands

---

2.11 Mott, N.F., Advanc. Phys. 13, 325, (1964)

2.12 " Theory of Magnetism in Transition Metals" Enrico Fermi Course No. 37, Academic Press (New York) 1967

with + and - spins (Fig. 2.3(a)). If ϵ electrons/atom (infinitesimal) are transferred from the - to + spin direction, then energy $\epsilon\ \delta E$/atom is required, where $2\ \delta E$ is now the energy difference between the two Fermi levels. (Fig. 2.3 (b)). Now the exchange and correlation energies are proportional to the

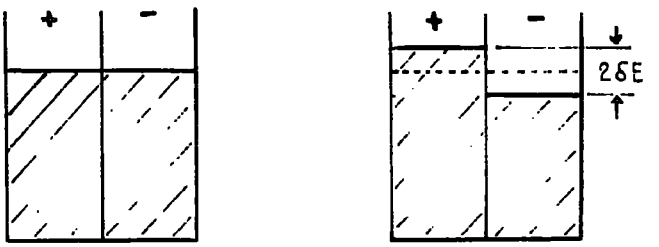

(a) (b)

Fig. 2.3

number of pairs of electrons in each half band. Thus for p electrons/atom the change in energy/atom from the paramagnetic to ferromagnetic state is

$$\epsilon\,\delta E - \left[\left(\frac{p}{2}+\epsilon\right)^2 + \left(\frac{p}{2}-\epsilon\right)^2 - 2\left(\frac{p}{2}\right)^2\right] W$$

where W is an exchange energy per pair of electrons (i.e. the energy required to replace a parallel pair of electrons with an anti-parallel pair). Thus the ferromagnetic state is stable with respect to the pure Pauli paramagnetic one for $2\epsilon^2 W > \epsilon\ \delta E$

2.13 (a) Stoner, E.C., Repts. Progr. Phys. 11, 43 (1947)
(b) Wohlforth, E.P., Proc. Roy. Soc. 195, 434 (1949)

and this reduces to

$$2 W N(E_F) > 1 \qquad \text{(Eqn. 2.5)}$$

where $N(E_F) = \epsilon/\delta E$ is the density of states at the Fermi level. The exchange energy W should really depend on the wave vectors of each pair of electrons but obviously in this analysis some sort of average over the different values must be understood.

Equation 2.5 is known as the Stoner condition (Ref. 2.13). The Stoner model has been very widely used in attempts to correlate diverse properties, such as moments, temperature behaviour and electronic specific heat, of itinerant electrons in transition metals. The model includes many simplifying assumptions but these allow the statistical-mechanical calculations to be made. A comprehensive list of references is given in Ref. 2.9 Chapter II.

When condition (2.5) is fulfilled, one half of the d-band should fill at the expense of the other until the gain in exchange energy in this process is limited by the loss in kinetic energy. This is obtained when the energy difference ΔE between the two Fermi levels (often called the exchange splitting) is equal to the ~~exchange~~ energy $\ln W$ where n is the number of electrons moved.

$$\text{i.e.} \ln W = \Delta E \qquad \text{(Eqn. 2.6)}$$

This condition can be rewritten as:

$$W = 1 / \overline{N(E)} \qquad \text{(Eqn. 2.7)}$$

where $\overline{N(E)} = n/\Delta E = \frac{1}{\Delta E}\int_{E_1}^{E_2} N(E)\,dE$ is the average density of states between two Fermi levels at E_1 and E_2 (i.e. $\Delta E = E_1 - E_2$).

Two points need to be emphasised about the preceeding analysis. Firstly the whole of the foregoing applies at 0° K and secondly we have spoken as though the Fermi levels were moved within a fixed band. In fact, of course, there is only one Fermi level and the sub-bands themselves are split by the exchange interaction. It is however conceptually easier to consider the bands as fixed and the Fermi levels moving.

II.5 (b) Alloys: Rigid Band Model

In an alloy we have to consider the effect of a localised perturbation V introduced by the impurity atom. Many of the important results about the scattering by V are due to Friedel and his collaborators (for review see Ref. 2.12). Firstly the total screening charge provided by the electron gas is simply related to the sum of the phase shifts of the scattered wave functions. Secondly a large fraction of the screening charge is contained within the impurity cell but there are also long range oscillations of the screening charge. Thirdly, and most important for the present concern, the effect on the density of

states is simple.

To first order in V it is found (Ref. 2.12) that the density of states may be written approximately as $N'(E) = N(E - c\bar{V})$ where c is the concentration and $\bar{V}$ is an average V. Thus the density of states curve is shifted rigidly in energy, without change in form, by the amount $c\bar{V}$. Again we shall find it easier to think of the Fermi levels moving rather than the band.

This is obviously the classical " Rigid Band Model " which has been used for many years (Ref. 2.14) as an ad hoc concept for the discussion of alloy properties. The use of the model for alloys of transition metals among themselves and with non-transition elements has been extensively reviewed (Ref. 2.11).

The model is a good approximation for small perturbations, i.e. for the case of neighbouring elements in the periodic table, but breaks down (Ref. 2.12) for strong perturbations V (i.e. widely differing elements) and in regions where the density of states of the matrix is abnormally large. Where V is strong enough bound states will occur which will be on the high or low energy side depending on whether V is repulsive or attractive. For sufficiently large repulsive V the bound states may be forced

---

2.14 Mott. N.F., and Jones, H., " Theory of the Properties of Metals and Alloys " Oxford University Press, 1936.

above the Fermi level so that states are removed from the band and thus, for materials where the magnetisation is saturated (i.e. spin-up band full), there should be a sudden lowering of magnetic moment. This is exactly what is observed in Ni and Co base alloys with elements to the left of Fe which show deviations from the Slater - Pauling curve (Ref. 2.11). These bound states are not discrete levels but are broadened by resonance with the conduction band and are called " virtual bound levels ".

II.5.(c) Localisation in the Band Model

As was stated earlier the localised and band models are two extremes which both seem appropriate in different circumstances. Recently models have been suggested which combine the important features of both these extremes.

The first insight was given by Friedel et.al. (Ref. 2.15) who criticised the usual bamd model outlined above on the grounds that it argues only in terms of energy, assuming all atoms behave in the same way: To extend the model therefore it is necessary to include a reasoning in space. They showed in a qualitative way that localised magnetic moments are not incompatible with the band approximation and that such moments can occur by a local piling up of electronic charge with one spin, compensated

---

2.15 Friedel, J., Leman, G., and Olszewski, S., J. Appl. Phys. 32, 325(s), (1961)

electrostatically by an equal local repulsion of electrons with opposite spin. They derived a condition for the existence of these moments which is identical with the previous condition for ferromagnetism (Eqn. 2.5) and showed that the minimum size of the central polarisation is of the order of the interatomic distance and that this is surrounded by " fringes " of spin polarisation of alternating sign [c.f. Section II.5 (b)] . The actual size of the central region and wavelength of the fringes was shown to depend on the average wave vector at the Fermi surface. It was further suggested that the overlap of these polarisations on neighbouring sites would result in a coupling which could be either ferro- or antiferromagnetic depending on the extent of the overlap.

This approach has been extended so that it now represents a really useful model for transition metals and it will undoubtedly undergo further refinement.

A quantitative theory of the one spin problem was first worked out by Anderson (Ref. 2.16) and the model has become known by that author's name. It was first presented in connection with

---

2.16 Anderson, P.W., Phys. Rev., 124, 41, (1961)

the problem of dilute alloys but has been extended to pure metals and the N-spin case has recently been presented by Liu (Ref. 2.17), treating a ferromagnetic metal as a lattice of overlapping Anderson-type localised moments.

The basic idea of the Anderson model is that the d states in transition metals act like scattering resonances of the conduction electrons. We consider a single atom with incomplete d shell in an environment of Bloch electrons generated by a broad conduction band, and assume that the energy, E, of the (localised) state is within the energy range of this band. In the Hartree-Fock approximation the true Hamiltonian will contain an interaction term of the d state with the plane-wave s states (hybridisation). As a result of this the energy of the state of spin σ is $E_\sigma = E + U < n_{-\sigma} >$ and the localised state is broadened over a range 2Δ. This is referred to as a " virtual" bound state. Depending on the values of E, U, and Δ the two different spin states may have the same or different occupations, i.e. the state for one spin direction may be above the Fermi level due to the effect of U .

In the N-spin case the metal is considered as a lattice of overlapping Anderson-type moments. This can obviously give rise to a coupling and Liu (Ref. 2.17) has shown that the relevant

---

2.17 Liu, S.H., Phys. Rev. 163, 472, (1967)

properties of the band model (fractional moments, conditions for ferromagnetism etc.) are contained within the properties of the band width Δ together with the relevant properties associated with the Heisenberg model (magnetic entropy, neutron diffraction etc.). Additionally the coupling may be either ferro-or antiferromagnetic.

II.6 Rare Earth Metals and the s-f Exchange Interaction

The Rare Earth elements, those between Lanthanum (Atomic Number 57) and Lutetium (71) are characterised by an incomplete 4f shell, tightly bound and localised in space, surrounded by filled 5s and 5p shells, and, usually, three valence electrons in $5d^1$ and $6s^2$. They have, consequently, very similar chemical properties since these depend primarily on the outer shells. The magnetic properties however, which derive almost entirely from the incomplete 4f shell, vary considerably. The elements Sc (21) and Y (39) are often included with the Rare Earths as they have very similar outer configurations i.e. $3s^2\ 3p^6\ 3d^1\ 4s^2$ and $4s^2\ 4p^6\ 4d^1\ 5s^2$ respectively. Neither, however, has an incomplete inner shell and, therefore, neither has a permanent magnetic moment. As already stated the 4f shell is very tightly bound and neutron diffraction results indicate that its radius is about one tenth of the interatomic distance. In addition, recent band calculations (Ref. 2.18) show that the 4f level is very sharp (about

0.05 eV) and lies a long way below the conduction band (about 11 eV). Thus it would seem reasonable to consider the metals as consisting of tri-positive ions immersed in a sea of conduction electrons. This view is supported by measurements of the high temperature susceptibilities which follow the Curie-Weiss law and have effective moments very close to the free $3+$ ion values. To calculate the properties of the Rare Earth metals then, we can first consider an isolated ion and then introduce the additional effects due to the metallic environment.

II.6 (a) Rare Earth Metals

The energy levels are calculated in the usual Hartree - Fock approximation. The most important contribution is due to the central potential which gives the $4f^n$ configuration. The f-f coulomb interaction is then introduced and partially removes the degeneracy of the configuration and the resulting terms are specified by the total moments L and S. The term with lowest energy is given by Hund's Rules (i.e. maximum S and maximum L consistent with that). In practice this is the only term we need to consider. The spin-orbit coupling lifts the term degeneracy and the resulting multiplets are specified by the total angular momentum J. For all the Rare Earths except Sm^{3+} and Eu^{3+} the spin orbit coupling is so large that

---

2.18 Dimmock, J.O., Freeman, A.J., and Watson, R.E., Proc. Int. Conf. on Optical Properties of Metals, ed. F. Abeles (Amsterdam 1966) p. 237

$E_{LS} \gg kT$, where E_{LS} is the multiplet separation. It is therefore only necessary to consider the ground state J value ($J = L \pm S$), and in calculating the susceptibility we consider only the $2J + 1$ levels (specified by M_J) arising from the ground state multiplet (c.f. Equation 2.4)

In a crystal each Rare Earth ion is surrounded by other ions on a regular lattice and this gives rise to an electric field (called the crystal field) of the appropriate symmetry on the ion. The effect of the crystal field is to partially remove the $(2J + 1)$ - fold degeneracy of each J level of the free ion so that new levels occur. For the Rare Earth metals, however, this crystal field splitting $E_c < kT$ as is evidenced by the success of the ionic model in accounting for the susceptibilities. The susceptibility is the main effect depending only on the isolated ion and all other properties (magnetic coupling, electrical resistivity) are concerned with the interactions of the ions with themselves and the conduction electrons.

The main interaction responsible for magnetic coupling in the Rare Earth metals is the indirect interaction via conduction electrons originally proposed for the 3d metals by Zener, though in an incorrect form (see the review Ref. 2.10). Additional reviews are (Ref. 2.19) and (Ref. 2.20). The interaction between the ion spin S and the conduction electron spin ϵ is usually taken to be of the scalar form:

2.19 de Gennes, P.G., J. Phys. Rad. 23, 510, (1962)

2.20 Elliot, R.J., in "Magnetism" Vol. IIa Chapter 7

$$\mathcal{H}_{s\epsilon} = -\Gamma\, S.\epsilon \qquad \ldots\ldots \text{(Eqn. 2.8)}$$

The conduction electrons are scattered under the influence of this interaction and strictly Γ should depend on the initial and final k states. The effect of exchange of this type was first examined by Rudermann and Kittel (Ref. 2.21) for the coupling of nuclei, by Yosida (Ref. 2.22) for Cu - Mn alloys and by Kasuya (Ref 2.23) for Gd, and is called, in consequence, the R-K-K-Y interaction.

The usual approximation is to treat the ionic potential as a delta function and the conduction electrons as free. Then the polarisation $P_n(R)$ of the conduction electrons in the neighbourhood of the ion (n) through the interaction (Equation 2.8) is given (Ref. 2.19) by

$$P_n(R) = \frac{9\pi Z^2}{4 Vo^2} \frac{\Gamma}{E_F} S_n \cdot F(2K_F R)$$

where

$$F(x) = \frac{(x \cos x - \sin x)}{x^4}$$

2.21 Rudermann, M.A., and Kittel, C., Phys.Rev. 96, 99, (1954)

2.22 Yosida, K., Phys.Rev. 106, 893, (1957)

2.23 Kasuya, T., Progr. Theoret. Phys. (Kyoto) 16, 45, (1956)

z is the number of conduction electrons/atom, V_o the atomic volume and R is the distance from the ion. The function F(x), and hence the polarisation, is long range and oscillatory. This polarisation acts on a second ion with spin S_m at position Rm as $-\Gamma\ S_m \cdot P_n(R_m)$ and this equivalent to a coupling $\mathcal{H}_{n,m} = -I_{n,m}\ S_n . S_m$

where $$I_{n,m} = \frac{9\pi}{4}\left(\frac{Z}{Vo}\right)^2 \cdot \frac{(\Gamma)^2}{E_F} \cdot F\,(2k_F\ R_m)$$

Thus the indirect interaction is long range and oscillatory, a property which derives from the singularity in $\mathbb{K}$ at K_F.

The principle problem in applying this R-K-K-Y interaction to the Rare Earth metals is to correctly include the effect of the spin—orbit coupling on the spins Sn, Sm. de Gennes has shown that for $E_{LS} \gg$ kT it is necessary only to make the substitution $Si = (g_J - 1)\ J_i$. The model accounts well for many of the properties of the Rare Earth metals (Refs. 2.10, 19 and 20) with approximately constant values of Γ , K_F and $\sum_{m \neq n} F(2K_F\ Rm)$. Additionally many alloy properties also vary with the de Gennes function $(g - 1)^2\ J\ (J + 1)$ which occurs in the formulae for different properties (e.g. paramagnetic Curie temperature).

Recent band calculations and Fermi surface determinations for

the R.E. metals (Ref. 2.24) show, however, that these are very far from being free-electron like but have mixed s-d character strongly resembling the transition metals. In view of this it is very surprising that the R-K-K-Y model has such success in accounting for the physical properties. Much of this must be taken as fortuitous. There have been very many attempts at improving the model from this point of view, however, though these all leave the essential features of the model intact. Perhaps the most fundamental improvement is the generalisation (Ref. 2.25) of the interaction for a nonspherical Fermi surface. In general the interaction is found to fall off as $^1/R^3$ and to oscillate with a period corresponding to a calipering of the Fermi surface in the R direction. Obviously the R-K-K-Y interaction is a fair approximation if an average K_F is taken and it constitutes a very useful starting point for the

---

2.24 Freeman, A.J., Dimmock, J.O., and Watson, R.E., Phys. Rev. Lettr. 16, 94 (1966)

Loucks, T.L., Phys. Rev. 144, 504 (1966)

Keeton, S.C., and Loucks, T.L., ibid 168, 672 (1968)

Williams, R.W., and Mackintosh, A.R. ibid 168, 679 (1968)

2.25 Roth, L.M., Zeiger, H.J., and Kaplan, T.A., Phys. Rev. 149, 519 (1966)

discussion of very many properties of R.E. metals, alloys and compounds.

II.6(b) Origin of the s-f interaction

We have so far described the s-f interaction using the phenonological pseudo-potential (Equation 2.8) without mention of the origin of Γ. There is considerable uncertainty experimentally over the size and even sign of the interaction and this will now be shown to result from different contributions to Γ. The most obvious contribution is that due to the exchange integral $\mathcal{J}_{int}$ (c.f. Section II.4) between the 4f shell and the conduction electrons. $\mathcal{J}_{int}$ must inevitably be positive and so produce positive conduction electron polarisation. The second contribution is termed interband mixing between the conduction electron and local-moment electron orbitals (Ref. 2.26). This is just the mechanism of the Anderson model (Section II.5(c) and gives a negative polarisation of the conduction electrons as follows. As before, hybridisation of the 4f and conduction electron states occurs, and, as a result, unoccupied conduction band states above the Fermi level with spin $\uparrow$ have their energy raised while the $4f\uparrow$ level is lowered. This is termed an " emission" process since an occupied 4f level has conduction-electron character part of the time. There is also an " absorption" process involving the $4f\downarrow$ virtual level (above the Fermi level) and an occupied $\downarrow$

2.26 Watson, R.E., Koide, S., Peter, M., and Freeman, A.J., Phys. Rev. 139 (A), 167 (1965)

conduction-electron. The effect of these processes is to increase the ↑ conduction-electron energies and reduce the ↓ resulting in a negative polarisation. This interband mixing is very sensitive (Ref. 2.26) to the conduction electron character so that the magnitude of the effective parameter Γ, being the sum of this and Ψ_{int}, depends on the exact band structure. It may also vary with conduction-electron K direction so that anisotropies result in the R-K-K-Y interactions.

Chapter III Background on Materials

III.1. Rare Earth Alloys and Compounds

The Rare Earth metals are prolific in their ability to form alloys and compounds, many of which have magnetic properties of considerable intrinsic importance and technological potential both exploited and latent.

Some of the best known Rare Earth compounds are the garnets, $R_3 Fe_5 O_{12}$, and the " substituted" garnets where another element (e.g. **Al**) is substituted for part of the Fe. These materials are of extreme technological importance as they are ferrimagnetic insulators and also can be produced as nearly perfect single crystals many of which are transparent. The orthoferrites, R Fe O_3, similarly are important materials. Of more recent interest are the compounds with the Group V elements (P, As, Sb, Bi) and Group VI (S, Se) of stoichiometry 1:1 and 4:3. Many of these compounds are magnetically ordered and semi-conducting and, as such, are receiving increasing attention.

The heavy Rare Earths readily form solid solutions among themselves and with Y and Sc. The magnetic properties of these alloys have a variety as great as that of the pure metals. Briefly, the addition of Y, Sc and Lu tends to stabilize the antiferromagnetic structure at the expense of the ferromagnetic, while lowering T_N. Lanthanum, however, generally, has the opposite effect and La - Gd

alloys are ferromagnetic down to 1% Gd, below which superconductivity sets in. Generally the Neel points, T_N, of the solid solutions vary as a universal function of the de Gennes factor (Section II.6.(a)).

The rich variety of the properties of rare earth compounds may be inferred from the length of even the brief review of Bozworth (Ref. 3.1), 50 pp., while a more extensive compilation (Ref. 3.2) runs to over 350 pp.

III.2. Rare Earth - Transition Metal Compounds

Of specific interest for the present work are the intermetallic compounds between the rare earth metals and the iron-group transition metals. The phase diagrams (Ref. 3.2) for the different rare earth, R, and transition metal, X, components show the presence of compounds of many stoichiometries, though not all these are the same for each system. The Yttrium-Cobalt system is perhaps typical; there are compounds of composition Y_3Co, Y_3Co_2 YCo, Y_2Co_3, YCo_2, YCO_3, Y_2Co_7,

---

3.1 Bozorth, R.M.,

3.2 Gibson, J.A., Harvey, G.S., " Properties of Rare Earth Metals and Compounds". Technical Report AFML-TR-65-43-, Air Force Materials Lab., Wright-Patterson Air Force Base, Ohio (1966).

YCo_5, and Y_2Co_{17}. Compounds of composition RX_4 have been reported as being congruently melting, but these are now considered (Ref. 3.3) to be a mixture of the RX_5 and R_2X_{17} compounds. Lemaire (Ref. 3.3) has shown that the crystal structures of many of these compounds may be simply related to the RX_5 structure.

The number of these compounds obviously precludes a detailed description here. The properties of many have been summarised in Ref. 3.1 and of the compounds with cobalt at some length in Ref. 3.3. Briefly, where a moment exists on both R and X these are generally coupled antiparallel for the heavy rare earths and parallel for the light. The moments on the X components vary in magnitude considerably depending on the composition and the R partner. These facts have been inferred from magnetisation measurements and in some cases confirmed by neutron diffraction.

The compounds RX_2 have received the greatest attention to date, and are the subject of the present work. These compounds will now be reviewed at greater length.

III.3 The RX_2 Compounds

III.3 (a) Structural Data: The Laves Phases

The compounds of stoichiometry RX_2 belong to the large class

---

3.3 Lemaire, R., Cobalt 32, 132, (1966) and 33, 201,(1966)

of intermetallics crystallising into the structures known as Laves phases. There are well over 200 binary compounds forming in these structures (Ref. 3.4) which are of three types; (i) $Mg\ Cu_2$, cubic (Strukturbericht Type C 15), 24 atoms/unit cell, (ii) $Mg\ Zn_2$, hexagonal (C 14 type), 12 atoms/unit cell, (iii) $MgNi_2$, hexagonal (C36 type), 24 atoms/unit cell. There are marked similarities between the three structures. They consist of double layers of hexagonal arrays of Mg atoms surrounded by tetrahedra of the other elements. In $Mg\ Cu_2$ the layers are stacked ABC, while in $Mg\ Zn_2$ they are ABAB. $Mg\ Ni_2$ may be considered as a transitional phase with stacking ABAC. Identification of the allotropic types is not easy since there is equivalence of many X-ray reflections (Ref. 3.5). The $Mg\ Cu_2$ type alone however has relatively few lines and is easily identified. All the RX_2 binary compounds form in this structure which is pictured in Figure 3.1.

The Laves phases represent a very efficient method of filling space and, with atomic size ratio $R_A/R_B = 1.225$, the average

---

3.4 Nevitt, M.V., in P.A. Beck, ed., " Electronic Structure and Alloy Chemistry of the Transition Elements". Interscience, New York, (1963)

3.5 Elliott, R.P., and Rostoker, W., Trans. A.S.M., 50, 617, (1958)

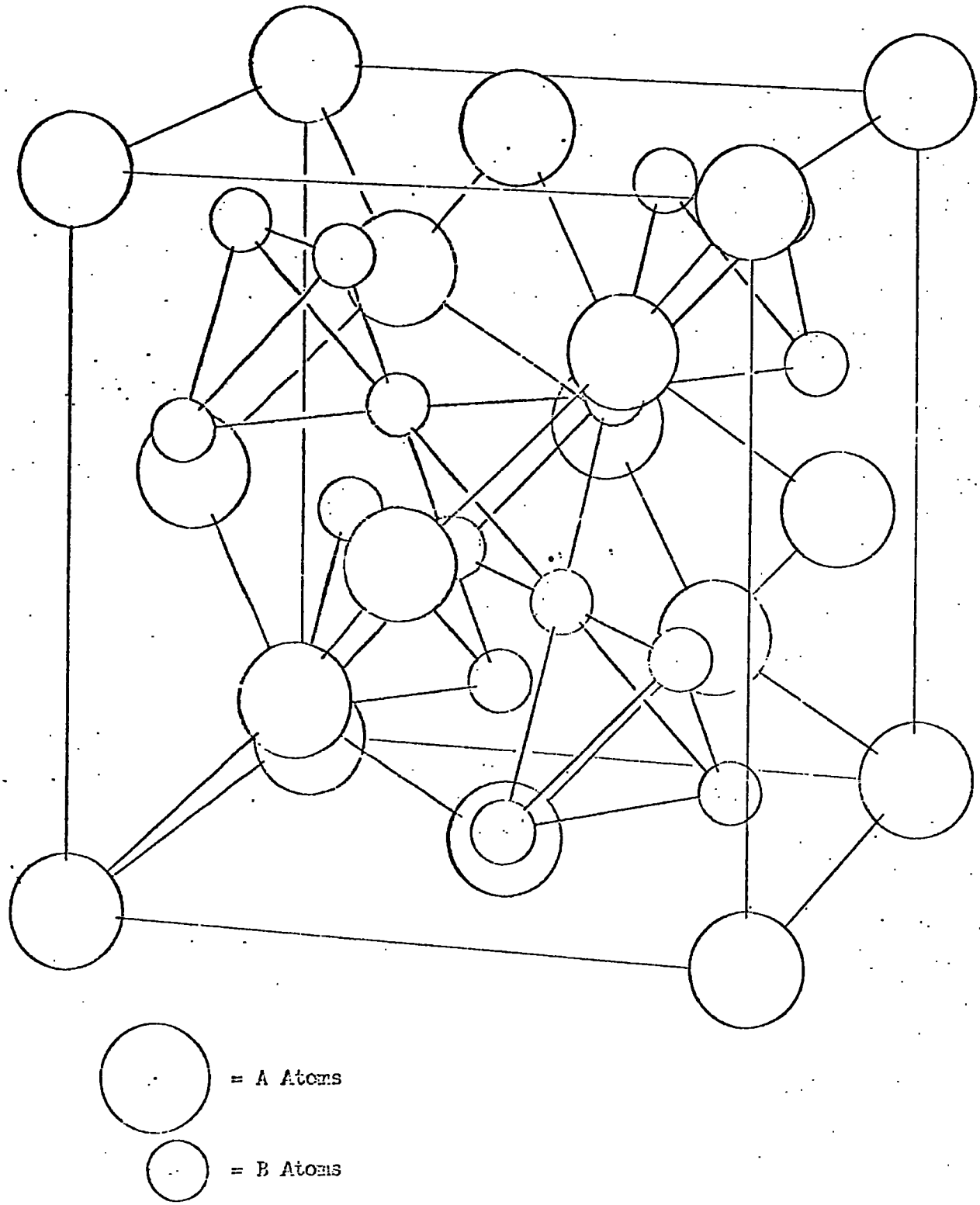

Figure 3.1 $MgCu_2$ Structure

number of nearest neighbours in the structures is $13\frac{1}{3}$. It was initially thought that the structures are size stabilized so that a size ratio close to this ideal value is required for the phases to form. Though this is undoubtedly to some extent true, compounds are formed with ratios between 1.10 and 1.46. The ideal ratio is the same for all three phases and there does not appear to be any discrimination between the types on size ratio so that other factors are involved. It was shown by Laves and Witte (see Refs. 3.4 and 3.5) on pseudo-binary and-ternary systems of the prototype Laves phases that the electron concentration is an operative factor in governing the range of miscibility of single-phase fields. This " valence" electron per atom concentration (VEC) dependence has subsequently been confirmed on compounds with transition metals (Ref. 3.5) and been related to the density of states variation obtained from hydrogen solubility, susceptibility, and electronic specific heat measurements (Ref. 3.6). This dependence is interpreted in terms of the interaction between the band structure and the Fermi surface. It is well known that, in the solid state, there is a tendency for any material to adopt a structure in which

---

3.6 Slick, et.al., J. Chem. Phys. 43, 2788, (1965) and

Wallace, W.E., and Craig, R.S., in " Phase Stability in Metals and Alloys" P.S. Rudman (Ed.) McGraw-Hill,(1967)

the Fermi surface is near a Brillouin zone boundary, where the density of states is high, since the energy of the Fermi surface will then be lower.

It appears from this work that the $MgCu_2$ type is stable for vec 1.33 to 1.72 and the $MgZn_2$ for vec 1.8 to 2.32. At higher vec the cubic type is again stable and the intermediate ranges are two-phase. There must however be other, as yet unknown, factors governing the stability of the Laves phases since many systems which satisfy the requirements of size ratio and vec do not form in these structures. Particularly noticeable are the compounds of copper with the rare earths and the scandium group metals of which not one forms in a Laves phase.

The previously reported lattice parameters for the RX_2 compounds, where X is iron, cobalt and nickel are shown in Table 3.I where the references are given at the end of the table and do not correlate with other references used in this chapter. These references are arranged in chronological order and since the accuracy probably improves with time, the last value cited in each case is probably the most reliable.

The considerable variation in properties reported in Tables 3.I and similarly for those reported later in Table 3.II almost certainly arises from the difficulty encountered in producing good single phases. This difficulty results from the peritectic nature

TABLE I

Previously Reported Lattice Parameters for RNi_2 compounds

Compound	a(°A)	Ref
YNi_2	7.181	8
	7.12	11
	7.184	12,13 *
	7.15	15
	7.16	17
$CeNi_2$	7.024	1
	7.192	2
	7.195	6
	7.202	10 *
	7.20	11
	7.18	15
	7.19	17
	7.2092	21
$PrNi_2$	7.206	4
	7.265	10 *, 16b
	7.25	15
	7.28	17
	7.2743	21
$NdNi_2$	7.270	10 *
	7.22	15
	7.23	17
	7.2560	21
	7.265	16b
$SmNi_2$	7.226	10 *
	7.22	11
	7.18	15
	7.20	17
	7.2180	21

Compound	a	Ref
$GdNi_2$	7.27	9
	7.202	10 *
	7.20	11,15
	7.206	16
	7.19	17
	7.1934	21
$TbNi_2$	7.160	10 *
	7.08	15
	7.16	17
	7.1631	21
$DyNi_2$	7.155	10 *
	7.17	11
	7.142	16
	7.14	15,17
	7.1490	21
$HoNi_2$	7.136	10 *
	7.13	11
	7.07	15
	7.12	17
	7.1318	21
$ErNi_2$	7.06	15
	7.11	10,17 *
	7.1175	21
$TmNi_2$	7.088	*
	7.06	15
	7.07	17
	7.0943	21

Compound	a	Ref
$LuNi_2$	7.085	*
	7.08	15
$Y Co_2$	7.22	11
	7.216	10,12 *
	7.17	15
	7.21	17
	7.217	19
$CeCo_2$	7.158	1
	7.161	10 *
	7.15	11
	7.162	14 ,16b
	7.13	15
	7.15	17
	7.146	18
$PrCo_2$	7.313	10,20 *
	7.17	11
	7.305	14 ,16b
	7.26	15
	7.32	17
	7.291	18
$NdCo_2$	7.30	14,19 *,16b
	7.27	15
	7.28	17
	7.283	18
$SmCo_2$	7.26	10,11,14 *,16b
	7.19	15
	7.23	17
	7.248	18

Compound	a	Ref
$GdCo_2$	7.225	10 *
	7.23	11
	7.22	15
	7.257	14,16
	7.24	17
	7.242	18
	7.259	19
$TbCo_2$	7.206	10 *
	7.209	15,16
	7.19	17
	7.195	18
$DyCo_2$	7.187	10 *, 16 b
	7.20	11
	7.190	14
	7.118	15
	7.14	16
	7.18	17
	7.175	18
$HoCo_2$	7.17	11
	7.168	10,14 *, 16 b
	7.13	15
	7.15	17
	7.159	18
	7.171	19

Compounds	a	Ref
$ErCo_2$	7.144	10 *
	7.151	14 , 16 b
	7.10	15
	7.13	17
	7.139	18
$TmCo_2$	7.121	10 *
	7.11	15
	7.10	17
	7.121	18
$LuCo_2$	7.122	10 *
	7.08	15
	7.057	18
YFe_2	7.273	10
	7.357	7,12,13 *
	7.29	11,15
$CeFe_2$	7.302	5
	7.303	10 *, 16 b
	7.25	11
	7.29	15
	7.26	17
	7.2859	21
$SmFe_2$	7.415	10 *
	7.45	11
	7.38	15
	7.4014	21
	7.411	16 b

Compounds	a	Ref
$GdFe_2$	7.44	4
	7.39	10 *, 16 b
	7.40	11,15
	7.3760	21
$DyFe_2$	7.325	10 *, 16 b
	7.29	11
	7.33	15
	7.3085	21
$TbFe_2$	7.30	15
	7.3414	21
	7.348	16 b
$HoFe_2$	7.300	10 *, 16 b
	7.28	11
	7.23	15
	7.2867	21
$ErFe_2$	7.273	10 *
	7.274	12
	7.28	15 ,16 b
	7.2603	21
$TmFe_2$	7.23	15
	7.247	X
$LuFe_2$	7.20	15
	7.222	*

References for Table 1

1. Füilling, Moeller, Vogel; Z. Matallk. 34, 253 (1942)
2. Nowtony; ibid 34, 247 (1942)
3. Endter and Klemm; Z. Anorg. Chem. 252, 377 (1944)
4. Vogel; Z. Metallk. 38, 97 (1947)
5. Jepson and Duwez; Trans. Am. Soc. Metals, 47, 543 (1955)
6. Samsonov et. al.; Doklady. Acad. Nauk. USSR. 119, 506 (1958)
7. Beaudry et. al.; Acta. Cryst. 13, 743 (1960)
8. Beaudry, Daane; Trans. AIME 218, 854 (1960)
9. Kleber; Research Report, Nucl. Corp. Am. (1960)
10. Wernick and Geller; Trans. AIME, 218, 866 (1960)
11. Nassau, Cherry, Wallace; J. Chem. Phys. Soc. 16, 123 (1960)
12. Dwight; Trans A.S.M. 53, 479 (1961)
13. Domogala et. al.; ibid 53, 137 (1961)
14. Baenziger and Moriarty; Acta. Cryst. 14 948 (1961)
15. Skrabek; PhD. Thesis, Pittsburgh (1962)
16. Ross and Crangle; Phys. Rev. 133 A509 (1964). b ; Nott^m Conf. ,240
17. Farrell; PhD. Thesis, Univ. of Pittsburgh (1964)
18. Harris, Mansey and Raynor; J. Less-Comm. Met 9, 270 (1965)
19. Lemaire; Cobalt. 33, 201, (1966)
20. Schweizer; Phys. Lett 24A, 739 (1967)
21. Mansey, Raynor and Harris; J. Less-Comm. Met. 14 329 (1968)

* Quoted by Nevitt in P.A. Beck, ed., 'Electronic Structure and Alloy Chemistry of the Transition Elements' Interscience, N.Y 1963 p.143

of the formation reaction, i.e. the compounds do not melt congruently, as shown in the phase diagrams (Ref. 3.2).

We note that in general the lattice parameters decrease as the X component changes from iron through cobalt to nickel.

III.3.(b) Magnetic Data for RNi_2.

The magnetic properties reported for these compounds are collected in Table 3.II. Again the references refer to the list at the end of the Table and are in chronological order so that the last entries for each compound should be the most reliable. The data for the three series will be considered separately commencing with the nickel series.

The Y, Ce and Lu compounds are Pauli paramagnets and the moment for Gd Ni_2 is close to that of the Gd^{3+} ion, so that it appears that the Ni ions have zero moment in these compounds and that Ce is in the $4+$ state. If we assume that Ni is non-magnetic in the other members of the series also, so that the measured moments are due to the rare earth components, it is evident that these are lower than the free tripositive ion values. The reduced moments have been attributed (Ref. 3.7) to partial quenching of the

---

3.7 Bleaney, B., Proc. Roy. Soc. A 276, 28, (1963) and in " Rare Earth Research", Vol 2, K.S. Vorres, ed., Gordon and Breach (1964)p.499.

TABLE II

Previously Reported Magnetic Data for RX_2 Compounds

Compound	M_{sat}[a]	T_c[b]	θ[b]	Reference
YNi_2	Pauli Paramagnet			3,10
$CeNi_2$	Pauli Paramagnet			3, 10
$PrNi_2$	0.73	8		3
	0.86 (c)	(c)	4	10
$NdNi_2$	1.68	20		3
	1.80	16	10	10
$SmNi_2$	6.30 (d)	77 (d)		3
	0.25	21		10
$GdNi_2$	6.74	90		3
	7.1	85	78	10
$TbNi_2$	5.85	46		3
	7.8	45	35	10
$DyNi_2$	7.1	32		3
	9.2	30	23	10
$HoNi_2$	7.1	23		3
	8.4	22	12	10
$ErNi_2$	5.7	14		3
	6.8	21	11	10
$TmNi_2$	2.5	14		3
	3.2 (c)	(c)	0	10

Compounds	M sat(a)	To(b)	θ(b)	Reference
$Lu Ni_2$	Pauli Paramagnet			3, 10
$Y Co_2$	0.3			1
	0.23	296		4
	1.10	320		10
	Antiferromagnetic; TN,			11
	No ordering down to 2°K			12
$Ce Co_2$	Paramagnetic			1,2,4,7
	No ordering down to 2°K			10
$Pr Co_2$	2.98	50		4
	2.6	50		7
	3.2	50	(e)	10
	3.7 (h)	-		13
$Nd Co_2$	3.46	126		4
	3.8	110		7
	4.2[e]	-		9
	3.8	116	107	10
$Sm Co_2$	1.6	530		1
	1.26	232,535		4
	1.4	215		7
	2.0	259		10
$Gd Co_2$	4.5	408		1
	4.31	408		4
	4.7	420		7
	4.9	-		10
	4.9	400		12

Compounds	Msat	Tc	θ	Reference
$TbCo_2$	4.38	245		4
	5.6	250		7
	6.8 (n)	237 (n)		9
	6.7	256	228	10
$DyCo_2$	6.72	169		4
	6.6	160		7
	7.6	159	129	10
$HoCo_2$	7.17	111		4
	6.9	95		7
	7.5 (n)	87 (n)		9
	7.8	95	(e)	10
$ErCo_2$	5.87	48		4
	5.6	40		7
	6.9 (n)	39 (n)		9
	7.0	36	28	10
$TmCo_2$	3.96	33		4
	4.7	18		10
$LuCo_2$	Pauli Paramagnet			4
YFe_2	...	535		1
	2.91	550		4
	...	552		14

Compounds	Msat	Tc	Q	Reference
$CeFe_2$	2.6	255		1
	6.97	878		2
	2.38	235		5
	2.4	221		6
$SmFe_2$	2.7	688		1
	2.50	700		4
	. . .	674		2
$GdFe_2$		813		2
	3.6	813		6
	3.35	782		8
$TbFe_2$	3.68	705		4
	3.9	696		6
$DyFe_2$	5.44	663		2
	5.4	750		6
	4.91	638		8
$HoFe_2$	5.3	610		1
	6.02	608		2
	5.11	614		4
	5.2	600		6
$ErFe_2$	5.02	473		2
	4.75	596		4
	4.7	450		6

Compounds	M sat	To	Θ	Reference
$Tm\ Fe_2$	2.92	613		2
	2.52	610		4
$Lu\ Fe_2$	2.97	610		4

(a) Saturation Moment; MB/ Formula Unit

(b) To, Curie Temperature;) 0, Curie-Weiss Temperature: (^{o}k)

(c) Magnetic state uncertain, may not be ferromagnetic at $2^{o}K$. Moment measured at $2^{o}K$, 20 KOe

(d) Serious Cd contamination; see Ref. 10

(e) Curie - Weiss behaviour not exhibited

(n) Neutron diffraction results.

References for Table II

1. Nassau; PhD Thesis, Pittsburgh, 1959
2. Wertheim and Wernick; Phys. Rev. 125, 1937 (1962)
3. Skrabek and Wallace; J. Appl Phys. 34, 1356 (1963)
4. Wallace and Skrabek; "Rare Earth Research", Vol 2. p.431 (1964)
5. Farrell and Wallace; J. Chem. Phys. 41, 1524 (1964)
6. Crangle and Ross; Proc. Int. Conf. Mag., Nottingham, p 240 (1964)
7. Ross and Crangle; Phys. Rev. 133, A509 (1964)
8. Mansmann and Wallace; J. Chem. Phys. 40, 1167 (1964)
9. Moon, Koehler and Farrell; J. Appl. Phys. 36, 978 (1965)
10. Farrell and Wallace; Inorg. Chem. 5, 105 (1966)
11. Taylor, Ellis and Darby; Phys. Lettr. 20, 327 (1966)
12. Lemaire and Schweizer; Phys. Lettr. 21, 366 (1966)
13. Schweizer; Phys. Lettr. 24A, 739 (1967)
14. Marci, Craig, Wallace and Tsuchida; J. Less-Comm. Met. 13, 391 (1967)

orbital moment by the crystalline field (see Section II.6 (a)). Bleaney (Ref. 3.7) estimated the energy level splitting due to the crystalline field in this series. Large splittings were found, in some cases larger than the exchange interaction, and the ground state moments were determined in good agreement with the measurements of Skrabek and Wallace (Ref. 3.8). The large splitting was subsequently investigated specifically (Ref. 3.9) but not confirmed. Bleaney's work, however, clearly shows that crystal field effects can account for the reduced rare earth moments.

The fact that Ni has zero moment in these compounds has been confirmed by neutron diffraction measurements (Ref. 3.10) on Tb Ni_2 and this has been attributed (Ref. 3.8) to electron transfer from the rare earth component to the Ni 3d shell putting it into the $3d^{10}$ state. This behaviour has been found also in rare earth-nickel compounds of other stoichiometries and attributed to the same cause.

III.3. (c) Magnetic Data for RCo_2

Comparing the moments for Gd Ni_2 and Gd Co_2, it seems reasonable

---

3.8 Ref. 3 in Table II

3.9 Ref. 10 in Table II

3.10 Felcher, G.P. Corliss, L.M., and Hastings, J.M., J. Appl. Phys. 36, 1001, (1965)

to ascribe a moment to each Co ion of about 1.1 μB coupled antiparallel to the Gd moment. Since the lattice constants for this series are larger than the corresponding ones in the Ni series, it is to be expected that quenching of the other rare earth moments should be not larger than in the latter. On this basis the same interpretation for the heavy rare earths (H.R.E.) as for Gd Ni_2 is consistent with the measurements. This is confirmed by neutron diffraction results (Ref. 3.11) which indicate a Co moment of 1.0 ± 0.2 μB antiparallel to the H.R.E. moment. In the light rare earth (L.R.E.) compounds, however, it appears that the Co moment is coupled parallel with the L.R.E. moment and that its values are lower than that given above. This is again confirmed by neutron diffraction (Ref. 3.11) which gives the Co moment in Nd Co_2 as 0.8 ± 0.2 μB. This behaviour is as expected since in the L.R.E. ions J = L-S while in H.R.E., J = L+S so that there is anti-coupling parallel between the rare earth and Co spins in both cases.

The measured Curie temperatures are consistent (Ref. 3.9) with the behaviour expected on the basis of a coupling mechanism via the conduction electrons in that they are proportional to the de Gennes function (Section II.6 (a)).

3.11 Moon, R.M., et.al., J. Appl. Phys. 36, 978, (1965)

There are, however, many complicating features in this series. As indicated above the Co moment in Gd Co_2 and several other compounds is about 1.1 μB, but in YCo_2 (see Table 3.II) this moment is very small and in Lu Co_2 and Ce Co_2 zero. These low moments are to be compared with the value of 1.7 μB in elemental cobalt, and have again been attributed (Ref. 3.12) to electron transfer from the rare earth component. Bleaney (Ref.3.7) suggested that the moment carried by Co in compounds with a magnetic partner is induced and should be proportional to $(g-1)\ M/g$, where M is the moment carried by the magnetic partner and g is its Landé factor. A measure of agreement was obtained with the experimental results.

Several of the compounds show anomalous magnetisation - temperature curves (see e.g. Ref. 3.9); some demagnetise in two steps and others have sharp discontinuities at the Curie temperature. This latter effect has been studied in some detail for the case of Ho Co_2 by Lemaire et.al.(see Ref. 3.3), who find that the transition at the Curie point is first order and shows thermal hysteresis, and that there is metamagnetism at higher temperatures.

3.12 Ref. 4 in Table II.

Further peculiarities (Ref. 3.9) are that (i) many of the compounds do not follow the Curie-Weiss law above Tc;(ii) $TmCo_2$ exhibits a compensation point at about 120°K which is far above the apparent Curie temperature (18°K); (iii) YCo_2, while having a very low moment, has a high Curie Temperature which patently does not correspond with the de Gennes function on which the others lie. With regard to (iii) Lemaire (Ref. 3.3) finds that the magnetisation of YCo_2 is linear with field at all temperatures down to 2°K, though the magnetisation - temperature curve is anomalous at low temperatures. Neutron diffraction of this compound did not reveal any ordered moment and Lemaire concludes that YCo_2 is paramagnetic with very low moment. It should be remembered however, that the errors in the neutron diffraction powder method are considerably greater than the moment measured for YCo_2 from bulk magnetisation.

Schweizer (Ref. 3.13) has studied Pr Co_2 by neutron diffraction and finds $\mu_{Co} = 0.50 \pm 0.25$ μB in this compound. He attributed the variation of cobalt moment to polarisation of the 3d electrons by the rare earth spin through the conduction electrons, the magnitude of the resulting moment being thus related to the rare

---

3.13 Schweizer, J., Phys. Lettr. 24A, 739, (1967)

earth spin. This is the same mechanism, presumably, as envisaged by Bleaney (vide supra).

III.3. (d) Magnetic Data for RFe_2

Again for this series it is to be expected that the rare earth moments should be less affected by crystal field quenching than in either of the two former series, because of the lattice dilation. Comparison of the moments here with those from the other series indicates that, in the H.R.E. compounds, iron has a moment of about $2\mu_B$, while in YFe_2 and $Lu\ Fe_2$ it has about 1.4 to $1.5\mu_B$. This reduction from $2.2\mu_B$ for elemental iron has again been attributed to electron transfer (Ref. 3.12) and, following Bleaney's reasoning on the RCo_2 compounds, the Fe moments were analysed by Wallace and Skrabek in terms of a permanent moment in all the compounds of $1.45\mu_B$ with an additional induced component proportional to $(g-1)$ M/g. With assumptions on the rare earth moments (M), and scaling the induced component from the $Gd\ Fe_2$ value, Wallace and Skrabek obtained fair agreement with the experimental measurements. This analysis seems to the present author, however, to be unsatisfactory. It is elementary to write down two simultaneous equations involving the rare earth, iron and observed moments which, when solved for M, yield values lower than those in the RNi_2 series. Reasons have already been given for believing that this is not the case. Further, the above analysis cannot include $Ce\ Fe_2$ which has a moment

lower than YFe_2.

This series has been investigated also through the Mössbauer Effect. Wallace (Ref. 3.14) has performed the most extensive study of the hyperfine field at the iron nucleus: he found that the hyperfine field was proportional to the moment carried by the iron atom, indicating that it results mostly from core polarisation. Strict proportionality was, however, not shown convincingly due to the uncertainty in the evaluation of the iron moments. Cohen has made (Ref. 3.15) a detailed Mössbauer effect study of the rare earth sublattice in $TmFe_2$. The temperature variation of the magnetic and electric nuclear interactions are well explained on a relatively simple theory assuming that the internal field (at the Tm nucleus) results entirely from the 4f electrons with little effect due to core or conduction electron polarisation. One very significant fact (in the view of the present author) emerging from this work was that the temperature variation of the Tm sublattice magnetisation is far from the " Brillouin" shape (see Section II.3) and is concave upwards between about 100° and 400°K.

Additional information on the hyperfine interaction is available from N.M.R. work. The field at the Gd nucleus in

---

3.14 Wallace, W.E., J. Chem. Phys. 41, 3857 (1964)

3.15 Cohen, R.L., Phys. Rev. 134, 494, (1964)

Gd Fe_2 is the same order of magnitude (400 kO_e) as in elemental gadolinium but of opposite sign (Ref. 3.16). The origin of the large positive contribution responsible for this is not apparent, but it is approximately constant for all RFe_2. There is a large variation, however, in the magnitude and sign of the hyperfine fields for different Gd X_2 compounds. Gegenwarth et al. consider that these results support the supposition of constant 4f core polarisation with the variations due to " valence" electron polarisation.

III.3 (e) Pseudo-Binary Series

The pseudo-binary series $Gd_xY_{1-x}Co_2$ has been investigated in two papers. Taylor et al. (Ref. 3.17) found the two-step demagnetisation curve (see Section III.3 (c)) for $x \geqslant 0.5$ and YCo_2 antiferromagnetic. They interpreted the series in terms of a triangular spin configuration. Lemaire and Schweizer (Ref. 3.18) on the other hand found no anomalous demagnetisation curves, and as stated previously (Section III.3 (c)), that YCo_2 was nonmagnetic. They interpreted the series in terms of a variable Co moment, though no mechanism for this variation was proposed.

Oesterreicher and Wallace (Ref. 3.19) measured the crystallo-

---

3.16 Gegenwarth, et al., Phys. Rev. Lettr. 18, 9, (1967)

3.17 Ref. 11 of Table II

3.18 Ref. 12 of Table II

3.19 Oesterreicher, H., and Wallace, W.E., J. Less-Common Metals 13,91,(1967)

graphic and magnetic (susceptibilities and saturation moments) characteristics for the systems Gd Al_2- Gd Fe_2, Gd Al_2 - Gd Co_2 and Er Al_2 - Er Co_2. The C14 structure was observed in all these series and the stability ranges for this and the C15 terminal phase were measured. An extended critique of their analysis is given later, in Chapter VI. Their essential results are presented in Table 3.3.

Table 3.3

System	Compositions in mol.% RAl_2 (± 2%)		
	RX_2 phase (C 15)	Intermediate (C14)	RAl_2 phase (C 15)
Gd Fe_2 - Gd Al_2	0 - 26	27 - 52	67 - 100
Gd Co_2 - Gd Al_2	0 - 24	49 - 73	74 - 100
Er Co_2 - Er Al_2	0 - 27	28 - 73	77 - 100

Mansey et al. (Ref. 3.20) have presented lattice spacings of several R $(X_1, X_2)_2$ pseudo-binary series. All the series investigated

---

3.20 Mansey, R.C., et al., J. Less-Common Metals, 14, 337, (1968)

were single phase (C 15) and the lattice parameters showed positive deviations from Vegards Law (linear interpolation) except for series involving Ce. The latter exception was explained by the variable valency of Ce. In some cases the deviations from Vegards Law were very large.

III.3 (f) Summary and Statement of Problem

The previous sections have outlined the properties of the RX_2 compounds and some general problems in their interpretation are obvious. Firstly the moment carried by the R component appears to be lower than the free tripositive ion value and secondly that on the X component is very variable. In the first case crystal field effects are obviously able to account for the reduction but the magnitude of the effect is uncertain because of the uncertainty in evaluating the component moments. The iron group component moments present a greater problem and the only explanation suggested so far has been electron transfer into the 3d shell together with induced moments in some cases. The transfer hypothesis seems to the author to be untenable as a major cause of the variable moments since the necessary degree of transfer varies so greatly for the different materials where elements with very similar electronegativities are involved. For example in Gd Ni_2, about 0.6 electrons /Ni atom are required while in Gd Fe_2

this is only about 0.2/Fe atom and, again, the values for YCo_2 and YFe_2 are about 1.7 and 0.8 per atom respectively. Lastly the induction process has been envisaged as proportional to the R spin but no physical process has been suggested and we have given reasons for considering that it is unable to account for the measurements satisfactorily.

The present work aims at elucidating some of these problems. Obviously the most serious hazard to the formulation of a useful theory of these materials is the uncertainty in the component moments. This could be resolved directly by neutron diffraction were single crystal specimens available; the powder method unfortunately has insufficient precision. In the absence of this, the author has considered the study of pseudo-binary series to be the most useful approach. In particular the substitution of Y for the rare earth components should provide information on the values of the components and the effect of variation in the rare earth spin. Also series of the type $Y\ (X_1, X_2)_2$ should yield direct information on the X component values and interactions.

The RFe_2 compounds seemed the most appropriate starting point since this series does not have the further peculiarities of the RCo_2 series. The series chosen initially was (Dy, Y) Fe_2 since a Mossbauer isotope is available for Dy so that the hyperfine

interaction at both nuclei could be studied and might provide further relevant information. In addition this work is concerned with the series Y $(Fe, Co)_2$, $Dy(Fe, Ni)_2$, and Y $(Fe, Ni)_2$ the last two in considerably less detail than the former for the reasons given later (Chapter VI).

CHAPTER IV EXPERIMENTAL DETAILS

In this work specimens of the different compounds were prepared by arc-melting in an inert atmosphere and their magnetic properties were measured, over a wide temperature range, with a vibrating sample magnetometer, and, at the highest temperatures, with an electro-magnetic servo-balance.

IV.1 Specimens

The raw elemental materials were obtained from the Koch-Light Laboratories Ltd., in the form of ingots of the Rare Earths and rods of the iron group metals. The stated purities were 3N + (with respect to other R.E.) for the Rare Earths and 4N8+ for the iron group metals. The stated analyses of the materials is given in Table 4.1.

Stoichiometric quantities of each component, for any given compound, were cut and weighed (to the nearest 0.001 gms) and the total weight of each specimen was made about 3-6 gms. The cutting and filing mechanisms were performed in an Argon atmosphere in a glove box. These components were then melted in an arc furnace. The furnace was evacuated to a pressure of less than 0.3 microns of mercury and flushed with high purity Argon (5N) to atmospheric pressure. It was then re-evacuated and filled to the working pressure of ~ 200 m.m. Hg and gettered for several minutes with

TABLE 4.1

Stated Analyses of Raw Materials

Showing impurities in parts per million

IRON	Ag	Al	Cu	Mg	Mn	Si		
	<0.5	<0.5	<0.5	3	3	3		
	No other metallic impurities							
COBALT	Ag	Al	Ca	Cu	Fe	Mg	Mn	Si
	<1	<1	<1	<1	3	1	2	3
NICKEL	Ag	Al	Cu	Fe	Mg	Si		
	<1	1	<1	2	2	<3		
	No other metallic impurities							

DYSPROSIUM	CaO	CuO	Fe_2O_3	NiO	SiO_2	Ta_2O_5	Y_2O_3	O_2
	100	100	200	200	100	1500	200	1500
YTTRIUM	Al_2O_3	CaO	Dy_2O_3	E_2O_3	Fe_2O_3	Gd_2O_3		
	300	50	500	100	100	20		
Ho_2O_3	Nd_2O_3	SiO_2	Ta_2O_5	Tb_4O_7	Yb_2O_3	O_2		
200	20	200	400	20	30	2000		

molten tantalum. The components were then melted together and the ingot turned over and remelted twice more before removal from the furnace. There was always a loss of approximately 2% by weight of the specimen during this process. In some instances the ingots were found to shatter during either cooling or remelting, presumably as a result of thermal stress caused by the rapid heating and cooling rates. The incidence of this shattering was, as far as could be ascertained, random and the same compound made at different times sometimes did and sometimes did not shatter.

Each specimen was examined visually on removal from the furnace and then broken in a pestel with a mortar, again in an Argon atmosphere in the glove box. A small amount was ground into a fine powder for x-ray diffraction. All the specimens were very friable and were easily broken and crushed.

The visual examination showed that the ingots had a good metallic lustre though some bluish discolouration, suggesting oxidation, was usually present on the surface. This surface layer was extremely thin and was easily removed by filing. Examination of the broken ingots revealed a coarse columnar structure with, apparently, grains running vertically through the ingot. These were examined in a few cases by the Laue back-reflection x-ray technique but only very low order was found. The normal x-ray diffraction examination was performed on the powdered specimens

with a Debye-Scherer type camera of diameter ~ 11 c.m., using cobalt K α radiation. Cobalt radiation was necessary since the more usual copper K α line causes fluorescence of the R.E. components. The results of these examinations are given in Section V.1.

IV.2 Apparatus

IV.2(a) Vibrating-Sample Magnetometer

The vibrating sample magnetometer used in this work was a modification of the instrument constructed and used by H.D. Ellis (Ref. 4.1). Mechanically only minor modifications were effected in order to facilitate easier interchange of the specimen tubes and a detailed description will not be given here. The essential features of the magnetometer are shown in the drawing (Figure 4.1) and photograph (Figure 4.2).

The apparatus was, however, fairly extensively rebuilt electronically so as to make it a null-output instrument, thus correcting the principal disadvantage of the previous instrument (Ref. 4.1). The block diagram for the magnetometer is shown in (Figure 4.3)

The " sample " and " monitor " pick-up coils, which are themselves twin coils connected in opposition (Ref. 4.1), are connected in series and the resultant signal is amplified before being passed

---

4.1 Ellis, H.D., Ph.D Thesis, University of Durham, 1967

FIGURE 4.1 Drawing of Magnetometer.

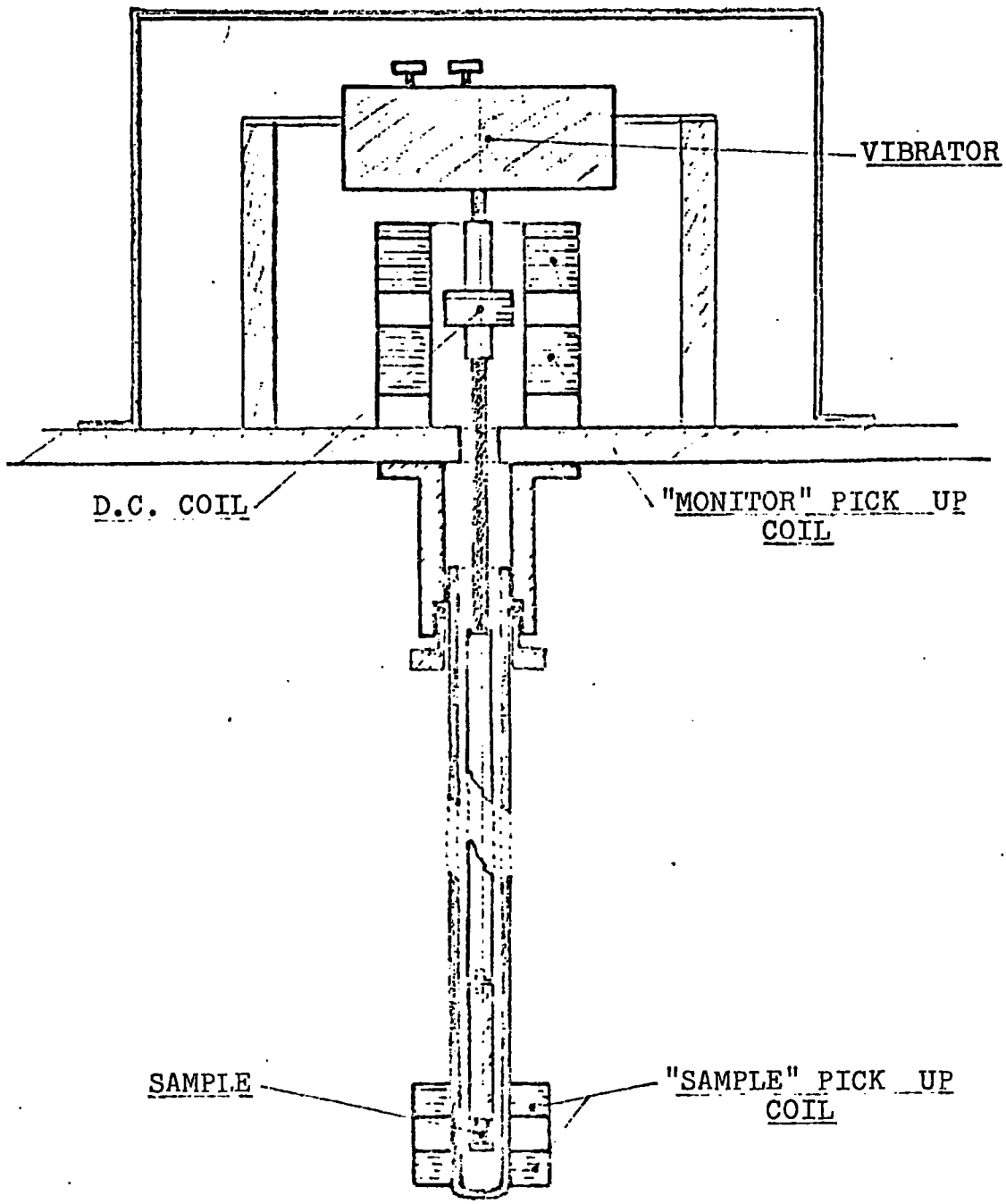

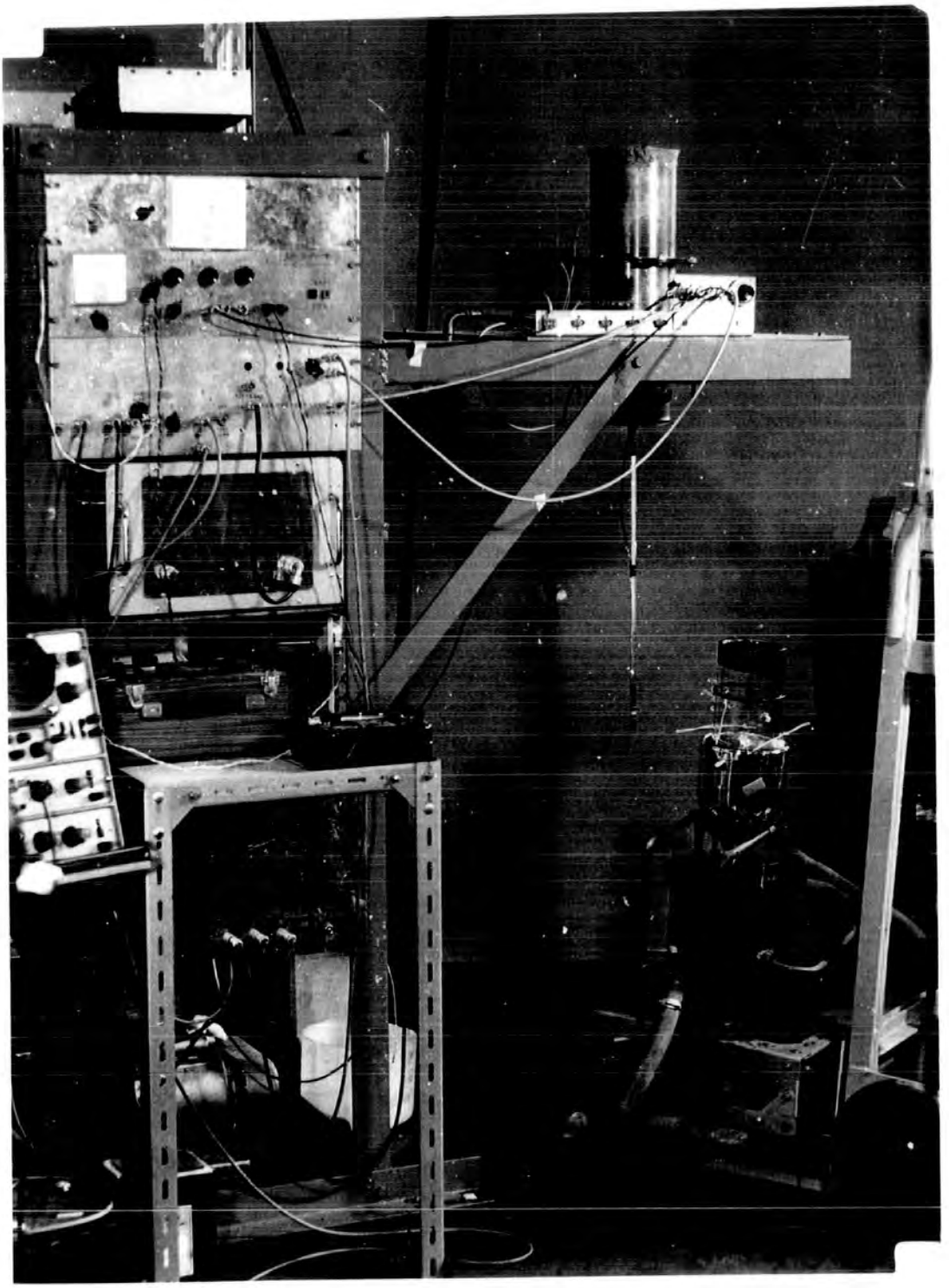

FIGURE 4.2 MAGNETOMETER

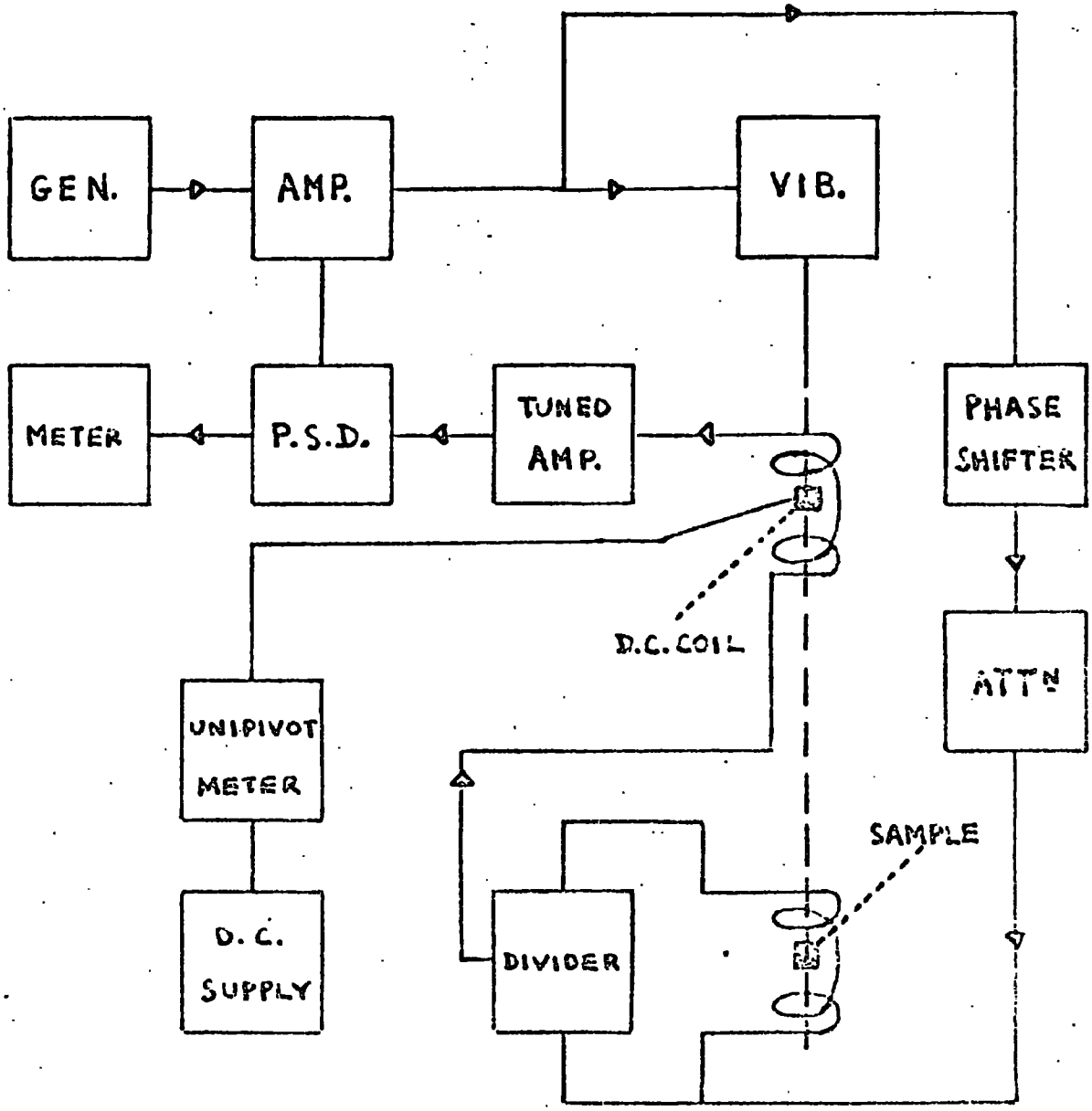

FIGURE 4.3 Block Diagram of Magnetometer.

to the phase sensitive detector and meter. The signal in the " monitor" pick-up coil is derived from the D.C. coil (Ref.4.1) which is supplied with variable (0 - 48 mA) current from a 6V source, this current being measured with a Cambridge Unipivot Type L milliammeter. The " sample" pick-up coil incorporates a 250 KΩ potential divider, with vernier setting, to reduce the magnitude of the signal if required. In use, the direction of the current in the D.C. coil is set to give a signal in the " monitor" coil in opposition to that in the " sample" coil. This current is then varied to give null output from the phase-sensitive detector. In this condition the current is proportional to the magnetisation in the sample.

The generator (Farnell Type LF solid state oscillator), vibrator (Advance), tuned amplifier (Grubb-Parsons T.A., high gain) and the phase-sensitive detector have all been described by Ellis (Ref. 4.1). The amplifier is a simple 2-stage amplifier for 70 c.p.s. whose circuit is given in Figure 4.4: the third stage provides the reference for the phase sensitive detector.

Considerable coherent noise is generated in the " monitor" coil, due to the proximity of the vibrator. This is eliminated by injecting a portion of the supply signal into the circuit. The circuit diagram for the phase-shifter and attenuator required

FIGURE 4.4 Amplifier Circuit Diagram

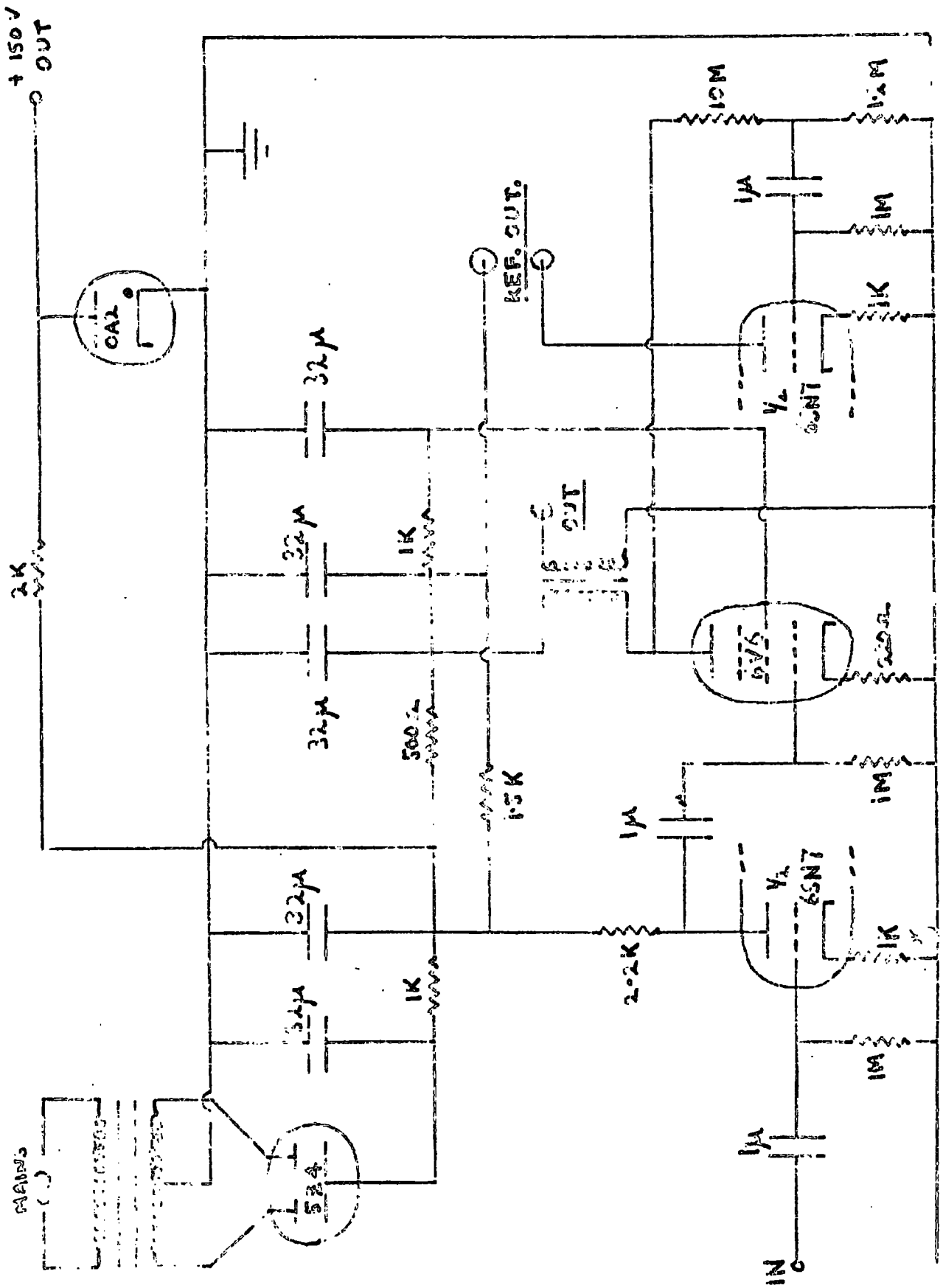

FIGURE 4.5 Phase Shifter and Attenuator.

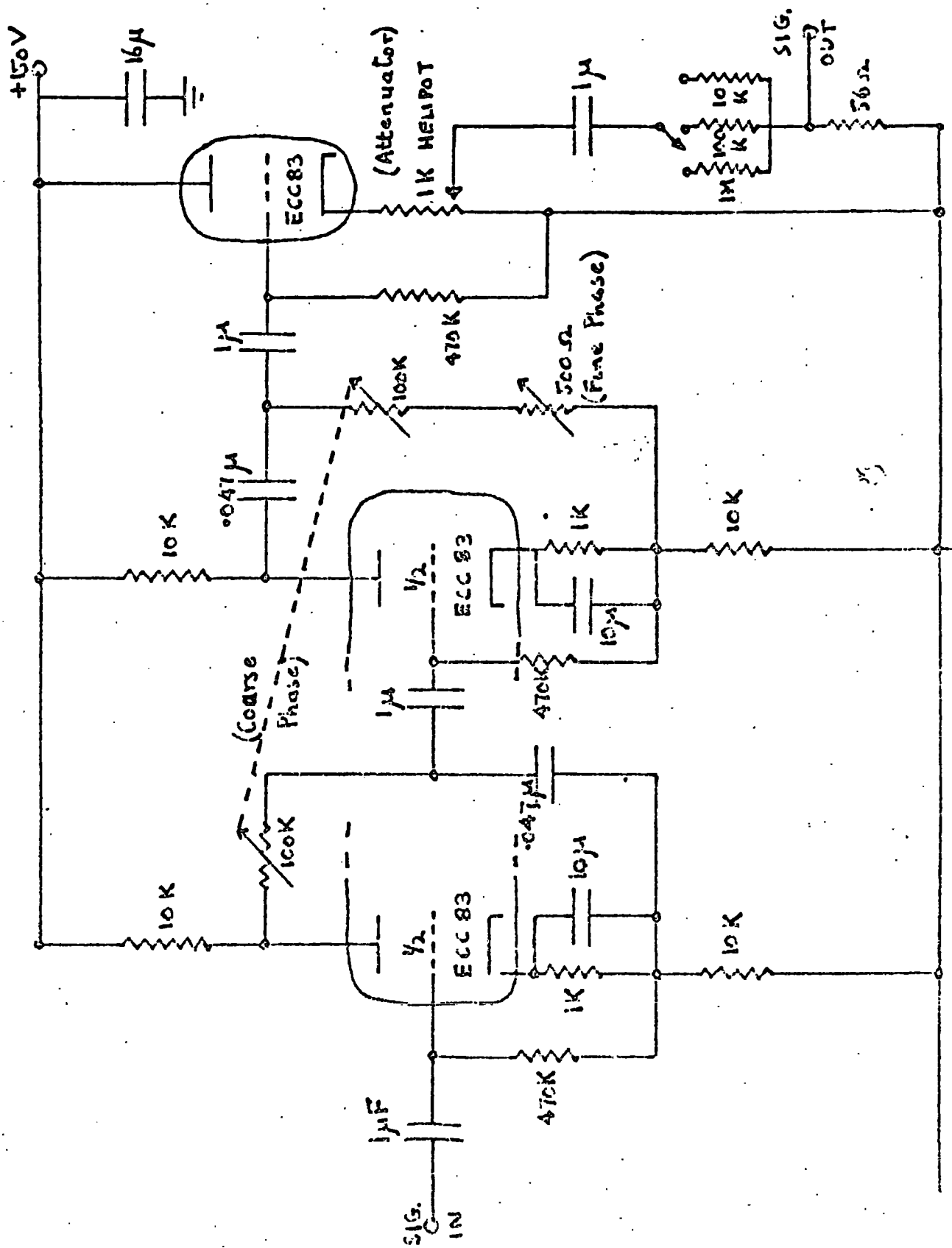

for this purpose is shown in Figure 4.5.

The effect of sample length in the magnetometer was investigated by Ellis who found (Ref. 4.1) that this must be less than 4.5 mms. Samples of length about 3 mms were therefore used, the pieces being selected as described in Section IV.4(c) and of weight about 80 m.gms. They were held in the silica tubes with " Durafix" cement for the low temperature work and with a waterglass cement for high temperatures. In use the " sample" pick-up coil was positioned so that its centre coincided with the centre of the sample itself, by measurement with vernier calipers with respect to a fixed point.

The solenoid and power supply used with this magnetometer have been adequately described previously (Ref. 4.1 and 4.2). The power supply is a Westinghouse 0-200 volts D.C., 50 K.W. Rectifier. There is considerable temporal fluctuation and ripple in the output. The solenoid is constructed of a number of " pancakes" of coiled copper strip and is water cooled. The previous calibration of this solenoid (Ref. 4.2) was confirmed with a Hall Probe. The field is linear with current at the rate of 42 Oe/Amp. giving a maximum field of about 9.5 KOe.

4.2 Hutchinson, F., Ph.D Thesis, University of Durham, 1958.

IV.2.(b) Susceptibility Balance

For measurements at the highest temperatures used in this study (> 600°K) the vibrating-sample magnetometer could not be used (see Section IV.3) and a susceptibility balance was used. This instrument was built and used by Thompson (Ref. 4.3). It is an electromagnetic servo-balance working on the Faraday method (see Ref. 4.4). The sample is placed in an inhomogeneous magnetic field in a solenoid and the force on the sample is measured electromagnetically and is proportional to the magnetisation. In this work the balance was not calibrated against an external standard but the magnetisation/temperature measurements taken with it were scaled against those from the magnetometer.

IV.3 Temperature Measurement and Control

Throughout this work, temperature measurement was effected by means of copper-constantan thermocouples in contact with the specimen. These were constructed from " high conductivity" copper, supplied by Lewcos, and " thermocouple telconstan", supplied by Telcon Metals, by melting the wires in a gas flame.

4.3 Thompson, D.R., Ph.D. Thesis, University of Durham (to be published)

4.4 Zijlstra, H., " Experimental Methods in Magnetism", Part 2, North-Holland Publishing Co., 1967.

The thermopotential from these couples corresponded with the British Standard tables (Ref. 4.5) at certain fixed points (liquid nitrogen, ice, boiling water, lead) and these tables were used for temperatures above -190°C. Below this temperature, values were obtained by interpolation between liquid helium and liquid nitrogen temperatures by comparison with standard tables. The thermo-emfs were measured with a Pye Portable Potentiometer. The reference junction was kept in liquid nitrogen for temperatures up to room temperature and ice for above.

At about 4°K constantan may have a large susceptibility so that the thermocouple could introduce an error into the measured magnetisation. In this magnetometer, however, the amount of constantan within the sensitive area is very small and measurements indicated that no correction was necessary for this.

Temperatures below room were obtained with liquid nitrogen and liquid helium contained in glass dewars. Above room temperature a small furnace was employed. This was wound with "Kanthal" wire around a silica tube, with the lower end closed, which fitted inside the solenoid. Below about 600°K Lissapol NX was used in this furnace

---

4.5 "Reference Tables for Copper v. Constantan Thermocouples" British Standard No. 1828, 1961.

tube as an oil bath to reduce the rate of temperature change so that measurements could be made with the temperature varying. At the highest temperatures measurements were taken in discrete steps in temperature as no suitable bath was available.

In the magnetometer, the " sample" pick-up coil was wound on a pyrophyllite former for high temperatures but a limit of about 600°K was set on measurements with this instrument by breakdown of the insulation of the copper wire forming this coil.

At all temperatures the magnetometer was filled with helium gas to act as a transfer gas to keep the sample at the temperature of the surroundings.

IV.4 Interpretation of Measurements

It has been shown that at any temperature and field setting the current, I_σ, in the D.C. coil can be measured. It remains to be shown how I_σ may be related to physically interesting parameters.

IV.4 (a) Calibration

The D.C. coil acts as a dipole whose moment depends on the current I_σ which must therefore be calibrated against magnetisation in the sample. This calibration was performed using several samples of pure iron and nickel against the absolute data of Weiss and Forrer (Ref. 4.6). I_σ was measured as a function of field at

---

4.6 Weiss, P., and Forrer, R., Ann. Phys. (Paris) 12, 297, (1929)

different temperatures and extrapolated to the saturation values. Values of the calibration constant Λ were then obtained from the equation

$$\sigma = \Lambda \cdot \frac{I_\sigma}{w}$$

where σ is the magnetisation/gm, from Ref. 4.6, and w is the mass of the sample. The values obtained for Λ for the different materials, samples and temperatures were within 1% and the average value was taken as the calibration of the instrument, i.e. $\Lambda = 0.0559$ e.m.u./mA.

The magnetometer could then be used with other materials, when the magnetisation in atomic units is given (using Equation 2.1) by

$$\sigma = \frac{0.0559.\ I_\sigma \cdot W_A}{w \qquad 5586} \quad (\mu_B/\text{molecule}) \quad \ldots(\text{Equation } 4.1)$$

w is measured in gms and I_σ in mA.

IV.4(b) Accuracy and Precision

Considering Equation 4.1 the quantities liable to error are Λ, I_σ, and w. I_σ could be measured to about 0.5%, and w was measured to about 1%. The overall precision is therefore put at $\pm$ 1.5% and the accuracy at $\pm$ 3% since here Λ must be considered also. The smallest magnetisation which could be measured was 5.10^{-3} e.m.u. corresponding to 0.1 mA.

IV.4(c) The Demagnetising Field

Since the magnetisation is required as a function of field, the influence of the sample on the applied field must be considered. The field inside the sample body is the internal field, Hi, composed of the applied field due to the solenoid, H, and the " demagnetising field", H_D, due to the poles of the sample itself; i.e. $Hi = H + H_D$. If the body is homogeneous and has the shape of an ellipsoid the demagnetising field is uniform and depends only on the dimensional ratio of the ellipsoid and is proportional to the magnetisation. If these conditions are not satisfied the demagnetising field is non-uniform and depends, additionally, on the susceptibility of the material and the fieldstrength. Under these latter conditions corrections can be made only approximately.

With the materials used in this work it was considered impracticable to machine the samples to a specific shape due to their reactivity. Samples were thus chosen so that corrections for the demagnetising field remained small. This requires, ideally, long rods magnetised along the axis or thin sheets magnetised in the plane. In practice samples where chosen of platelets of the material with the length at least 2-3 times the width. For samples of this shape the demagnetisation factor N_D ($H_D = - N_D M$, where M is the magnetisation) is (e.g. Ref. 4.4 Ch.2) about 0.1 so that the correction to the applied field H is of the order of a few percent.

In the whole of this work this correction is ignored and Hi is taken equal to H. Specific calculations were made with a few samples of the effect of the demagnetising field on the calculated saturation moment (Section IV.4 (d)). The error introduced by the above assumption was well within the previously stated experimental error.

IV.4 (d) Atomic Moment and Curie Point

The Bohr magneton number, p, of a material is related to the magnetisation by Equation 2.1. That is the atomic moment is given by the absolute saturation magnetisation. The measurement of this quantity, however, requires either infinite field or zero temperature so extrapolation is necessary from high fields at the lowest temperatures. The variation of the spontaneous magnetisation at low temperatures has been discussed in Sections II.1 and II.2 so that, if the spontaneous magnetisation could be measured at different temperatures, the absolute saturation value could be obtained.

Since in zero applied field the domains have random orientation it is not feasible to measure the spontaneous magnetisation within a domain. In applied fields of about 10^3 to $3\ 10^4$ Oe it is found that, for many materials the empirical relationship (see Ref. 4.7)

$$\sigma_{H,T} = \sigma_{S,T} \left(1 - \frac{a}{H} - \frac{b}{H^2}\right) + cH \quad \ldots\ldots \quad \text{(Equation 4.2)}$$

4.7 Morrish, A.H., " The Physical Principles of Magnetism" Wiley (1965) Ch. 6.

at low temperatures

is followed. Here a $>$ b $\gg$ c are constants and $\sigma_{S,T}$ is termed the saturation magnetisation. For fields of the order suggested, the difference between $\sigma_{S,T}$ and $\sigma_{0,T}$ is negligible.

In this work it was not feasible to obtain σ versus H data at very low fixed temperatures other than at the liquid helium temperature. Consequently the saturation magnetisation was obtained at 4.2°K, from Equation 4.2, by extrapolation of the σ versus $^1/H$ plot to $^1/H = 0$, and this value was taken to give the atomic moment.

It has been shown, at the start of Chapter II, that for an isolated atom p = gJ and the expression for g was given. g may be related (Ref. 2.8) to the magnetisations associated with orbital and spin angular momentum, Morb and Msp respectively, by g = 2(1 + Morb/Msp). In a Ferrimagnetic material, or in an alloy assumed to consist of separate sublattices, the effective g value may be related to the g values and magnetisations of the different sublattices (Ref. 4.8). Thus, in principle, measurement of p and g for a material leads to a knowledge of Morb and M spin and hence to some aspects of the electric structure.

We turn now to the determination of the Curie point. From general thermodynamic considerations, Belov (Ref. 4.9) has shown

---

4.8 Smit, J., and Wign, H.P.J., " Ferrites ", Philips Technical Library (1959)
and Meyer, A.J.P., and Asch. G., J. Appl. Phys. 32(s), 330 (1961)

4.9 Belov, K.P., " Magnetic Transitions ". Consultants Bureau, New York, (1961)

that at constant temperature in this region $\sigma_{H,T}^2 = \sigma_{0,T}^2 + aH/\sigma_{H,T}$. Hence the spontaneous magnetisation may be obtained from plots of σ_H^2 against H/σ_H. The isotherm passing through the origin thus gives the Curie point ($\sigma_0 = 0$). This is, however, a tedious procedure and for routine measurements we can, as before, take the magnetisation in a field < 10^4 Oe as representing the spontaneous magnetisation at temperatures not too near the Curie point. On the molecular field model (Section II.1), expansion of the Brillouin function for small x in Equation 2.2 yields $\sigma_{o,T}^2 \propto (Tc - T)$. Thus Tc may be obtained by extrapolation of the linear portion of σ^2 versus T.

CHAPTER V RESULTS

V.1. Crystal Structures and Lattice Parameters

The series $DyFe_2$ - YFe_2 and YFe_2 - YCo_2 were found to be single-phase with the C15 structure. In both the series $DyFe_2$ - $Dy Ni_2$ and YFe_2 - YNi_2 the terminal phases were C15 but, in addition, the C36 phase was found for some intermediate compositions. The lattice parameters are given for these four series in Tables 5.1 to 5.4, respectively, and, for the first three, are plotted in Figures 5.1, to 5.3.

For the cubic C15 phases the lattice parameters are calculated using the Nelson-Riley extrapolation (Ref. 5.1) for the elimination of systematic errors. For the hexagonal phases the least squares method of Cohen was used with the extrapolation function employed previously.

Some of the compounds investigated were subjected to annealing after manufacture. The as-cast material was sealed into a silica tube under a vacuum of $\sim 10^{-4}$ Torr and heated for several days at about 700°C. Subsequent X-ray diffraction revealed no change in the lattice parameters measured or in the phase composition. In those compounds where the C15 and C36 phases were found there existed some diffraction lines which were not indexed as either

---

5.1 Nelson, J.B., and Riley, D.P., Proc. Phys. Soc. 57, 160(1945)

of these so that additional phases were present. These extra phases had much lower concentration than the Laves phases.

Composition x	Lattice Parameter (A) ± 0.002A	Atomic Volume ± 0.02 A^3
1.0 ($DyFe_2$)	7.318	16.33
0.80	7.333	16.43
0.65	7.339	16.47
0.50	7.343	16.50
0.40	7.345	16.51
0.35	7.348	16.53
0.30	7.348	16.53
0.15	7.353	16.56
0.08	7.352	16.56
0 (YFe_2)	7.354	16.57

Table 5.1 Lattice Parameters for (Dy, Y)Fe_2

Composition u	Lattice Parameter (A) ± 0.002 A	Atomic Volume ± 0.02 A^3
2.0 (YFe_2)	7.354	16.57
1.67	7.350	16.54
1.33	7.340	16.47
0.98	7.312	16.29
0.59	7.270	16.01
0.35	7.251	15.88
0.14	7.234	15.77
0 (YCo_2)	7.222	15.69

Table 5.2 Lattice Parameters for $Y(Fe,Co)_2$

Composition	Structure	a_o	c_o	c/a	At.Vol
2 ($DyFe_2$)	C15	7.318			16.33
1.6	C15	7.311			16.28
1.2	C15	7.291			16.15
	C36	5.028	16.51	3.28	15.05
0.8	C15	7.237			15.78
	C36	4.991	16.45	3.30	14.79
0.4	C15	7.200			15.55
	C 36	4.962	16.39	3.30	14.56
0 ($DyNi_2$)	C15	7.148			15.22

Table 5.3 Lattice Parameters for Dy $(Fe, Ni)_2$

Composition	Structure	a_o	c_o	c/a	At.Vol
$YFe_{1.4}Ni_{0.6}$	C36	5.088	16.61	3.26	15.52
	Other Phases Not Indexed				
$YFe_{1.0}Ni_{1.0}$	C36	5.024	16.48	3.28	15.01
	Other Phases Not Indexed				
$YFe_{0.7}Ni_{1.3}$	C36	4.999	16.45	3.29	14.83
	Other Phases Not indexed				
YNi_2*	C15	7.18			15.42

* values from Table 3.1

Table 5.4 Lattice Parameters for Y $(Fe,Ni)_2$

FIGURE 5.1

LATTICE PARAMETERS FOR

$Dy_{x}Y_{1-x}Fe_2$

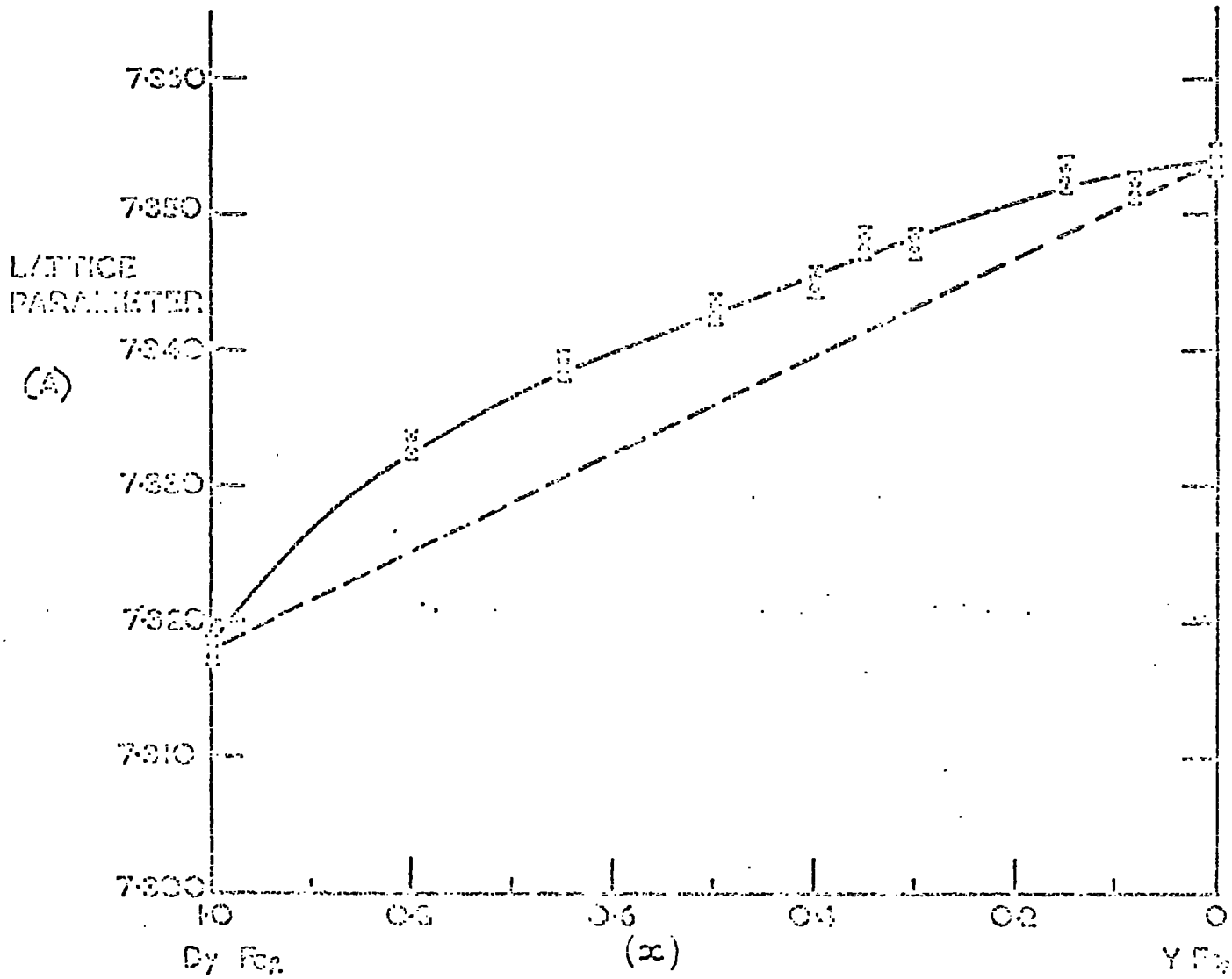

FIGURE 5.2

Lattice Parameters for $Y(Fe,Co)_2$.

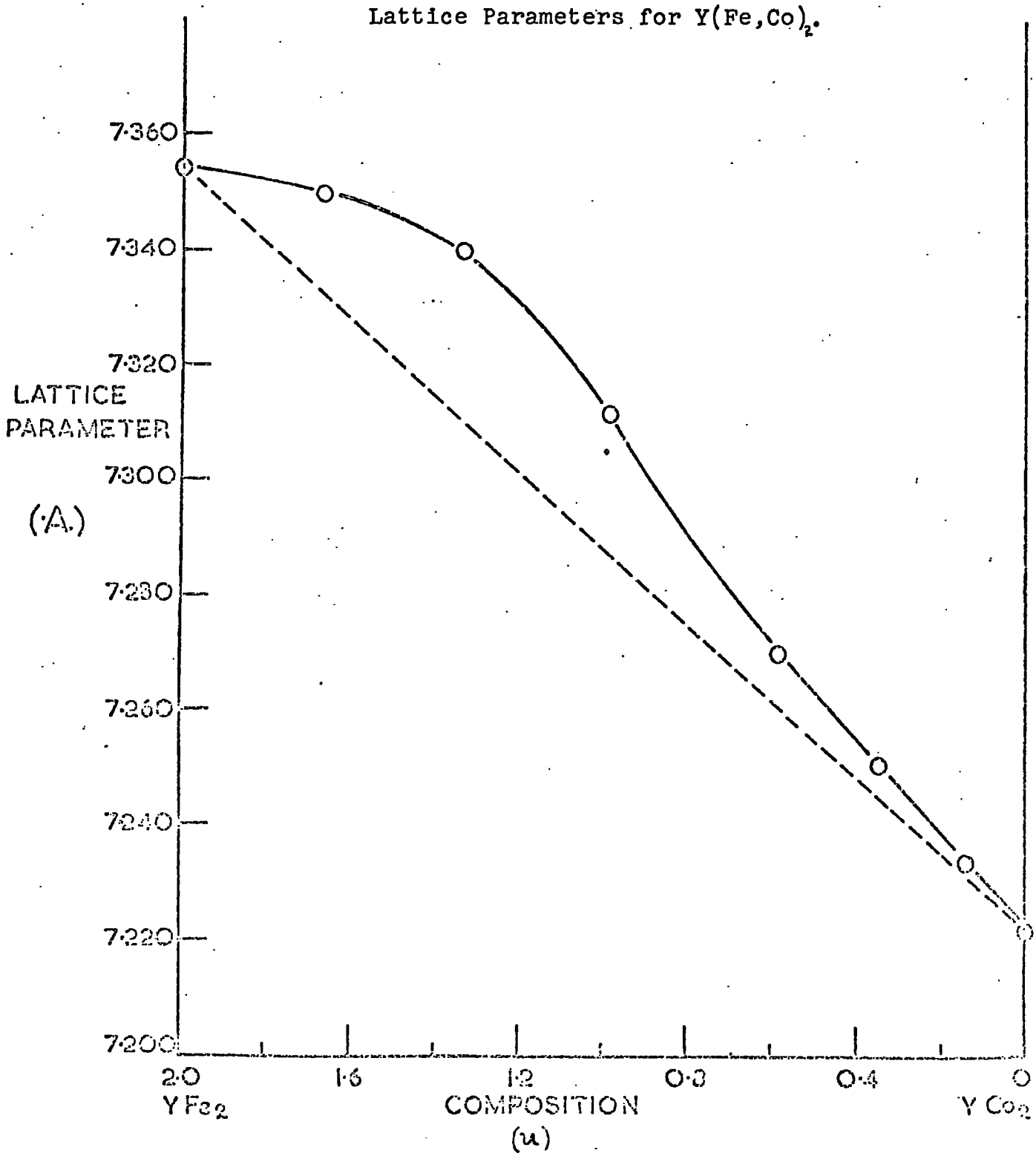

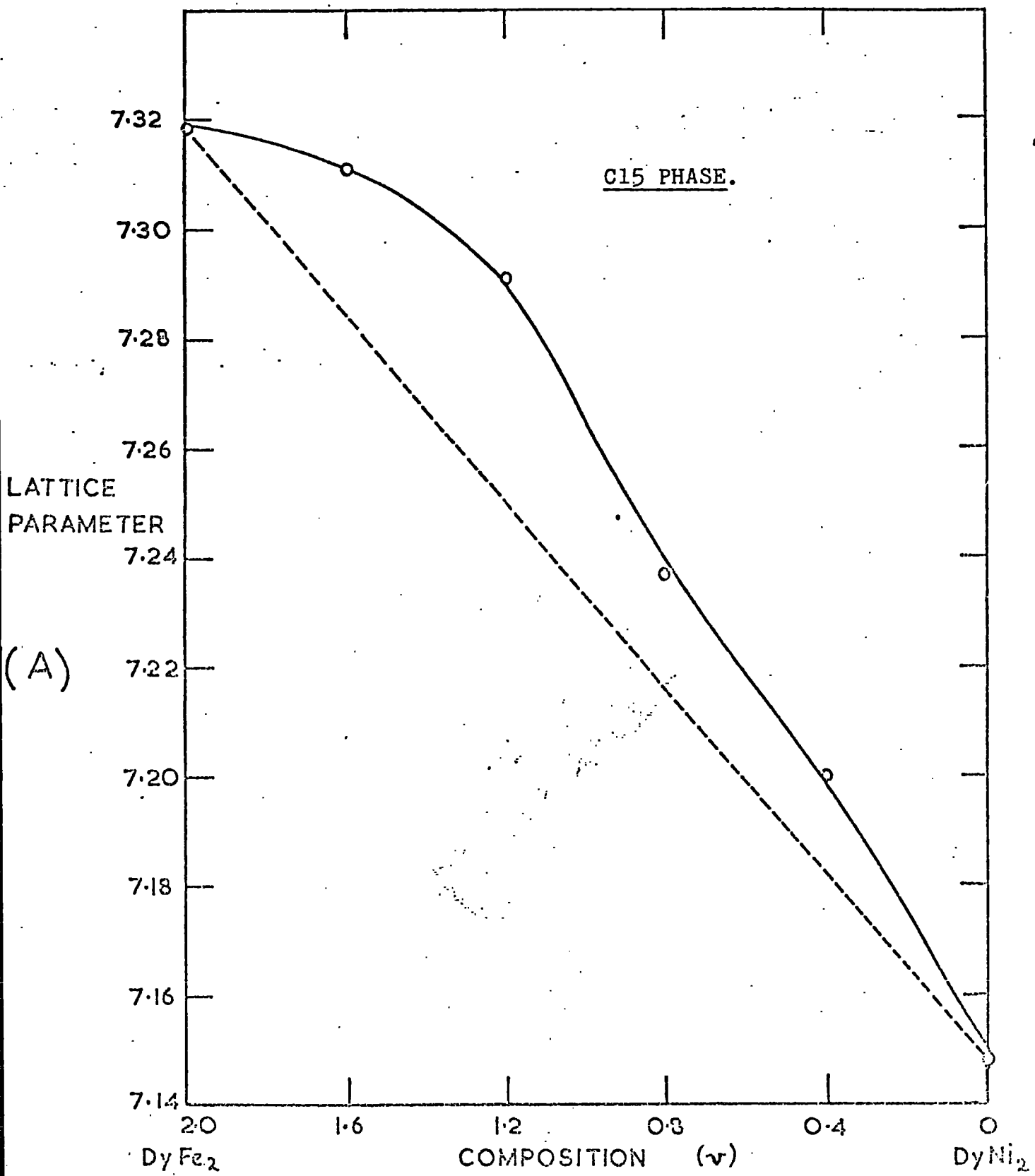

FIGURE 5.3 Lattice Parameters for $Dy(Fe,Ni)_2$.

V.2. Magnetic Properties

The magnetic properties reported here are the saturation moments (σ_s) at 4.2°, 77°K and room temperature (taken as 290°K), the ferromagnetic Curie temperature (T_c), and the magnetisation - temperature behaviour. The saturation moments were determined by extrapolation of σ_H versus $^1/H$, as indicated in Equation 4.2, to $^1/H = 0$. The Curie points were determined by extrapolation of σ^2 versus T to $\sigma^2 = 0$ (see Section IV.4.(d)). The σ/T behaviour is given in most cases by a single curve at a field sufficient for σ to approach the saturation value.

The σ_s and Tc values are collected into Table 5.5 and Figure 5.4 for $DyFe_2$ - YFe_2 and in Table 5.6 and Figures 5.6 and 5.7 for YFe_2 - YCo_2. These tables also contain values for the relative saturation at 4.2°K which is the ratio of the magnetisation at the highest field used to the saturation value. Table 5.7 contains some data on the remaining two series. These data are less extensive since measurements indicated the presence of multiple phases at some compositions.

The σ/T curves are presented in Figures 5.8 to 5.24.

In Table 5.5 the values for σ_s at 4.2°K for the compounds $x = 0.4$, 0.35 and 0.3 are given only approximately since saturation could not be approached. These values were obtained by magnetising

the specimens to the highest field at 77°K and reducing the temperature to 4.2°K, in this field. The resulting magnetisations were then scaled with the relative saturation ratios obtained at 77°K to yield the approximate values quoted.

Composition x	Saturation Moments μ_B/mol ± 3%			Curie Temperature	Rel. Sat.*	Coercive Field, 4.2°K
	4.2°K	70°K	290°K	°K ± 5	%	(KOe)
1.0 ($DyFe_2$)	5.26	5.20	3.36	633	94	0.7
0.80	3.91	3.67	2.21	618	92	1.7
0.65	2.73	2.42	1.28	5.93^{+15}_{-5}	85	3.1
0.50	1.44	1.21	1.07	590	68	5.5
0.40	~ 0.95[1]	0.93		586	-	8.5
0.35	~ 0.70[1]	0.65	0.63	579	-	>10
0.30	~ 0.45[1]	0.53	0.75	577	-	>10
0.24	0.64	0.83	1.18	568	89	4.0
0.15	1.50	1.50		564	92	2.4
0.08	1.86	1.86	2.07	559	96	0.9
0 (YFe_2)	2.80	2.80	2.53	554	96	0

1. See Text

TABLE 5.5 Magnetic Data for $(Dy,Y)Fe_2$

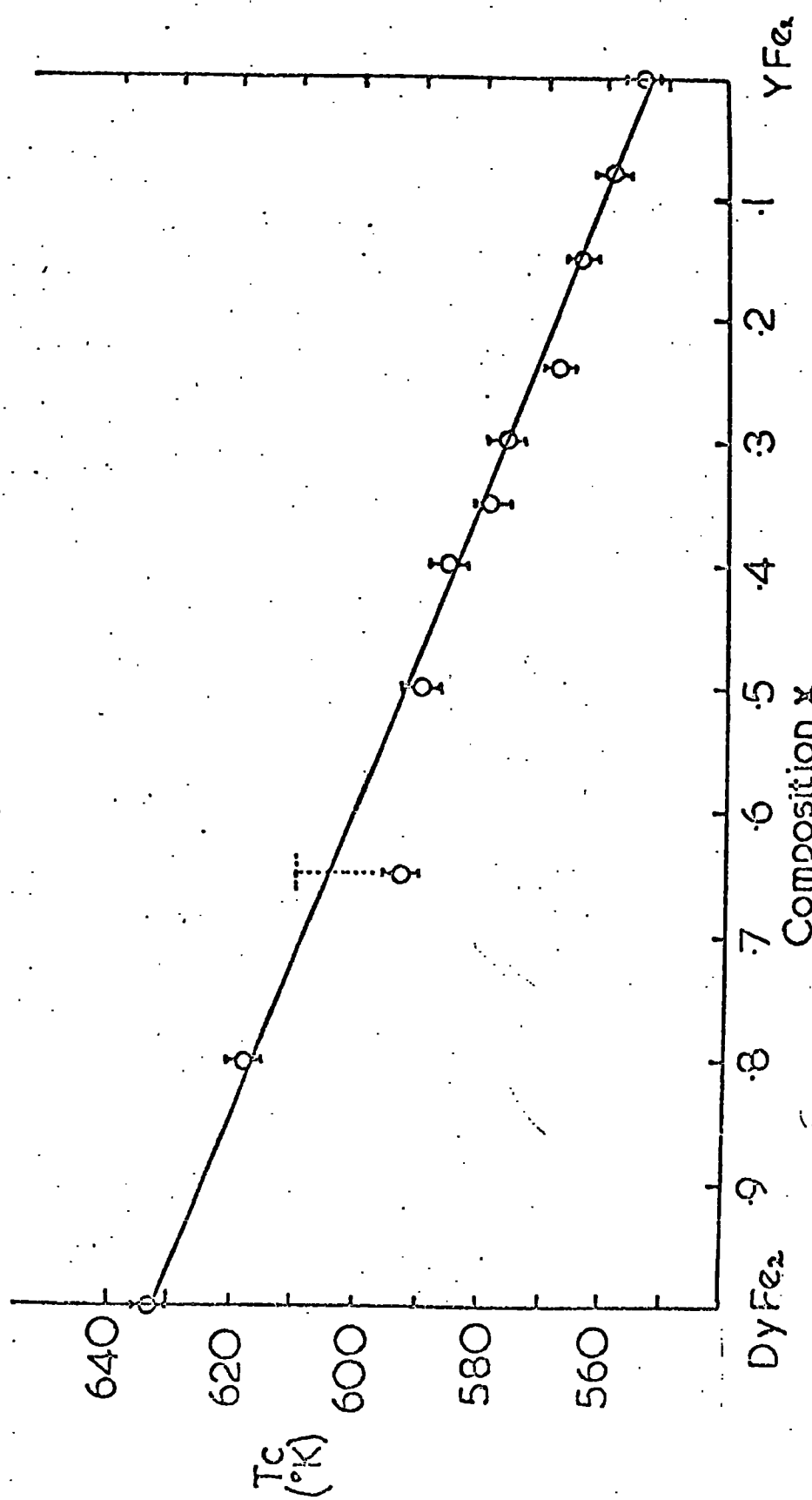

FIGURE 5.4 Curie Temperatures for $(Dy,Y)Fe_2$

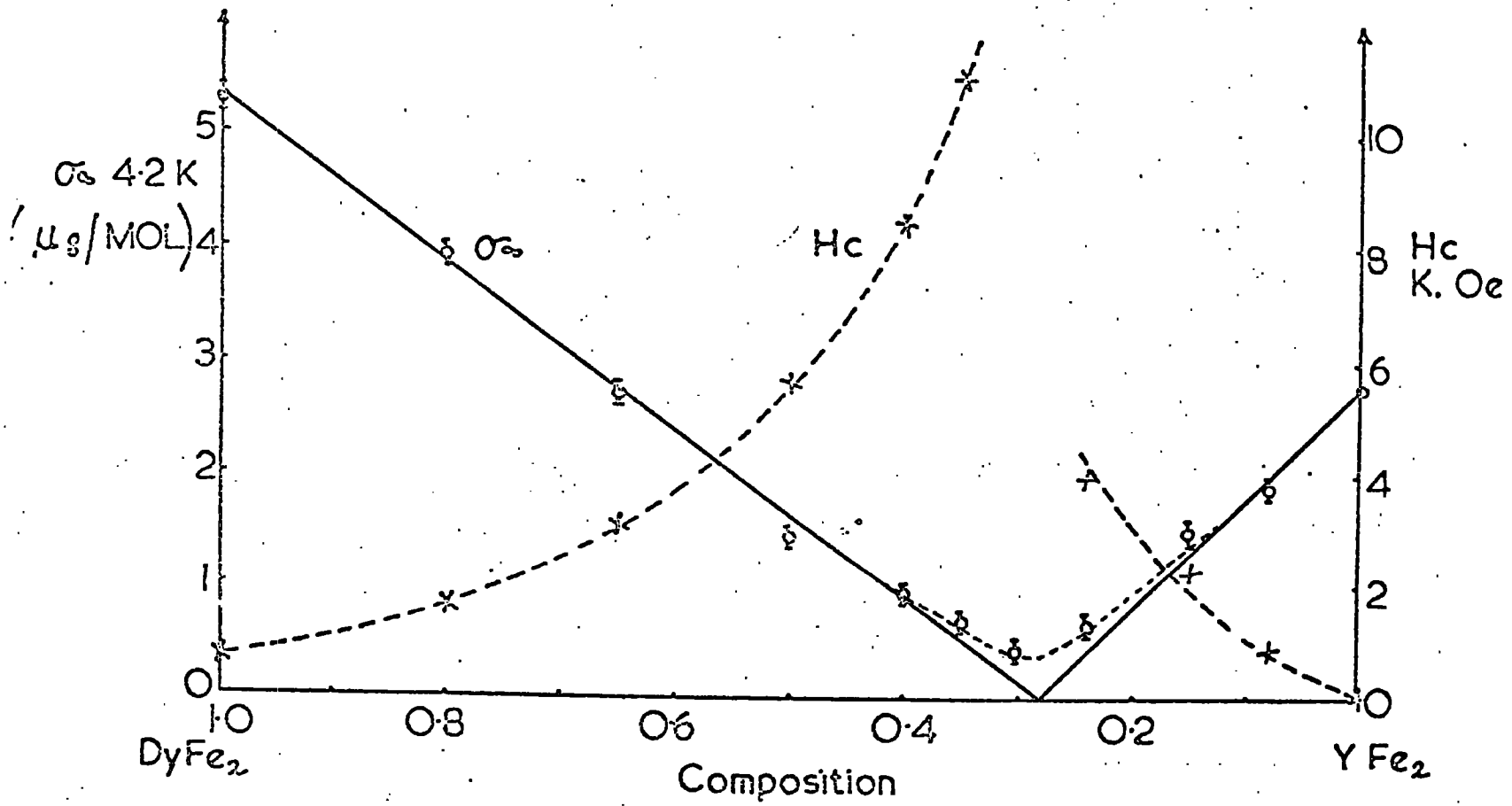

FIGURE 5.5 Saturation Moments for $(Dy,Y)Fe_2$.

Composition u	Saturation Moments μ_B/mol ± 3% 4.2°K	77°K	290°K	Curie Temperature	Relative Saturation*
2.0 (YFe_2)	2.80	2.80	2.53	554	97
167	3.13	3.11	2.80	600	99
1.33	3.14	3.12	2.74	700	98
0.98	3.13	3.01	2.53	682	99
0.59	2.58	2.55	2.24	633	76
0.35	1.86	1.76	1.12	571	89
0.14	0.56	0.55	0.52	458	92
0 (YCo_2)	0.09	0.10	-	307	92

* Ratio, at 4.2°K, of the magnetisation at 9.4 kOe to the saturation value

TABLE 5.6 Magnetic Data for $Y(Fe,Co)_2$

5.14

FIGURE 5.6

Curie Temperatures for $Y(Fe,Co)_2$.

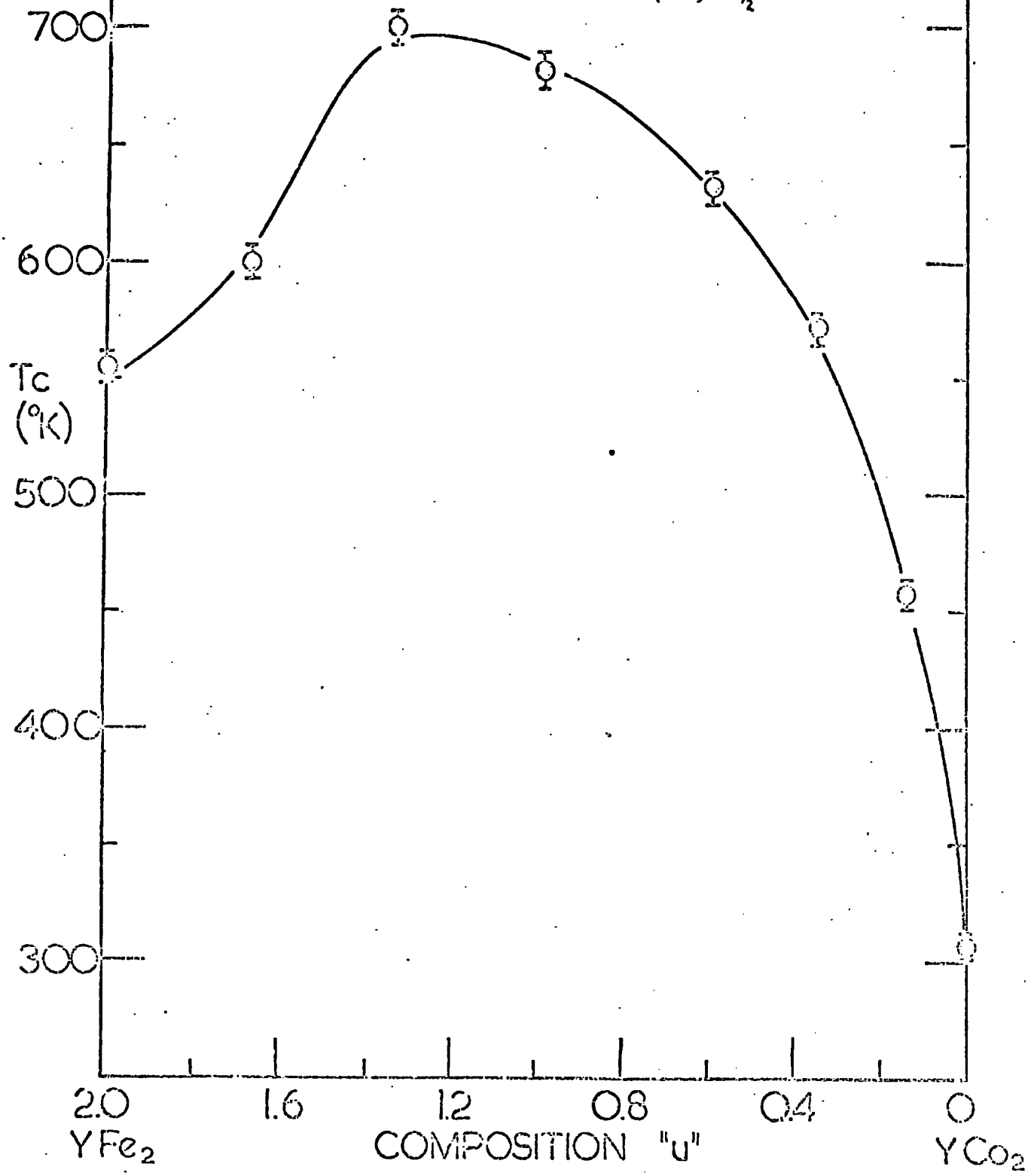

FIGURE 5.7.

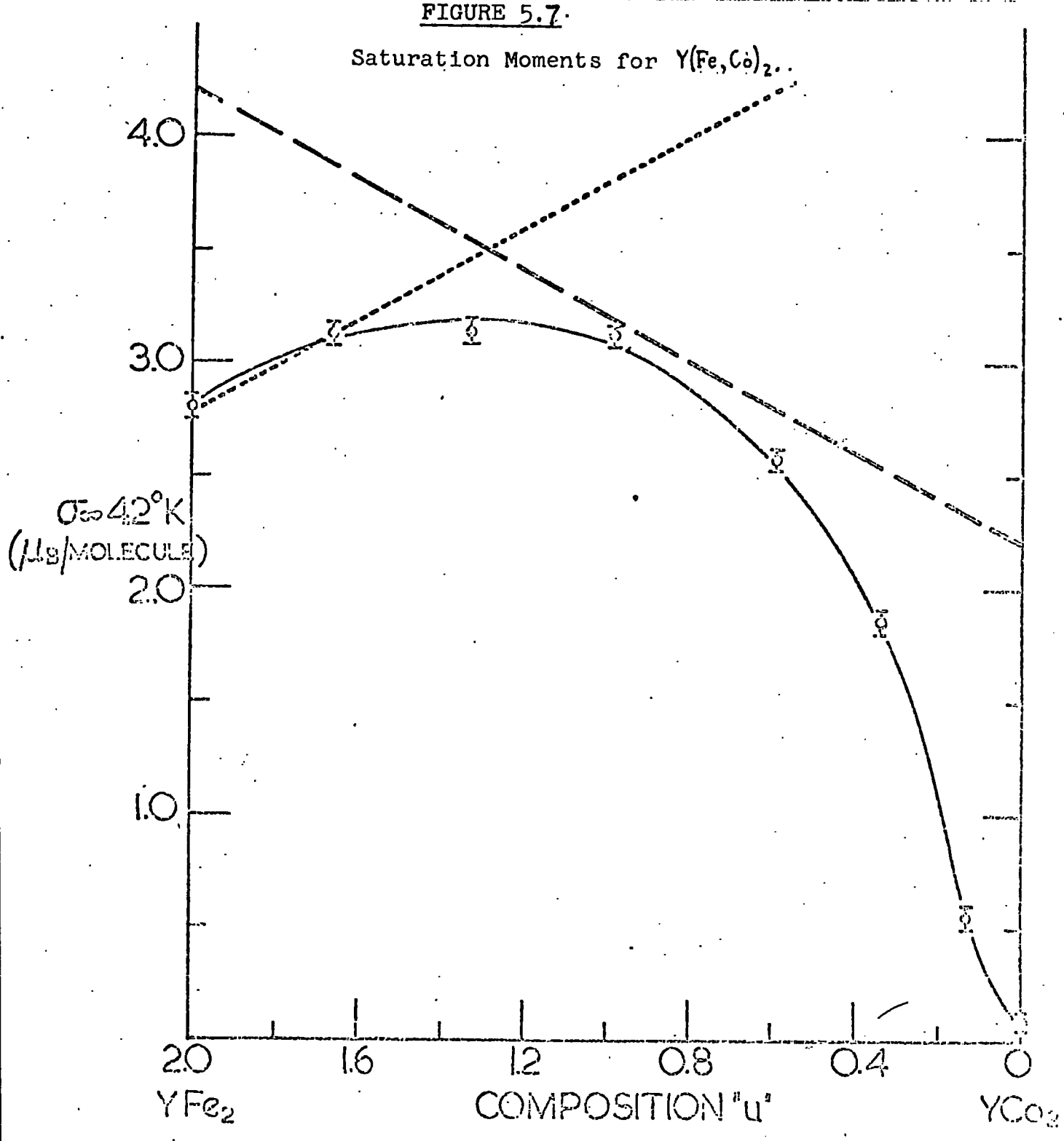
Saturation Moments for Y(Fe,Co)2..
4.0
3.0
2.0
1.0
σ≈4.2°K
(μB/MOLECULE)
2.0
1.6
1.2
0.8
0.4
0
YFe2
COMPOSITION "u"
YCo2

Composition	Saturation Moments μ_B/mol		Curie Temperature (°K) ± 10
	4.2°K	77°K	
$DyFe_{1.6}Ni_{0.4}$	5.2	-	620
$DyFe_{1.2}Ni_{0.8}$	6.0	-	610
$DyFe_{0.8}Ni_{1.2}$	6.0	-	365
$DyFe_{0.4}Ni_{1.6}$	6.9	-	270
$YFe_{1.4}Ni_{0.6}$	-	2.4	>300
$YFe_{1.0}Ni_{1.0}$	-	1.9	>300

Table 5.7 Magnetic Data for $Dy(Fe,Ni)_2$ and $Y(Fe,Ni)_2$

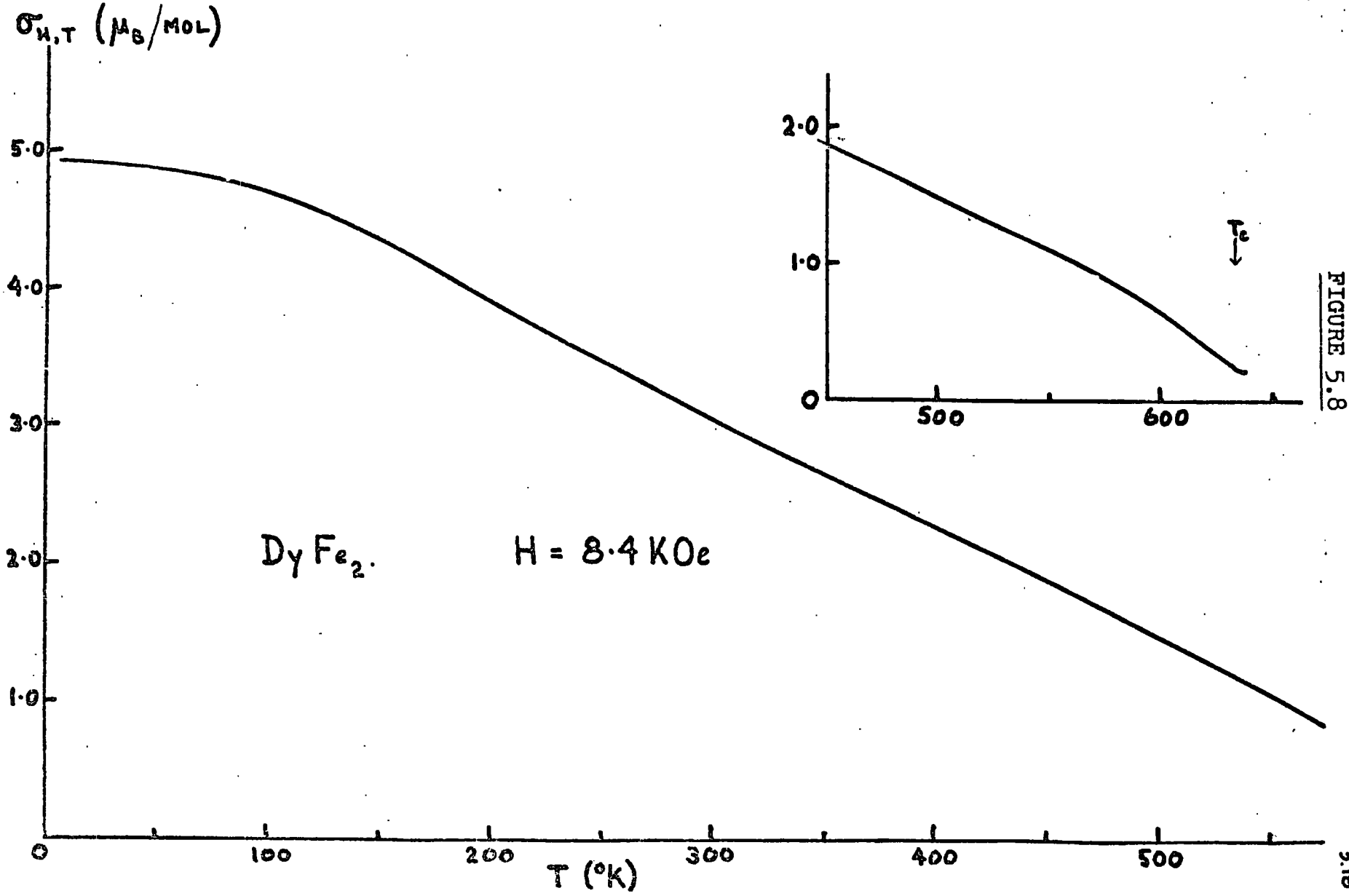
$\sigma_{H,T}$ (μ_B/MOL)
5·0
4·0
3·0
2·0
1·0
0
100
200
300
400
500
T (°K)
$DyFe_2$.
H = 8·4 KOe
2·0
1·0
0
500
600
T_c

FIGURE 5.8

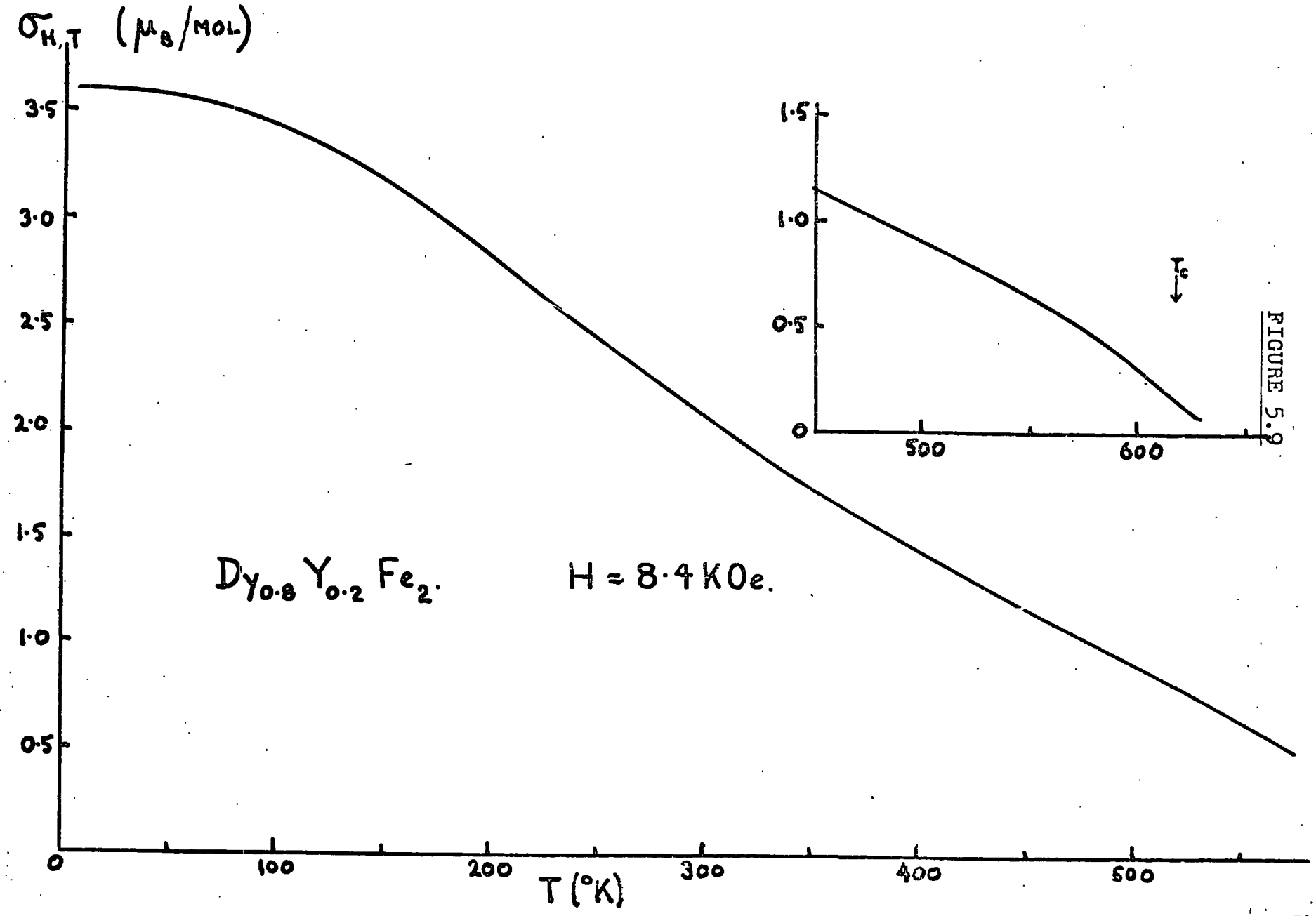
$\sigma_{H,T}$ (μ_B/MOL)
3·5
3·0
2·5
2·0
1·5
1·0
0·5
0
100
200
300
400
500
T (°K)
$Dy_{0.8}Y_{0.2}Fe_2$.
H = 8·4 KOe.
1·5
1·0
0·5
0
500
600
T_c

FIGURE 5.9

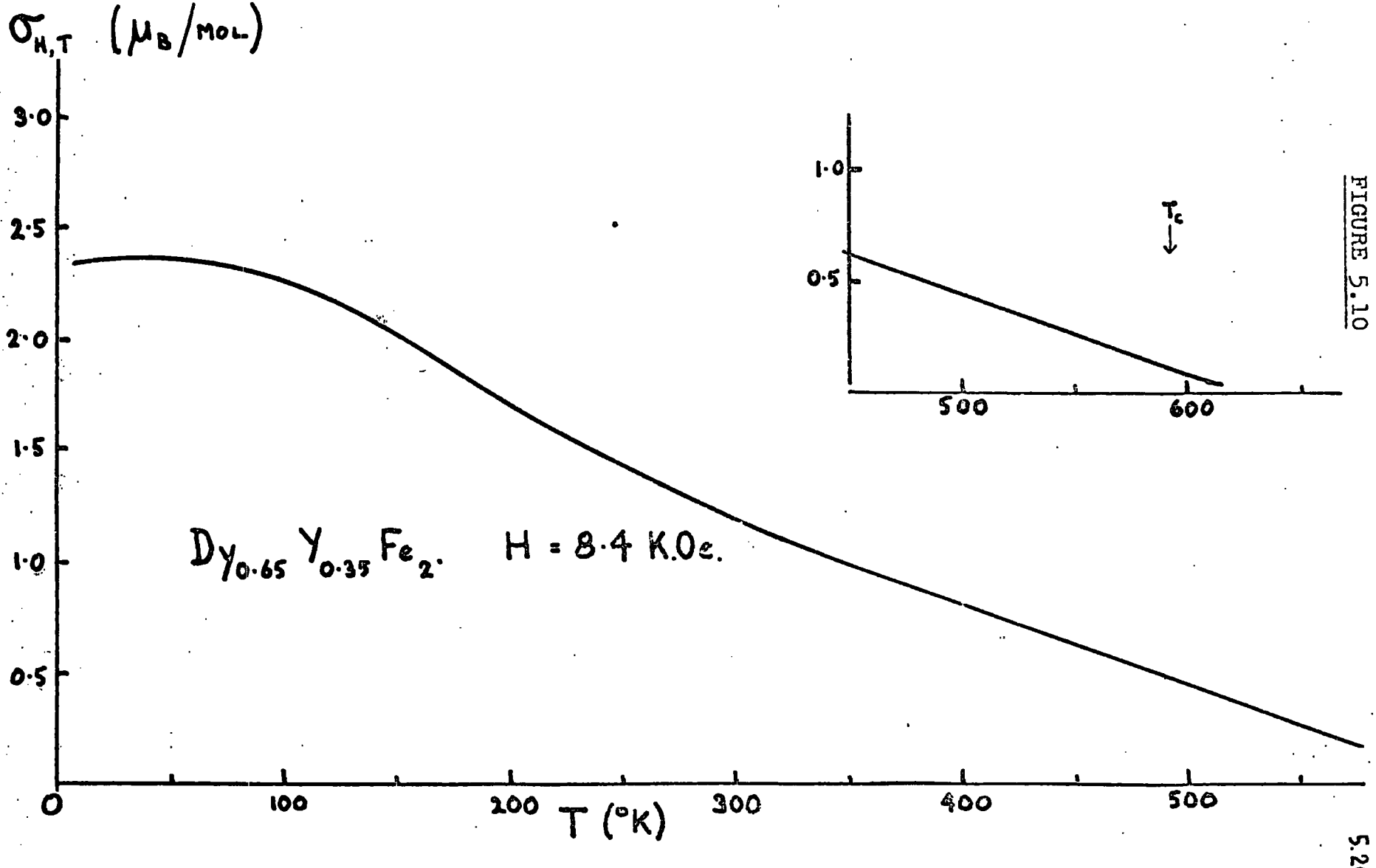
$\sigma_{H,T}$ (μ_B/MOL.)
3·0
2·5
2·0
1·5
1·0
0·5
0
100
200
300
400
500
T (°K)
$Dy_{0.65}Y_{0.35}Fe_2$. H = 8·4 K.Oe.
1·0
0·5
500
600
T_c

FIGURE 5.10

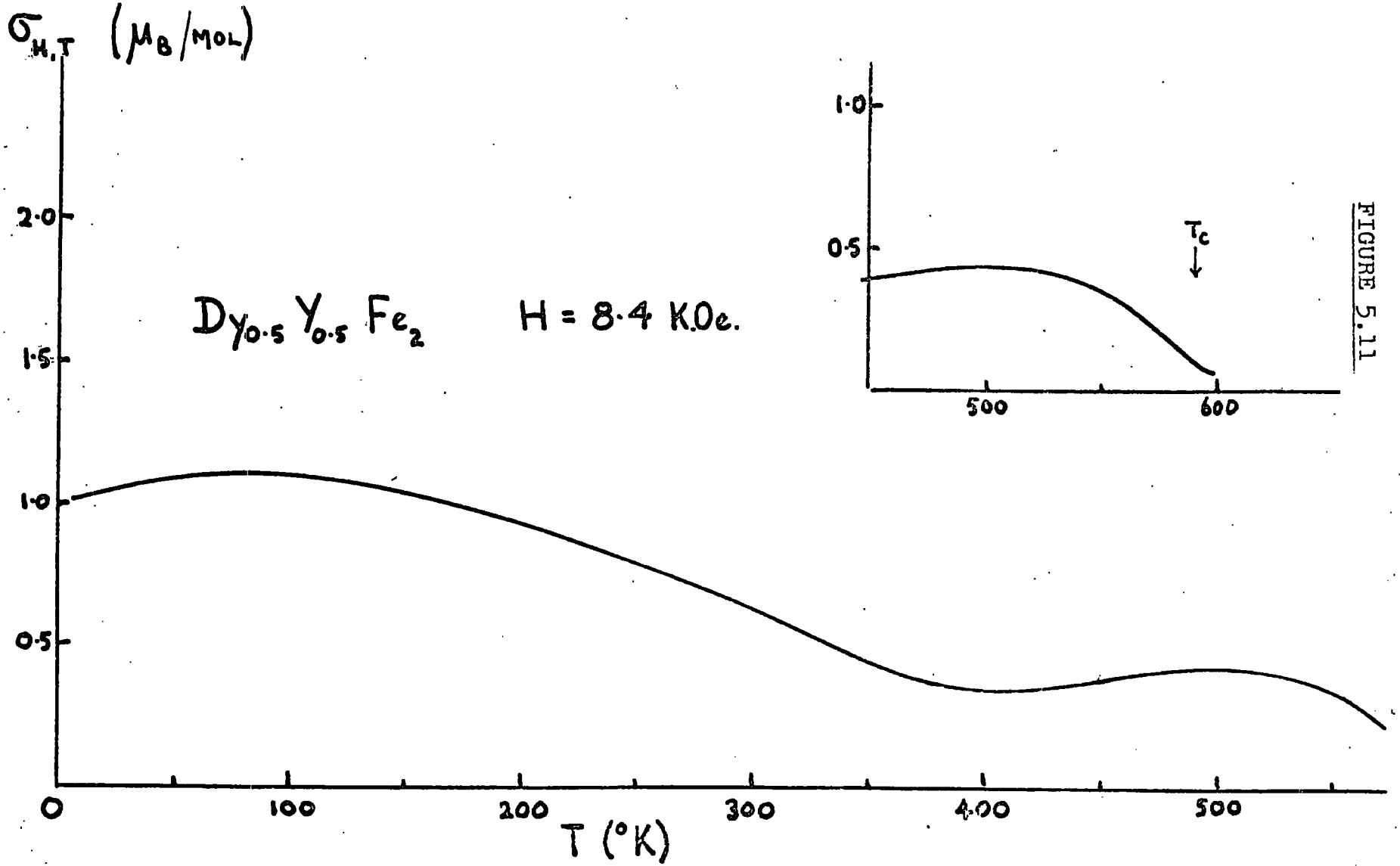
$\sigma_{H,T}$ (μ_B/MOL)
$Dy_{0.5}Y_{0.5}Fe_2$
H = 8·4 K.Oe.
2·0
1·5
1·0
0·5
0
100
200
300
400
500
T (°K)
1·0
0·5
T_c
500
600

FIGURE 5.11

FIGURE 5.12

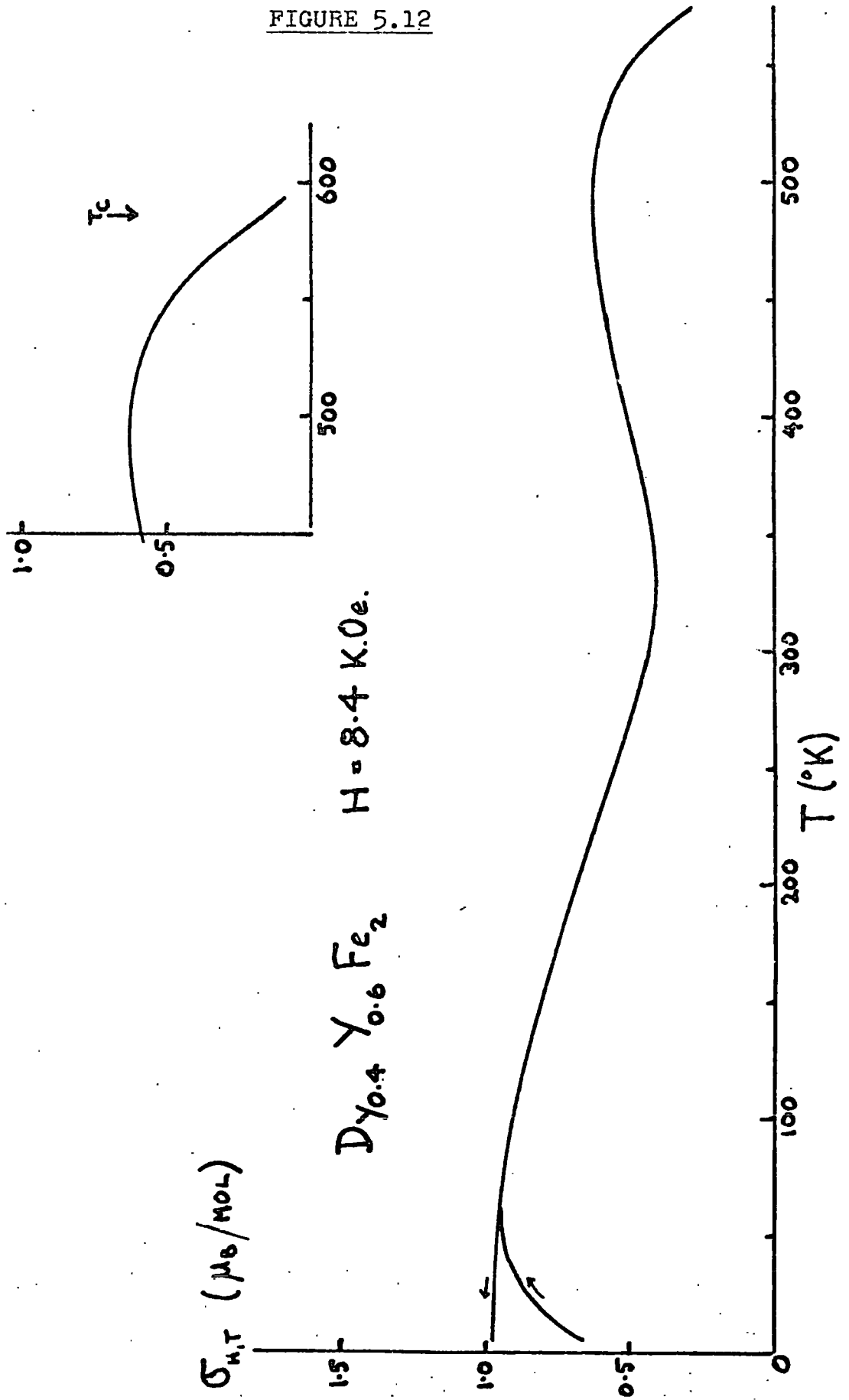
$\sigma_{H,T}$ (μ_B/MOL)
1·5
1·0
0·5
0
100
200
300
400
500
T (°K)
$D_{Y_{0.4}}Y_{0.6}Fe_2$
H = 8·4 K.Oe.
T_c
1·0
0·5
500
600

FIGURE 5.13

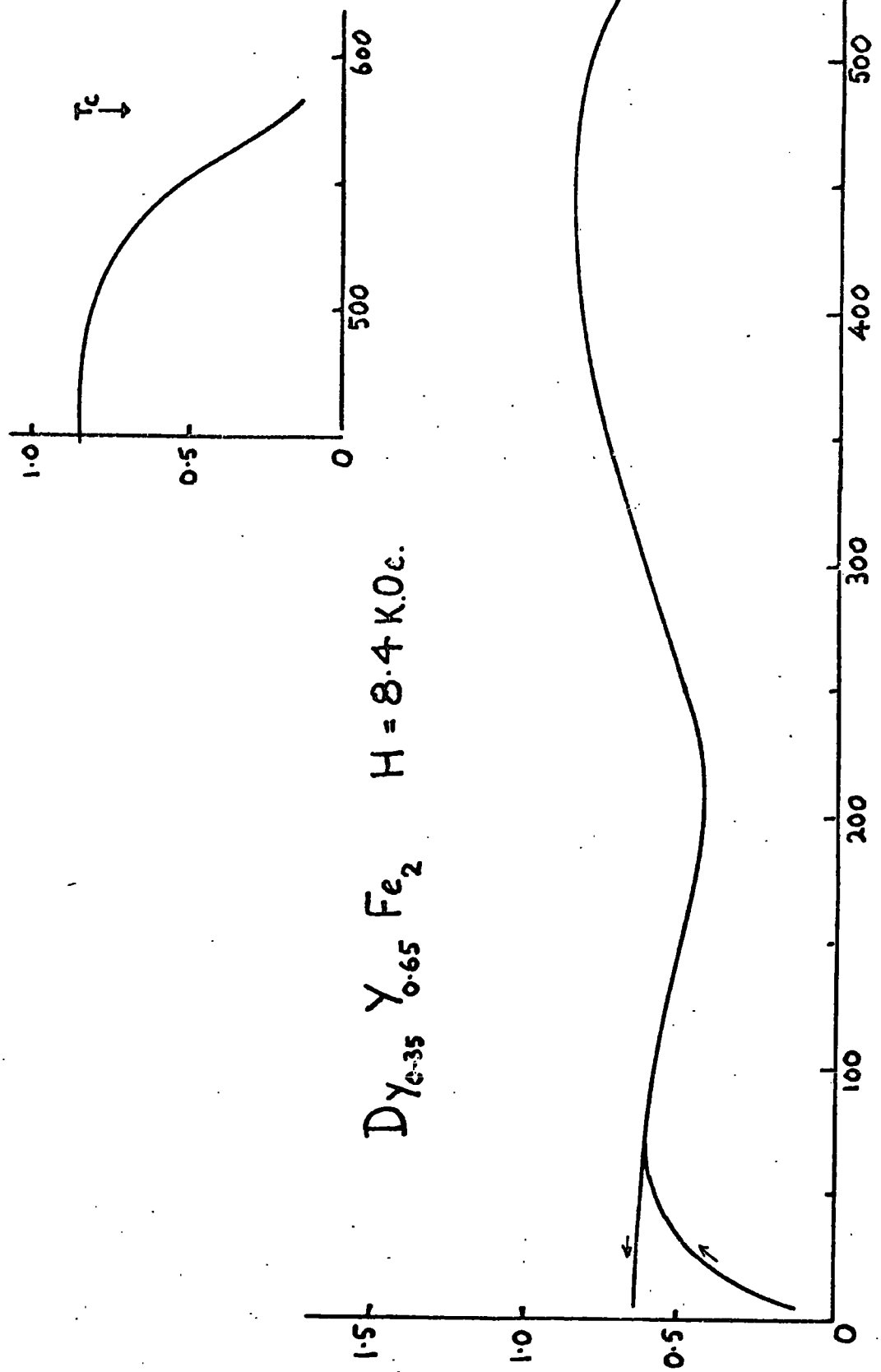
$D_{Y_{0.35}}\ Y_{0.65}\ Fe_2$
H = 8.4 K.Oe.
T_c
1.5
1.0
0.5
0
100
200
300
400
500
600
1.0
0.5
0
500

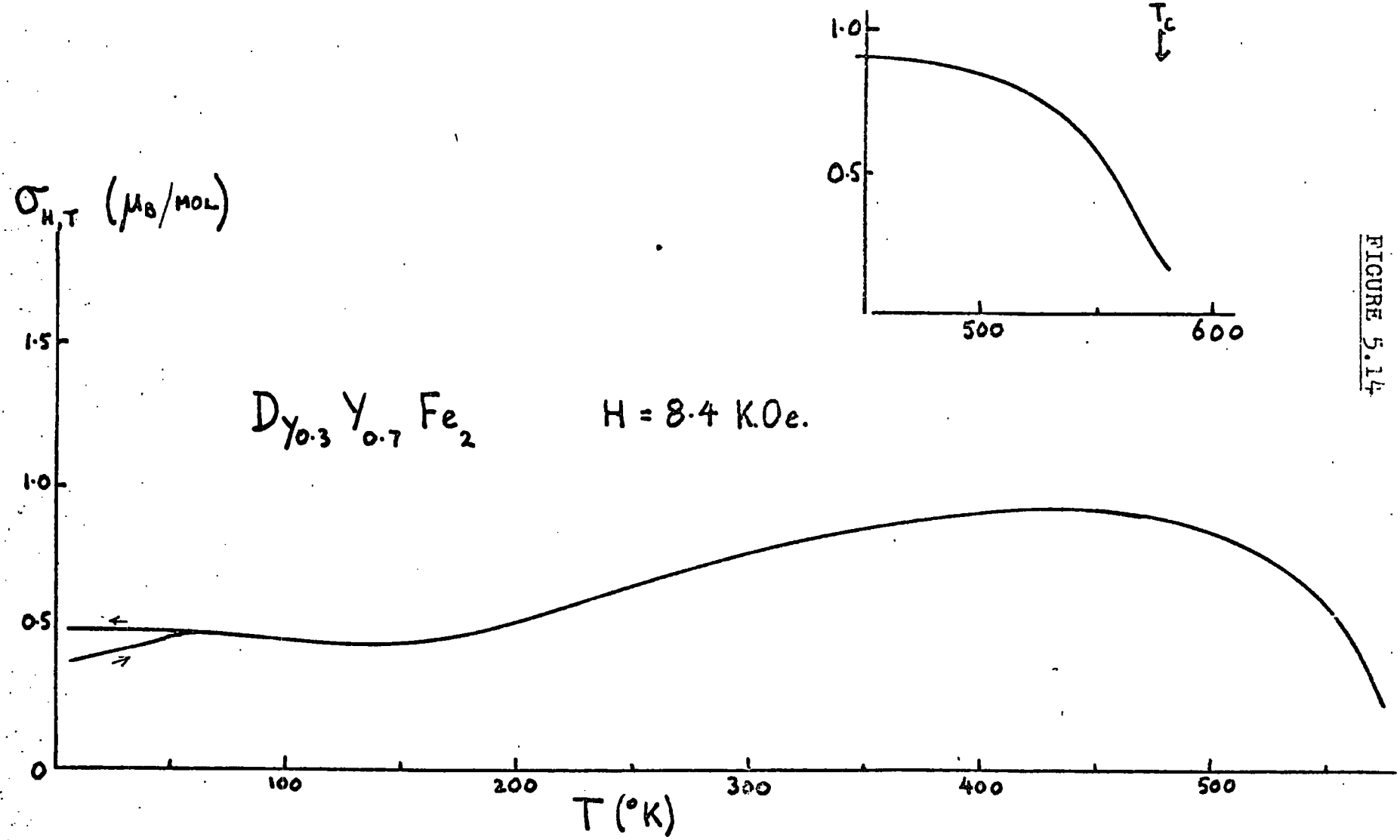
T_c
1.0
0.5
500
600
$\sigma_{H,T}$ (μ_B/MOL)
1.5
1.0
0.5
0
$D_{Y_{0.3}} Y_{0.7} Fe_2$
H = 8.4 K.Oe.
100
200
300
400
500
T (°K)

FIGURE 5.14

FIGURE 5.15

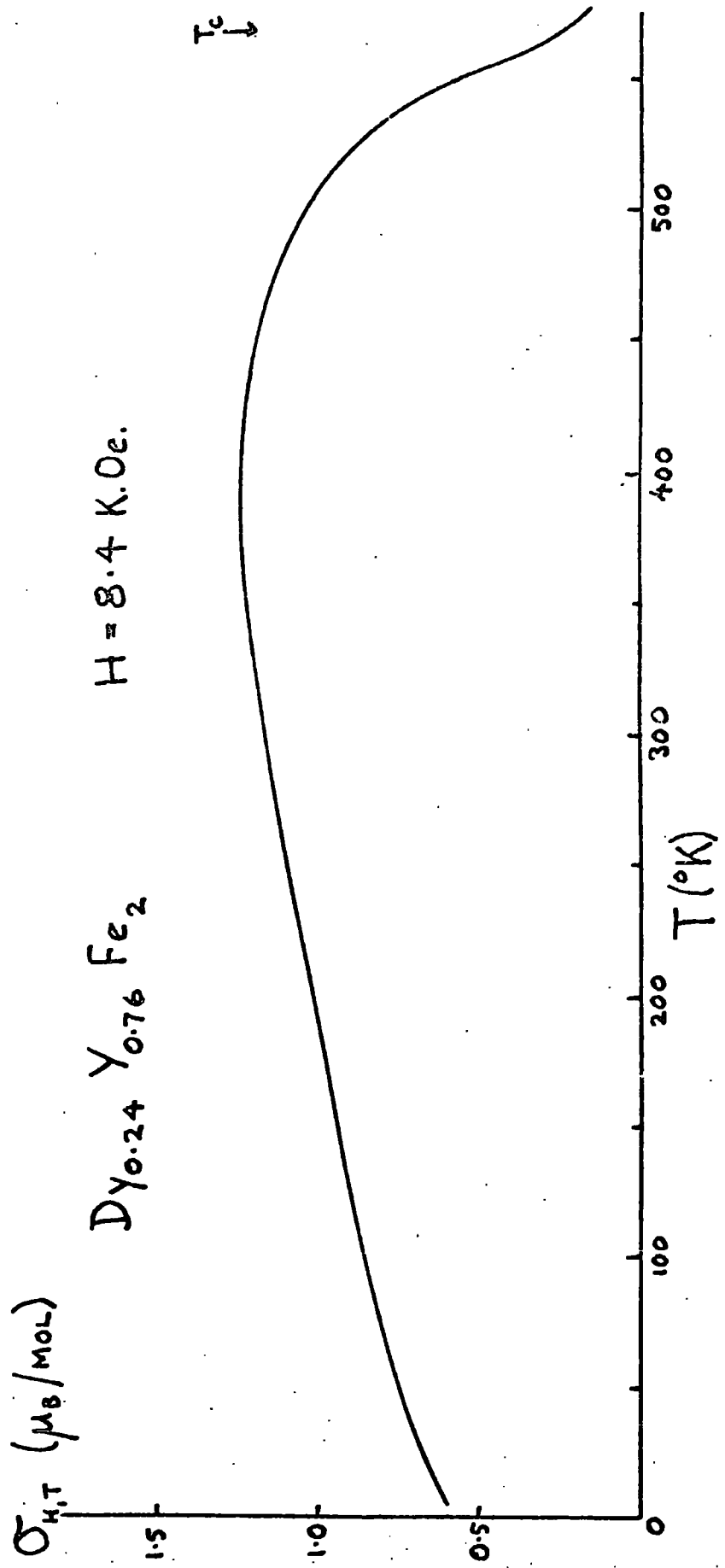
T_c
$\sigma_{H,T}$ (μ_B/MOL)
$Dy_{0.24}Y_{0.76}Fe_2$
H = 8·4 K.Oe.
T (°K)
0
100
200
300
400
500
0·5
1·0
1·5

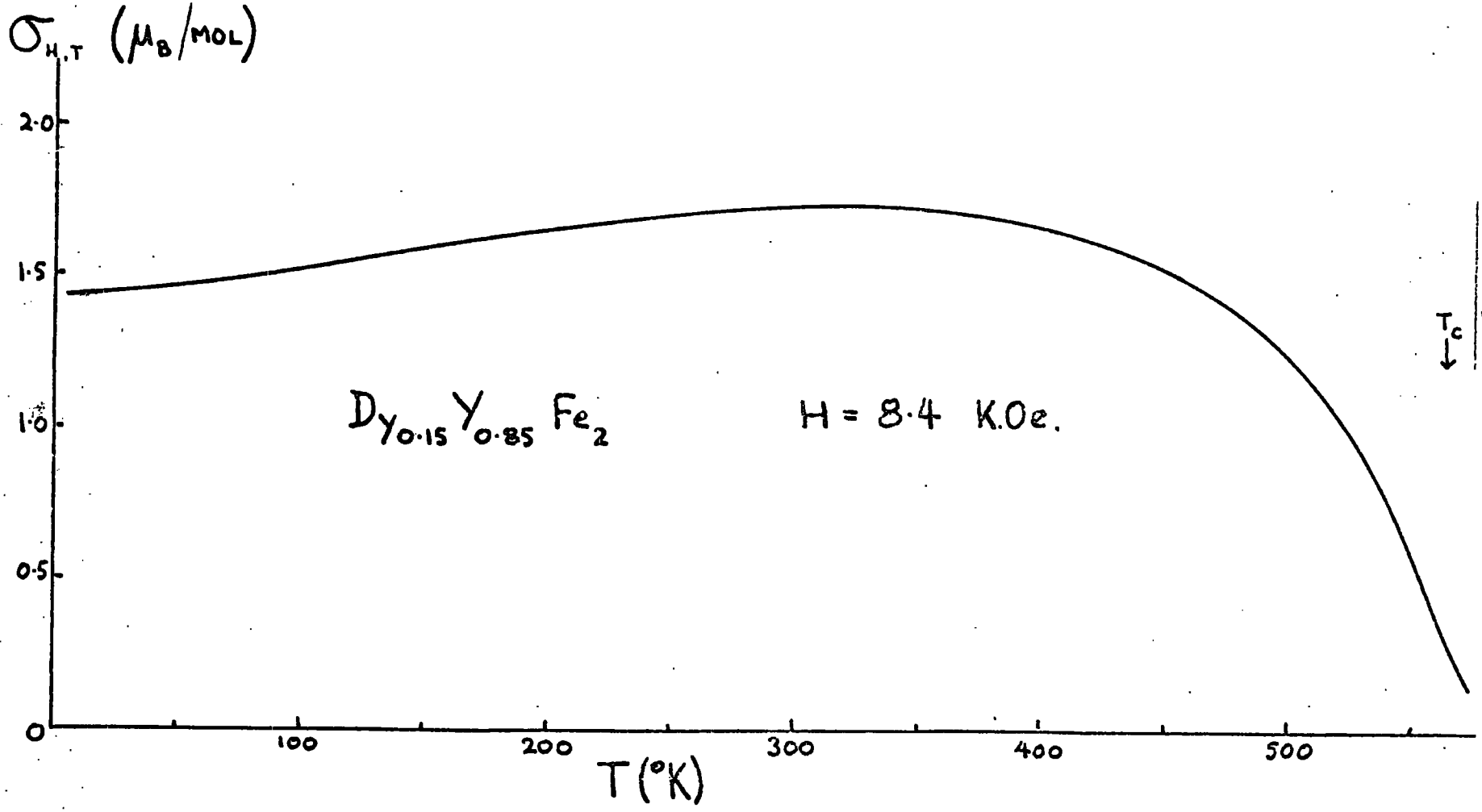
$\sigma_{H,T}$ (μ_B/MOL)
2·0
1·5
1·0
0·5
0
100
200
300
400
500
T(°K)
$Dy_{0.15}Y_{0.85}Fe_2$
H = 8·4 K.Oe.
T°K

FIGURE 5.16

FIGURE 5.17

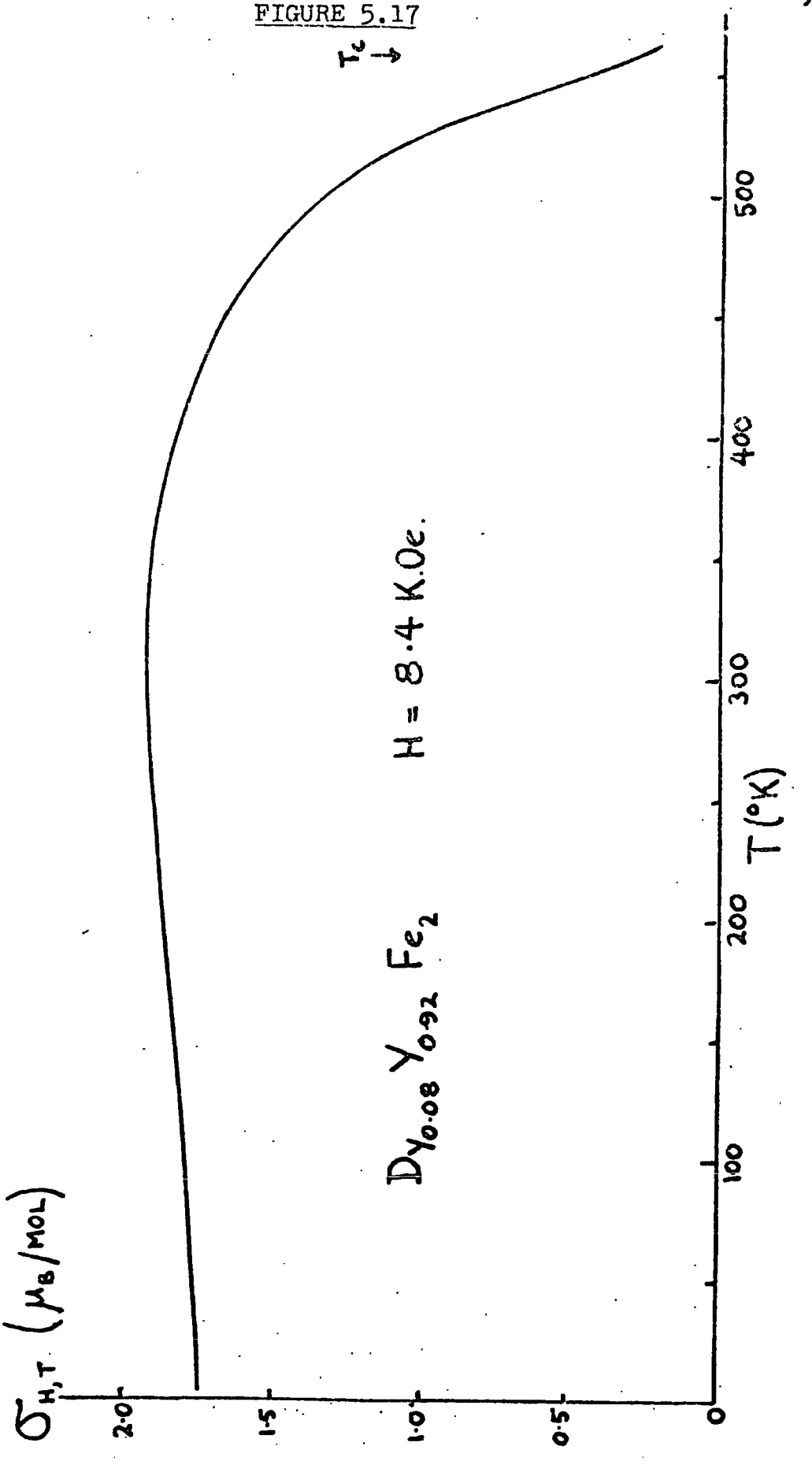
T_c →
$\sigma_{H,T}$ (μ_B/MOL)
2·0
1·5
1·0
0·5
0
100
200
300
400
500
T (°K)
$Dy_{0.08}Y_{0.92}Fe_2$
H = 8·4 K.Oe.

FIGURE 5.18

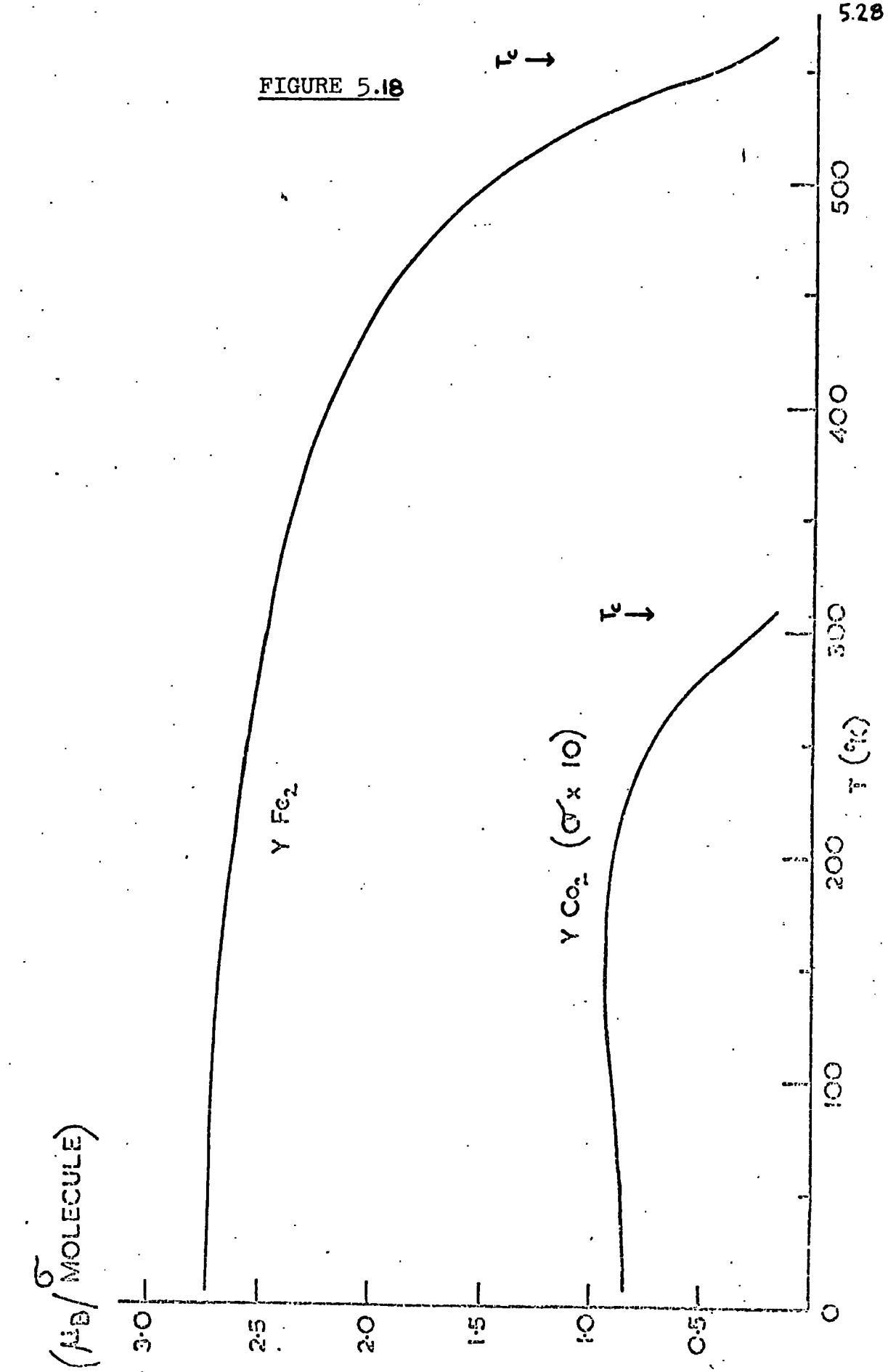
$T_c \rightarrow$
$T_c \rightarrow$
Y Fe_2
Y Co_2 (σ x 10)
$(\mu_B/\sigma$ MOLECULE)
3·0
2·5
2·0
1·5
1·0
0·5
0
100
200
300
400
500
T (°K)

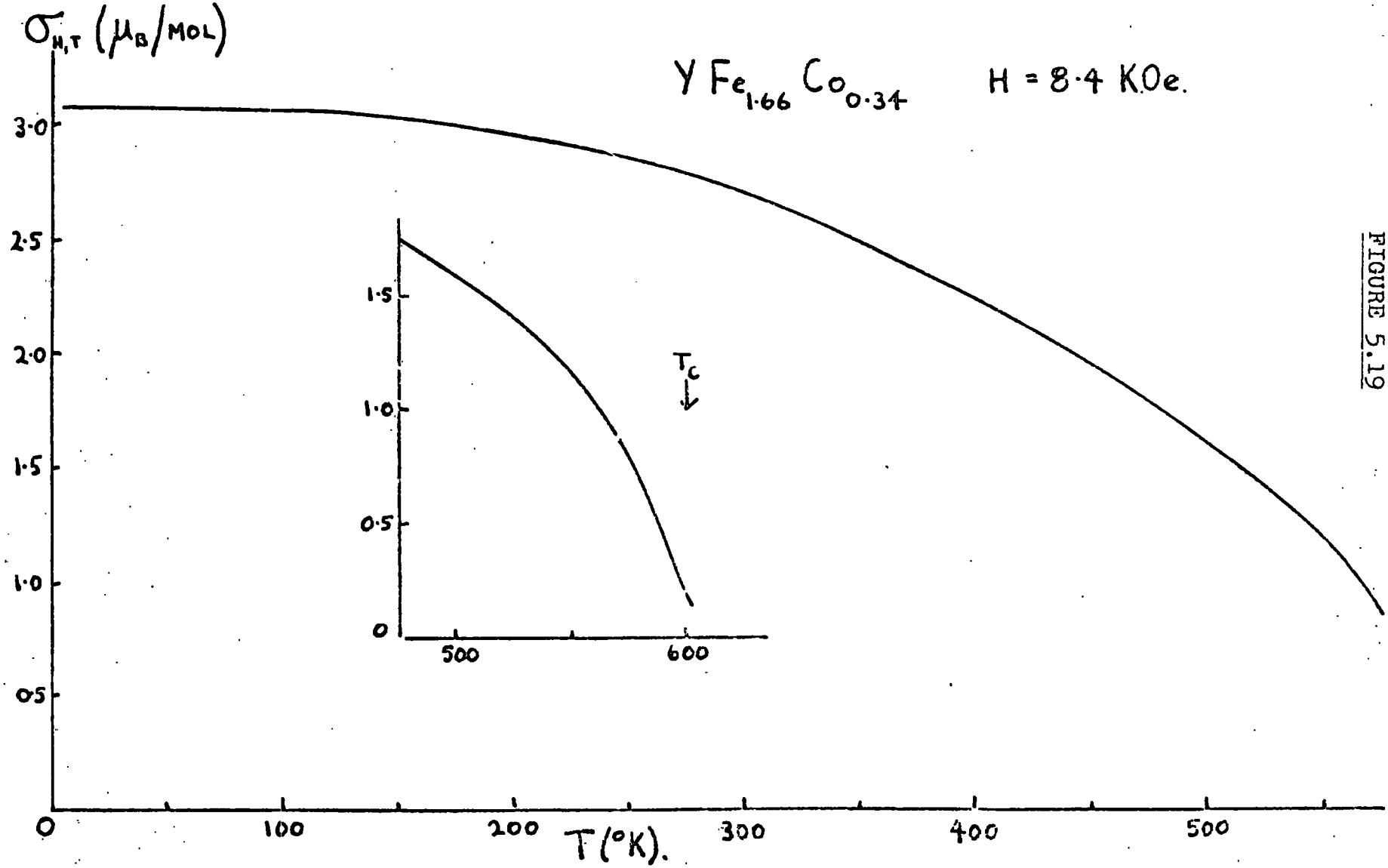
$\sigma_{H,T}$ (μ_B/MOL)
$Y Fe_{1.66} Co_{0.34}$ H = 8·4 KOe.
3·0
2·5
2·0
1·5
1·0
05
0
100
200
300
400
500
T(°K).
1·5
1·0
0·5
0
500
600
T_c

FIGURE 5.19

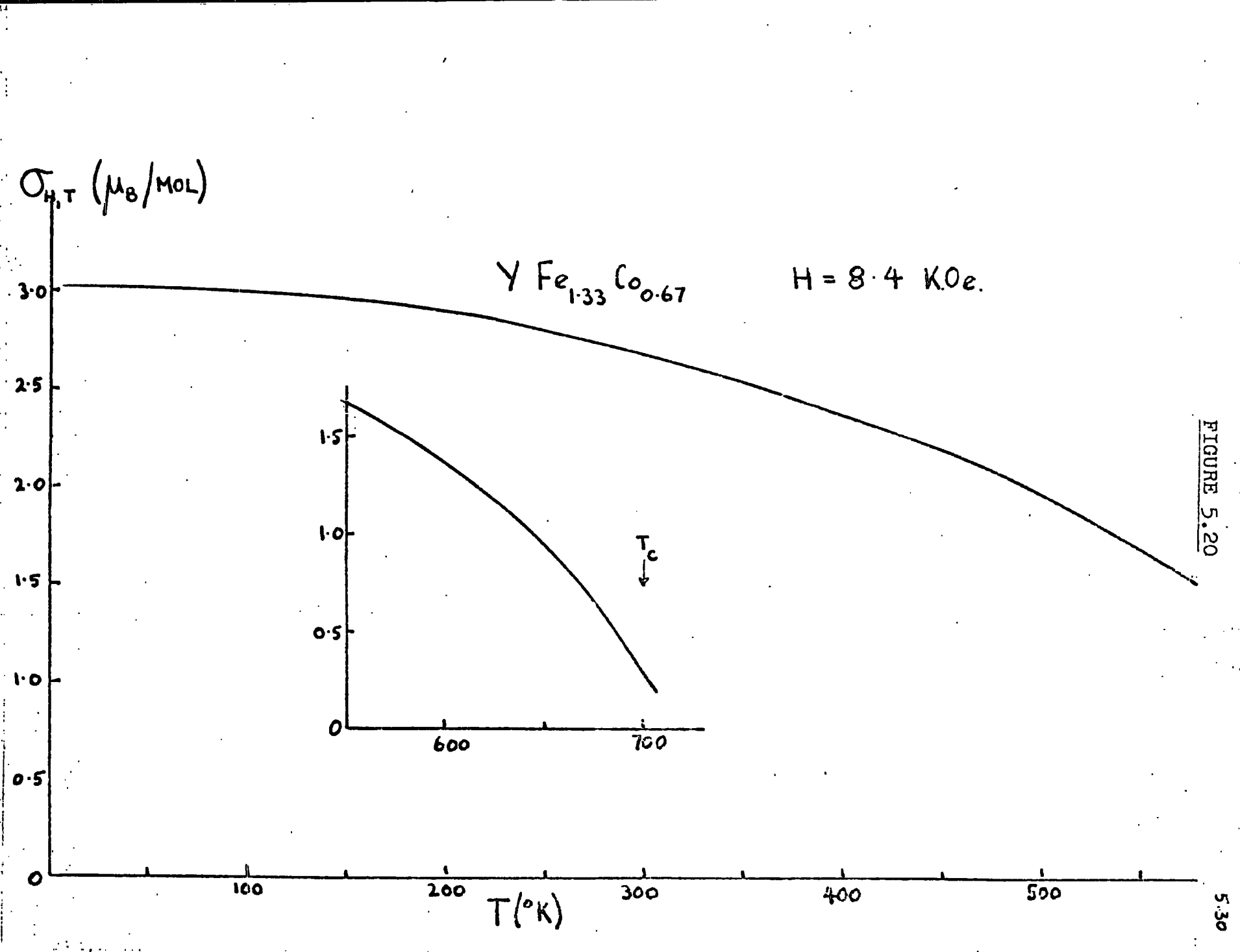
$\sigma_{H,T}$ (μ_B/MOL)
Y $Fe_{1.33}$ $Co_{0.67}$
H = 8·4 K.Oe.
3·0
2·5
2·0
1·5
1·0
0·5
0
100
200
300
400
500
T(°K)
1·5
1·0
0·5
0
600
700
T_c

FIGURE 5.20

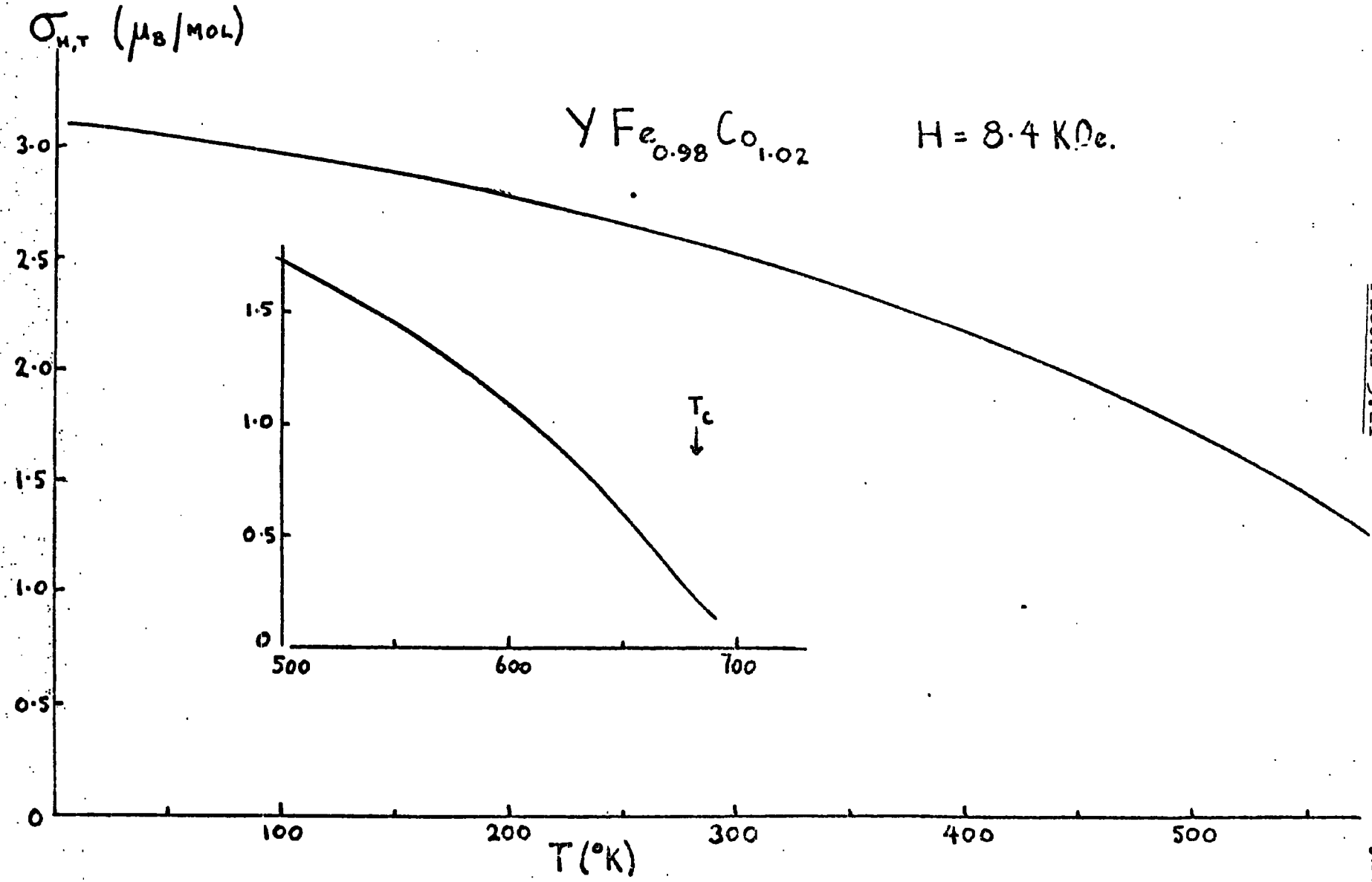
$\sigma_{H,T}$ (μ_B/MOL)
$Y Fe_{0.98} Co_{1.02}$
H = 8·4 KOe.
3·0
2·5
2·0
1·5
1·0
0·5
0
100
200
300
400
500
T (°K)
1·5
1·0
0·5
0
500
600
700
T_c

FIGURE 5.21

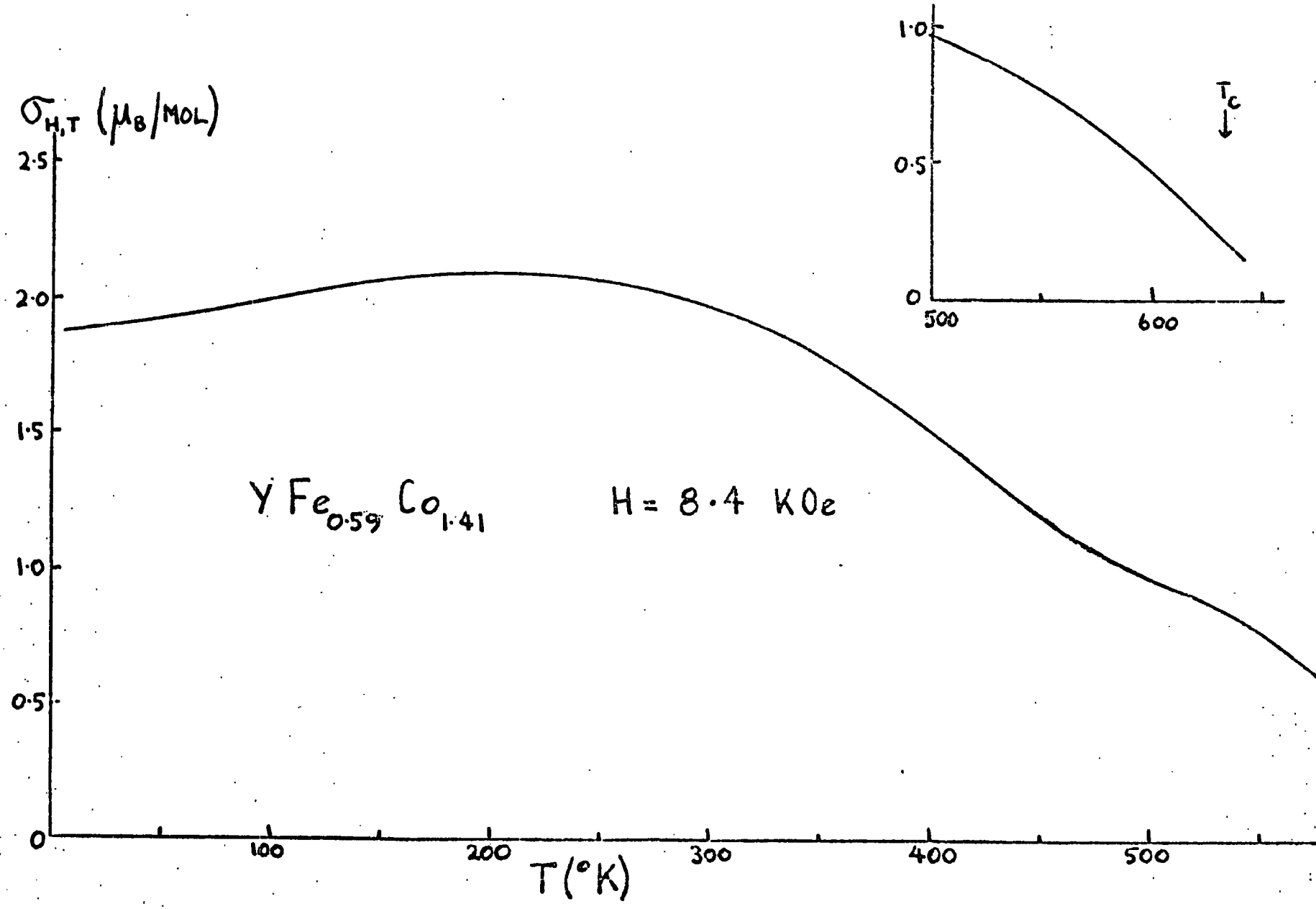
$\sigma_{H,T}$ (μ_B/MOL)
2·5
2·0
1·5
1·0
0·5
0
100
200
300
400
500
T(°K)
Y $Fe_{0.59}$ $Co_{1.41}$
H = 8·4 KOe
1·0
0·5
0
500
600
T_c

FIGURE 5.22

FIGURE 5.23

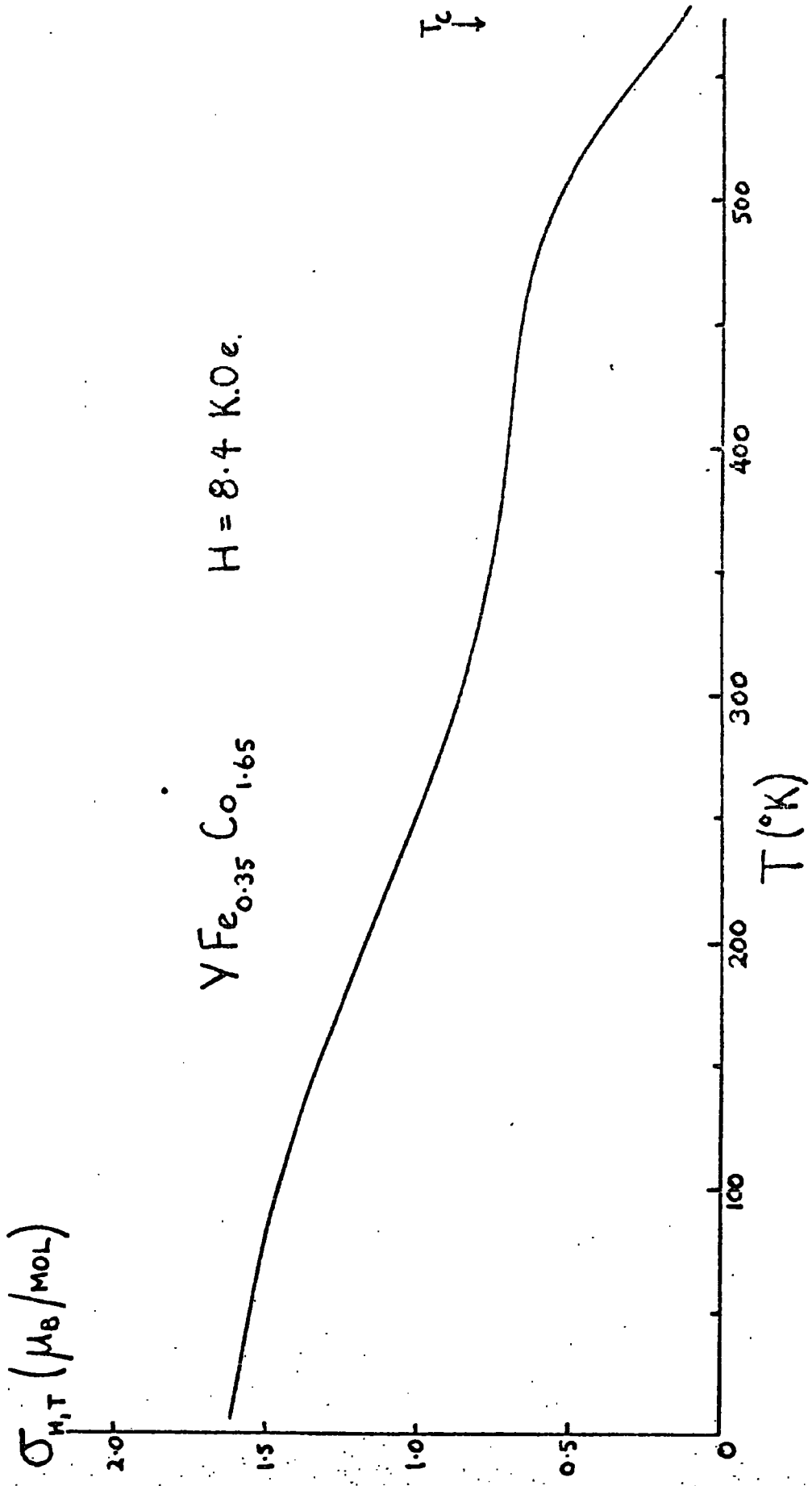
$\sigma_{H,T}$ (μ_B/MOL)
2·0
1·5
1·0
0·5
0
100
200
300
400
500
T (°K)
T_c →
$Y Fe_{0.35} Co_{1.65}$
H = 8·4 K.Oe.

FIGURE 5.24

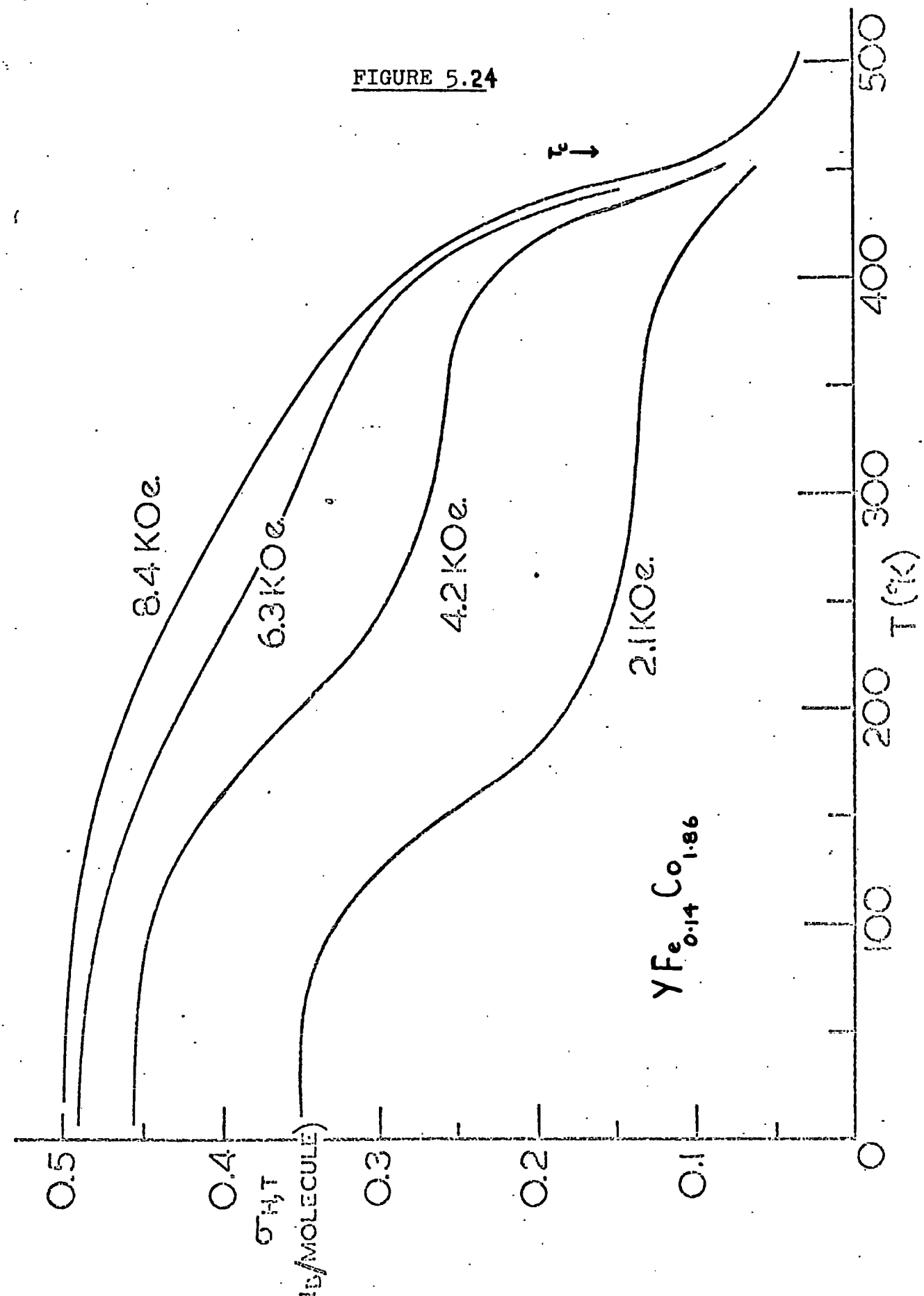
8.4 KOe.
6.3 KOe.
4.2 KOe.
2.1 KOe.
H
$YFe_{0.14}Co_{1.86}$
0.5
0.4
0.3
0.2
0.1
0
100
200
300
400
500
T (°K)
$\sigma_H T$
B/MOLECULE)

CHAPTER VI DISCUSSION

The results presented in Chapter V are considered in the following. The structures and lattice parameters are discussed first and then the magnetic properties under the different series. It is perhaps misleading to separate the series as a single model is presented for all the compounds, but the length of this discussion is so considerable that some sub-division is desirable.

VI.1 Structures and Lattice Parameters

The variations of the lattice parameter of the C15 phases show positive deviations from Vegards Law (linear interpolation between the terminal compounds), indicated by the dashed lines, in each case. This is in agreement with measurements on other series (Section III.3(d)) of this type.

Though metallic systems rarely follow this law accurately the extent of the fluctuations observed is surprising. This is particularly so for the series $(Dy,Y)Fe_2$ (Fig. 5.1) where the difference between the terminal values is only 0.5%. Small deviations may be accounted for on the basis of compressive energy but where the ion radii are apparently so close this effect must be very small. The deviation may result from variation of the electronic state of the Fe component. For the series where the 3-d metal component varies (Figures 5.2 and 5.3) the deviations from Vegards Law are much greater.

Comparing these series, however, it may be seen that the variation is very similar for the two cases: the deviation is greatest at the Fe-rich end of the series and there is an inflection in the centre of the curve. It is possible that the curves as presented, representing the lattice parameters measured at room temperature, are misleading. It has been shown for similar compounds (Ref. 6.1) that there is a discontinuity in the thermal expansion coefficient at the Curie point, as is expected in general. Thus, since the Curie points are at variable temperatures above or below the measuring temperature, the shape of the curves must change with temperature. It is possible that the deviation from Vegard's Law is less at a temperature above the highest Curie point in the series. The magnitude of the discontinuity demonstrated in Ref. 6.1 is, however, such as to cause only a relatively small change in the shape of these curves.

The striking similarity of the variation in the two series is shown in Figure 6.1 where the reduced lattice parameters (terminal values 0 and 1) are plotted together with those for the series $Er(Fe, Co)_2$ and $Er(Fe,Ni)_2$, (Ref. 6.2): Remarkably, a single curve can be satisfactorily drawn for all the points. It should be

---

6.1 R.C. Mansey, G.V. Raynor, and I.R. Harris, J. Less-Comm. Met. 14, 337 (1968)

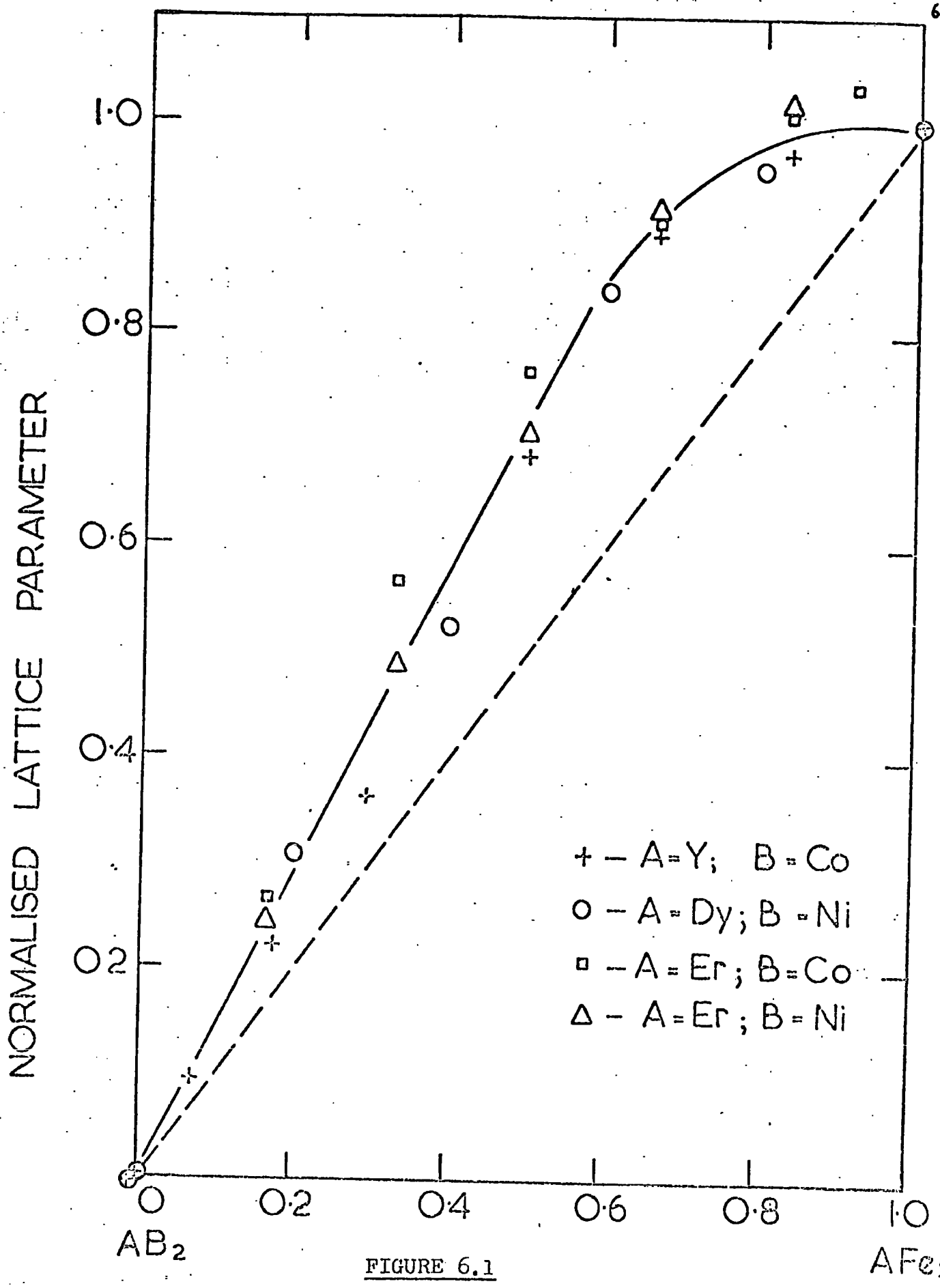
NORMALISED LATTICE PARAMETER
1·0
0·8
0·6
0·4
0·2
0
0·2
0·4
0·6
0·8
1·0
AB2
AFe2
+ – A=Y; B=Co
o – A=Dy; B=Ni
□ – A=Er; B=Co
Δ – A=Er; B=Ni

FIGURE 6.1

noted that Fe is a constituent of all the compounds shown in Figure 6.1 and it is found that other series (e.g. Er $(Co, Ni)_2$- Ref. 6.2) do not show the same variation though there is some evidence of a common behaviour here also. The lattice parameter is obviously related to the electronic structure and to the details of the coupling mechanism and the variations will be discussed further, briefly, in Section VI.5.(a) from this point of view.

The tendency towards the formation of other phases, in some of the series, does not appear to be related to the extent of the deviation of the lattice parameter from additivity though the atomic volume of the intermediate phase is, in every case, less than that for the C15 phase and indeed shows a large negative deviation from additivity (Fig. 6.2). It is further surprising that the intermediate phase formed should be the C36 type since the discrimination between the Laves phases (see Section III.3.(a)) is thought to be on the grounds of vec and not size effects. The vec for these series of compounds are very similar and obviously some other mechanism is important in determining which of the Laves phases should form. It is not clear at this time what this mechanism can be. Additional pertinent facts are that $ScFe_2$ is the

---

6.2 Mansey, R.C., et al., J. Less-Comm. Met. 14, 329 (1968)

FIGURE 6.2

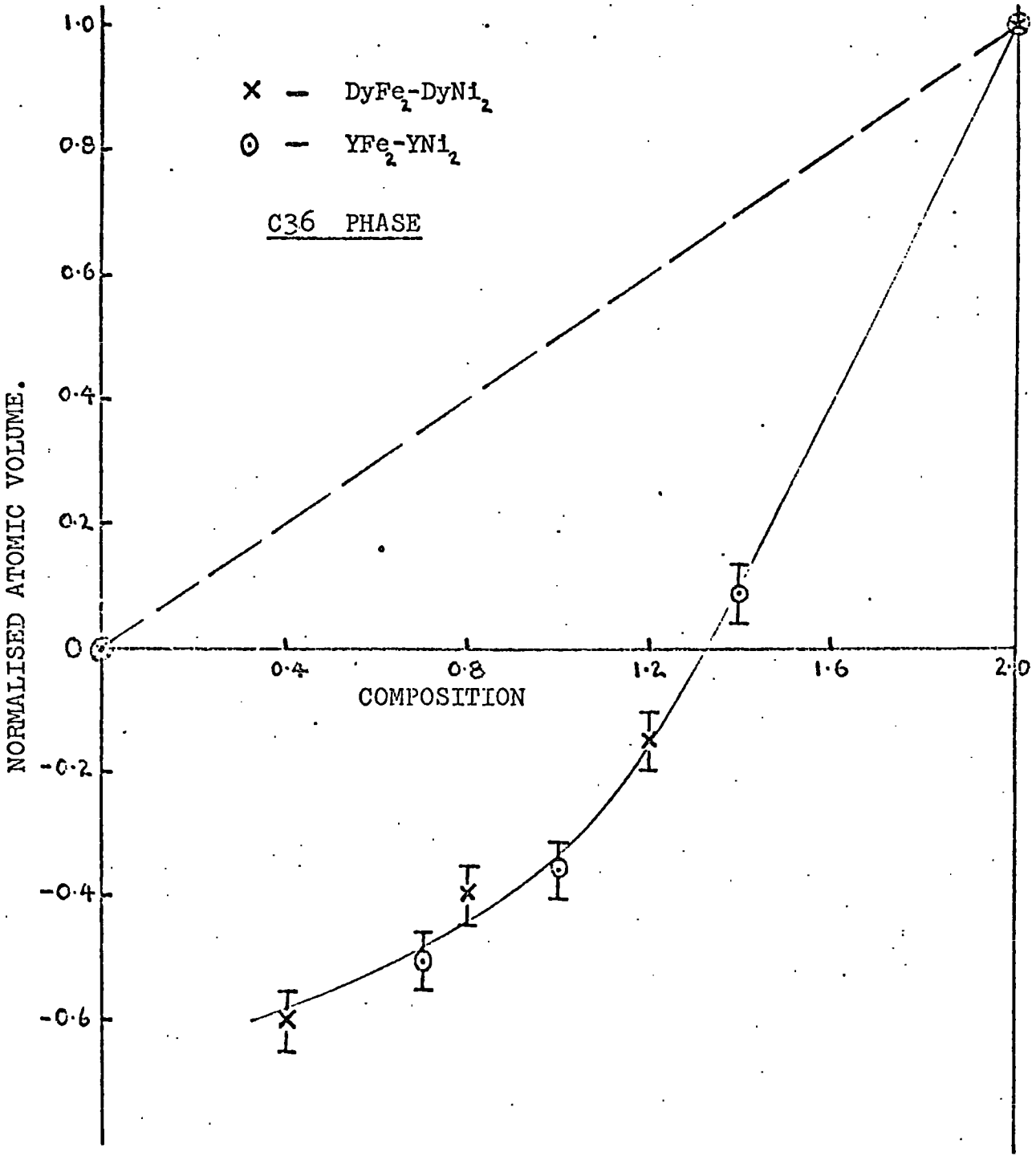
1·0
0·8
0·6
0·4
0·2
0
-0·2
-0·4
-0·6
NORMALISED ATOMIC VOLUME.
× — DyFe2-DyNi2
⊙ — YFe2-YNi2
C36 PHASE
0·4
0·8
1·2
1·6
2·0
COMPOSITION

only " Rare Earth" - iron group compound forming in the C36 phase (Ref. 6.3) and that no intermediate phases have been reported in the practically identical series Er $(Fe, Ni)_2$ (Ref. 6.2).

VI.2 (Dy, Y) Fe_2 Series

The data for the terminal compounds agree well with the previously published values given in Tables 3.1 and 3.2 and, together with the data for the intermediate compositions and the magnetisation - temperature (σ /T) curves, clearly show that these compounds are ferrimagnetic.

The σ /T curves for the whole series have the usual form demonstrated in Section II.3; in particular the curves for $0.65 \geqslant x \geqslant 0.3$ show a compensation point (T_K). The compound $x = 0.65$ is obviously very close to the critical composition shown in curve (6) of Fig 2.1(c) where the magnetisation approaches zero with $d\sigma/dT = 0$, effectively a compensation point occurs at the Curie point ($Tc = T_k$). This makes the evaluation of Tc difficult for obviously the previously described procedure is inapplicable in this case. The value of Tc reported for this compound in Table 5.5 is that obtained by the usual method and is given a larger error limit because of the above. Figure 5.4 clearly shows that this value is too low, as expected.

6.3 Nevitt, M.V., in P.A. Beck, ed., " Electronic Structure and Alloy Chem. of the Transition Elements ", Interscience (1968)

The fact that the minima in the σ/T curves are indeed compensation points has been demonstrated experimentally. A sample of the compound $x = 0.3$ was attached to a thread and magnetised in a strong field whilst immersed in liquid nitrogen. It was then allowed to warm up while suspended in a low field and observed to reverse its direction suddenly at the compensation temperature.

The σ/T curves show that the critical composition (4) of Fig. 2.1 (c), where the absolute saturation magnetisation is zero (i.e. $T_K = 0$), occurs between $0.3 > x > 0.24$ and the saturation moments and coercive fields of Fig. 5.5 indicate that this composition is $x_c = 0.28\ (\pm 0.01)$. We will term this composition the " equilibrium concentration" since here the iron and dysprosium sublattice moments exactly cancel. If the component moments remained constant then the equilibrium concentration would occur at $x = 0.35$, i.e. $\mu_{YFe_2}/(\mu_{DyFe_2} + \mu_{YFe_2})$. This value is obtained also on the basis of Dy and Fe moments (μ_{Dy} and μ_{Fe}) varying linearly with composition so that the experimental value clearly indicates that these conditions do not apply. Hence either μ_{Dy} or μ_{Fe}, or both, must vary non-linearly with x.

We consider first the values of these moments in the terminal compounds. Here, and in the whole of this chapter, the discussion of the component moments should include that due to the polarisation

of the conduction electrons but since there is no independent measure of this quantity in these results it will be assumed added to μ_{Dy} or μ_{Fe} depending upon its sign. In YFe_2 the moment is due entirely to the Fe ions so that $\mu_{Fe} = 1.40\ \mu_B$ here. We have given evidence in Chapter III that the values of μ_{Dy} in $DyNi_2$ and $DyCo_2$ are 9.2 and 9.6 μ_B respectively and shown that/value in $DyFe_2$ should be not less than this. If we take $\mu_{Dy} = 9.6\ \mu_B$ in $DyFe_2$ then $\mu_{Fe} = 2.17$. We now distinguish two extreme models for the intermediate compositions; (a) μ_{Fe} varies linearly between these values, and μ_{Dy} is allowed to vary non-linearly, (b) $\mu_{Dy} = 9.6\ \mu_B$ throughout the series and μ_{Fe} varies non-linearly. In case (a) μ_{Dy} is required to decrease through the series (with x) and at x_c its value is in excess of 11.5 μ_B. This is so much greater than the free ion value of 10 μ_B as to be discounted, even when allowance is made for conduction electron polarisation effects. μ_{Fe} therefore varies non-linearly and Figure 6.3 shows this variation for case (b). In reconstructing this variation the value $x_c = 0.29$ has been used since, for 0.28, μ_{Fe} falls below it's value at YFe_2. It is probable that the condition μ_{Dy} = constant is not followed and that it increases slightly with the addition of Y (decreasing x). This effect would arise from the conduction electron polarisation, which may be expected to decrease less slowly than the ion moment, and would allow μ_{Fe} to increase slightly in the region $0 < x < 0.3$

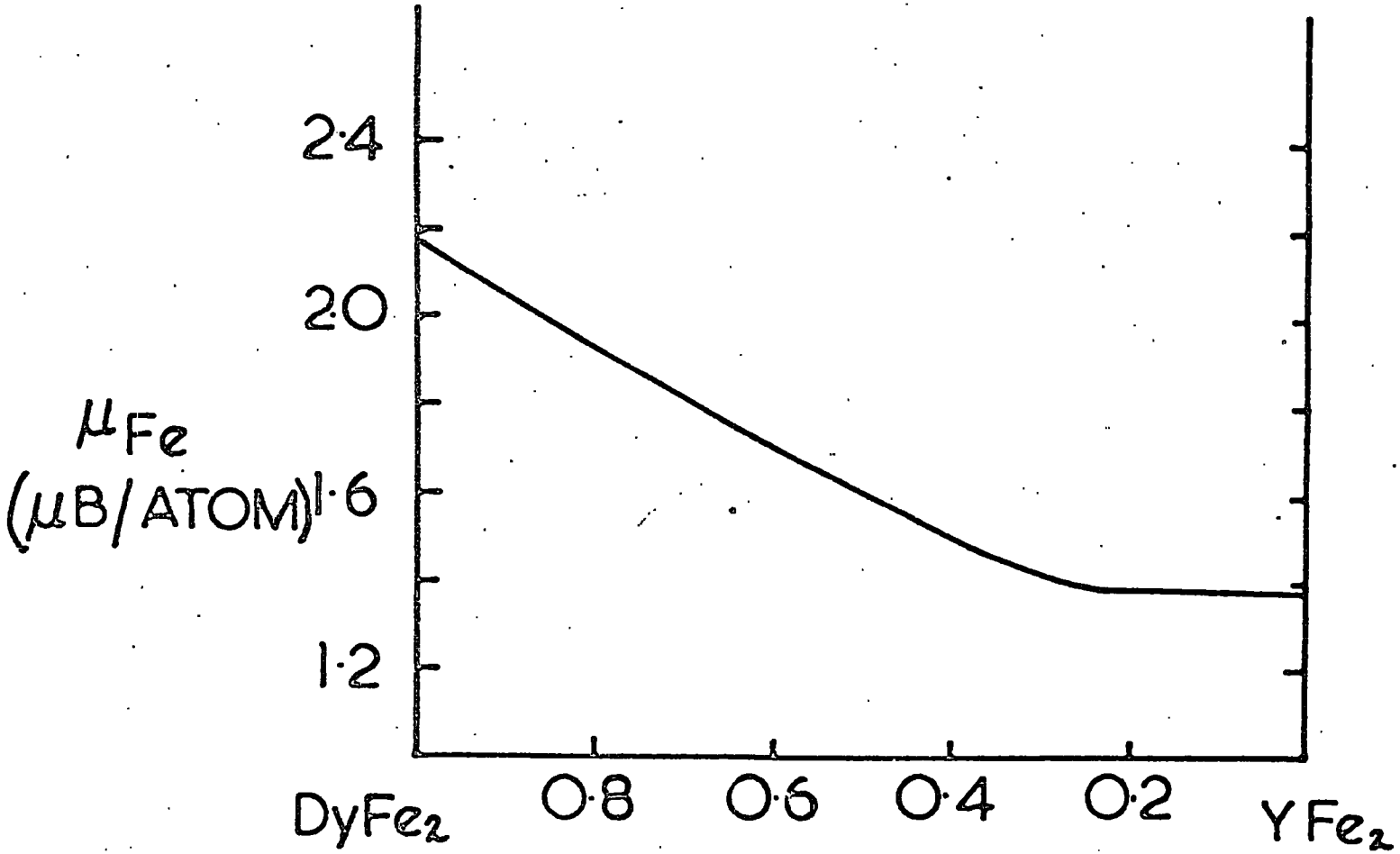

FIGURE 6.3 Variation of μ_{Fe} in $(Dy,Y)Fe_2$.

where it is constant in Fig. 6.3.

In attempting to account for the variation of μ_{Fe} shown in Figure 6.3 we consider first the previous models reported in Chapter III. Such a variation could be describable in terms of transfer of electrons from the rare earth component to the iron 3d shell, but such an argument is very tenuous. Even if the transfer differs for Dy and Y to account for the extremal values, which seems unlikely since these elements have similar electronegativities, the variation through the series between these values must logically be linear. The second model, with an induced moment proportional to (g-1)M, gives a linear variation also. The behaviour is, however, explained quite naturally if the iron moment is considered on a collective electron model.

The interatomic distances in these compounds are similar to those in metallic iron and it seems, therefore, that the 3d electrons in the compounds are as likely to form a band as in the element. Further a rigid band model seems particularly appropriate for this series due to the great similarity of Dy and Y as regards electronegativity, outer electronic arrangements, and size. Then, since μ_{Fe} is greater in $DyFe_2$ than in YFe_2, the d-band magnetisation in the latter must be unsaturated, i.e. holes in both spin directions (Section II.5(a)). The Fermi-level for one spin direction

must therefore be held in a region of low density of states, in YFe_2. Then as the exchange energy is increased by the addition of Dy, as reflected in the Curie temperatures, μ_{Fe} should increase slowly until the Fermi-level passes through this low density of states region. This is precisely the variation shown in Figure 6.3. This model is considered further in later sections of this chapter.

Finally, for this series it may be noted that the saturation moments near the equilibrium concentration do not go to zero (dotted curve in Figure 5.5) and also that the σ /T curves do not go to zero at the compensation points. This behaviour is to be expected to a small degree as a result of local variations in composition but the magnitude of the present effect is rather too large to result from this effect. For example, the measured saturation magnetisation for the composition $x = 0.3$ is comparable with the expected value for $x = 0.35$ and would be produced by a uniform composition range of approximately $0.4 < x < 0.2$ so that the variation would have to be, in practice, even greater than this. The behaviour may result from a non-colinear arrangement of the Dy and Fe moments at the compositions close to the equilibrium concentration, and a canted arrangement about 8° off antiparallel would reproduce almost exactly the measured values. It has been found (Ref. 6.4), from Mössbauer effect measurements, that there

---

6.4 Bowden, G., Ph.D Thesis, University of Manchester, 1968

is anisotropy in the RFe_2 compounds and that the easy direction of magnetisation is in the $[1, 0, 0]$ direction for $DyFe_2$ and $[1, 1, 1]$ for YFe_2. If the easy direction is determined by whether the rare earth or iron sublattice predominates, as appears to be the case (Ref. 6.4), then there must be a tendency towards a canted arrangement when these are of comparable magnitude. It is most improbable that the sublattice magnetisations would align along these directions exactly, since the angle between them is about 55° and the anisotropy energy appears to be quite small, as deduced from the magnetisation curves, compared with the exchange energy between the sublattices. An angle of less than 10° however would not seem to be impossible.

At the compensation points the same anisotropy effects may occur to account for the magnetisations observed. Some additional rather tenuous evidence has been collected for this case. Measurements were made of the remanent magnetisation on passing through the T_K and compared with the values obtained at constant temperature above T_K. Now the magnetometer measures magnetisation in a single direction so that if the easy axis changes in passing through T_K then the value measured in the first case is the component in the direction of the first easy axis. The value obtained at constant temperature above T_K is the component in the direction of the second easy axis. Thus the angle between these two directions was obtained and found to be almost exactly that

given above for the direction between [1,0,0] and [1,1,1]. This correspondence is almost certainly fortuitous since the remanent magnetisation must be considerably influenced by the magnetostatic energy on passing through T_K. The direction of the easy axis in the region of T_K may be revealed by Mossbauer work but the possibility of a canted arrangement near the equilibrium concentration must await neutron diffraction study.

VI.3 $Y(Fe,Co)_2$ Series

The data presented for the terminal compounds in this series are again in good agreement with the previously published values (Table 3.1 and 3.2). The compound YCo_2, about which there has been uncertainty (Table 3.2), has consistently shown the magnetic behaviour reported here, as prepared on several separate occasions.

The variation of the moment through the series (Figure 5.7) again seems to preclude a simple localised description where the moment is determined by the occupation of discrete 3d orbitals, since in that case it must presumably vary linearly between the terminal values. The variation can be readily interpreted, however, within the framework of the rigid band model of the last section.

Again throughout this discussion we ignore conduction electron polarisations and, since we have no measure, assume that the g values for the Fe and Co ions are both 2.0, i.e. the moment

results from spin only and the number of electrons (holes) in the band is given directly by the Bohr magneton number. This is almost certainly an incorrect assumption, but the g values should not be too far different from 2.0 and not appreciably dependent on composition so that the following analysis should not be greatly affected when the correct values are included.

Assuming, in line with the discussion of Section VI.2, that there is a minimum in the density of states for YFe_2 and, further, that this minimum is at the Fermi level in the spin-down ($\downarrow$) sub-band, then as electrons are added to the band by substitution of Co the moment should increase. This occurs because the " paramagnetic " Fermi level ($\updownarrow$) moves away from the minimum, so that when the Fermi level, under the influence of the exchange interaction, again reaches this minimum, the difference between the spin-up ($\uparrow$) and $\downarrow$ levels is greater. This is shown schematically in Figure 6.4. Under the conditions shown in this figure, where the $\downarrow$ Fermi level remains at the same position, the moment obviously increases at a rate corresponding to the addition of one electron/atom. This is shown by the dotted line in Figure 5.7. After the $\uparrow$ Fermi level reaches the top of the band the moment must decrease due to the filling of the $\downarrow$ sub-band. The dashed line in Figure 5.7 represents the approximate position of the top of the band, taken

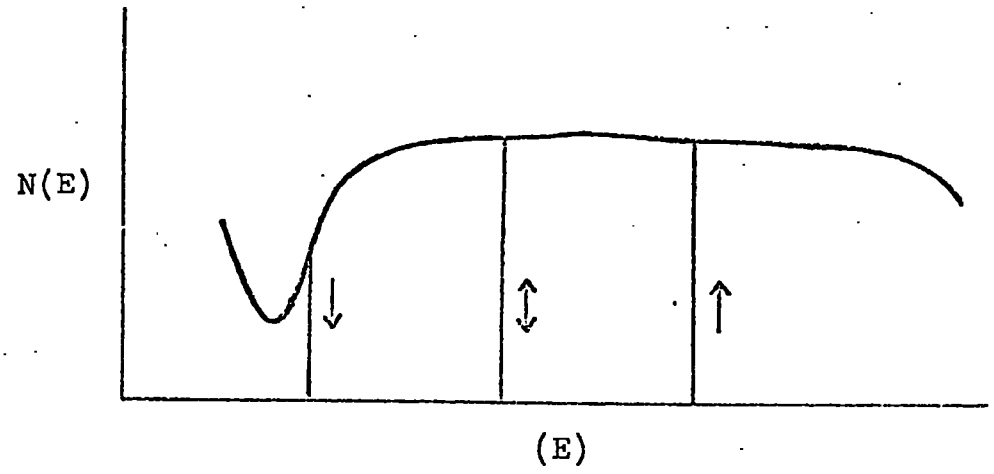

(a) YFe_2 (Schematic).

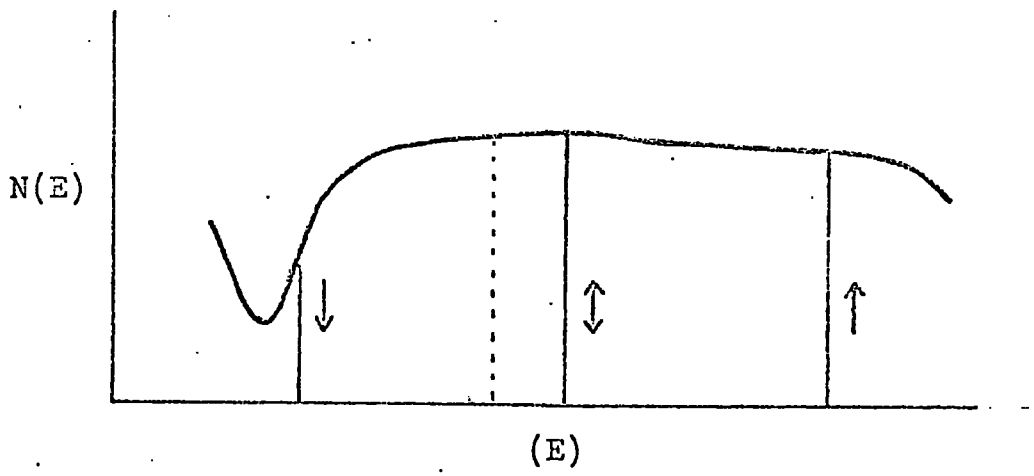

(b) After substitution of Co.

FIGURE 6.4.

to be linear between the two extreme values which have been placed as explained later (Section VI.3(a)). At the cobalt-rich end of the series the moment falls below the saturation value, given by this dashed line, as a result of the reduced exchange energy which is indicated by the falling Curie temperatures (Figure 5.6); i.e. the ↓ Fermi level moves to the right in Figure 6.4.

At the iron-rich end of the series it should be noted that although the Curie temperature increases with increasing Co concentration (Figure 5.6) the ↓ Fermi level does not pass through the minimum, i.e. the moment does not go above the dotted line in Figure 5.7. Indeed, near the 67 atomic % Fe compound, the Fermi level does not reach the minimum even though this compound has the highest Curie temperature of those measured. It is evident therefore that the ↑ density of states decreases considerably as the top of the band is approached so that near YFe_2 the density at the ↑ Fermi level is almost equal to that at the ↓ level, i.e. at the minimum. We can say further that this minimum must be very sharp on the lower side since a relatively small increase in the exchange energy (Curie temperature) in the series (Dy, Y) Fe_2 is sufficient to allow the Fermi level to pass through this region.

The origin of the variation of the Curie temperature (Fig.5.6) through the series is obscure. In the RCo_2 compounds, reported

Curie temperatures are much lower than those for the corresponding RFe_2 compounds (see Table 3.2) but in the present case as Co is substituted for Fe the Curie temperature initially increases. This effect will clearly arise from the details of the coupling mechanism in these compounds and may be related to the changes in lattice parameter: Figures 5.2 and 5.6 show that the region $u > 1.3$ is anomalous for both properties.

The two step magnetisation-temperature curves found for some compositions (Figures 5.23 and 5.24) have been observed in some RCo_2 compounds (see Section III.3(c)). There is evidence in the present compounds that the step is reduced in higher fields (Fig. 5.24) suggesting that it may not be a property of the spontaneous magnetisation but may arise from a variation in the magnetocrystalline anisotropy energy. This view is supported by the difference in magnetic hardness above and below the step (in Fig. 5.24 the curves are relatively more widely spaced at higher temperatures) and by the field dependence of the step temperature. Further these compounds are difficult to saturate at low temperatures (Table 5.6) as are the compounds which exhibit an initial increase in the magnetisation-temperature curve ($u = 0$ and 0.59). This latter effect probably results from anisotropy variation also. Some preliminary work on the polycrystalline magnetostriction in these compounds shows that there is a negative linear magnetostriction below the temperature

of the step which disappears above this temperature.

VI.3(a) Position of Band Top

The d-band top (dashed line in Figure 5.7) is placed between 2.1 holes/atom for YFe_2 and 1.1 holes/atom for YCo_2 for the following reasons. Oesterreicher and Wallace (Ref. 6.5) have shown, in the system Gd Co_2 - Gd Al_2, that the Co moment decreased with increasing Al concentration and extrapolated to zero at 36 mole % Gd Al_2. This result indicates that the 3 electrons/atom from Al enter the d-band and that 1.08 electrons/atom are sufficient to fill this band. These authors showed also that the C15 terminal phase was unstable and that the C14 phase was stable for the compositions 49-73 mole % Gd Al_2. On the basis of the above model the valence electron concentration corresponding to these compositions are 1.64 and 2.28 electrons/atom which are in reasonable agreement with the values obtained with other Laves phases (see Section III.3(a)) of 1.80 and 2.32. This seems to establish fairly well that 1.1 holes/atom is the correct value for Gd Co_2 and this indeed corresponds with the maximum moments found on Co in the RCo_2 compounds (see Section III.3(c)). There is no good reason for

---

6.5 H. Oesterreicher and W.E. Wallace; J. Less-Comm. Met. 13, 91,(1967)

believing that the value in YCo_2 is different.

Oesterreicher and Wallace considered also the Gd Fe_2 - Gd Al_2 system, where they found that the Fe moment extrapolated to zero at about 90 mole % Gd Al_2 and that the intermediate phase was stable between 27 and 67 mole %. They suggested that the Fe d-band is again filled by Al. However, the above values then give about 2.7 holes/atom in the d-shell and 1.19 and 1.99 as the critical vec. The present author believes that this interpretation is incorrect since the hole number seems large and the vec are inconsistent with the previous values for the phase stability. Their data may be analysed far more satisfactorily on the assumption that the conduction electrons from aluminium do not eneter the d-band for the Fe compounds. We ignore the moment extrapolation, which for the series under discussion is dubious in any case since one of the three values is obtained for a compound in the intermediate phase, noting that a reduction is expected on the rigid band model since the Curie temperature falls. Then, taking 2.1 holes/atom in the d-band for the Fe compounds, and thus 0.1 conduction " s " electrons/atom, the critical vec are 1.59 and 2.36 in far better agreement with the previous values. The value of 2.1 holes/atom is in agreement with the maximum moments found in the RFe_2 compounds (Section III.3(d)) and with the value suggested

(Ref. 6.6) from the paramagnetic moment of YFe_2 and is, of course, 1 hole/atom larger than for Co which is intuitively expected.

It may be noted that the two opposite behaviours suggested for the effect of Al substitution occur for the elemental Iron group metals (for review see Ref. 6.7).

VI.3.(b) Calculation of N(E)

Some qualitative details have been proposed in this chapter for the 3d band structure of the compounds under discussion. These are that there is a minimum near the position of the Fermi level for YFe_2 and that the magnitudes of the density of states at the Fermi level for this compound in both sub-bands are similar. In the present sub-section a semi-quantitative calculation of the density of states, from the previous results, is given.

Taking the results of the previous sub-section for the number of holes in the d-band for YFe_2 and YCo_2 the positions of the " paramagnetic " (↕) Fermi levels for all the compounds were evaluated. Then the ↑ and ↓ Fermi limits were evaluated from

---

6.6 Marei, S.A., et.al, J. Less-Comm. Met. 13,391,(1967)

6.7 Mott, N.F, Advanc. Phys. 13, 325 (1964)

the measured moments. For example for YFe_2, (moment = 1.40 μ_B/Fe atom and, in each sub-band, ↕ = 1.05 holes from the band top) the ↑ limit is 0.35 (= 1.05 - 0.70) and the ↓ limit is 1.75 holes from the top. The average density of states was then evaluated from the elementary rigid band theory with some assumptions, as under.

The condition for an equilibrium of the type shown in Fig. 6.4 to exist is, from Eqn. 2.6, $\ln W = \Delta E = E_F \uparrow - E_F \downarrow$. Now W must be related to the ordering temperature and we assume $\ln W = B\ T_c$ where B is a constant. The ΔE values for each of the $n\uparrow$ and $n\downarrow$ limits were thus calculated and the average density of states $n/\Delta E$ evaluated for these limits for each compound. The average density was then evaluated over smaller regions from these values. The resulting histogram is shown in Figure 6.5 where the ordinate is the usual density of states in units of $1/10^3$B, and the abscissa is holes/atom/sub-band. On this figure the region to the right of n = 1.750 is evaluated from the series Y $(Fe, Co)_2$. The region to the left is uncertain due to the uncertainty in evaluating the Fe moment in the series (Dy, Y) Fe_2. In this latter region the full line gives the value obtained using $DyFe_2$ results alone and the broken line indicates how this is modified when a further value is used (0.65).

FIGURE 6.5.

Calculated Density of States.

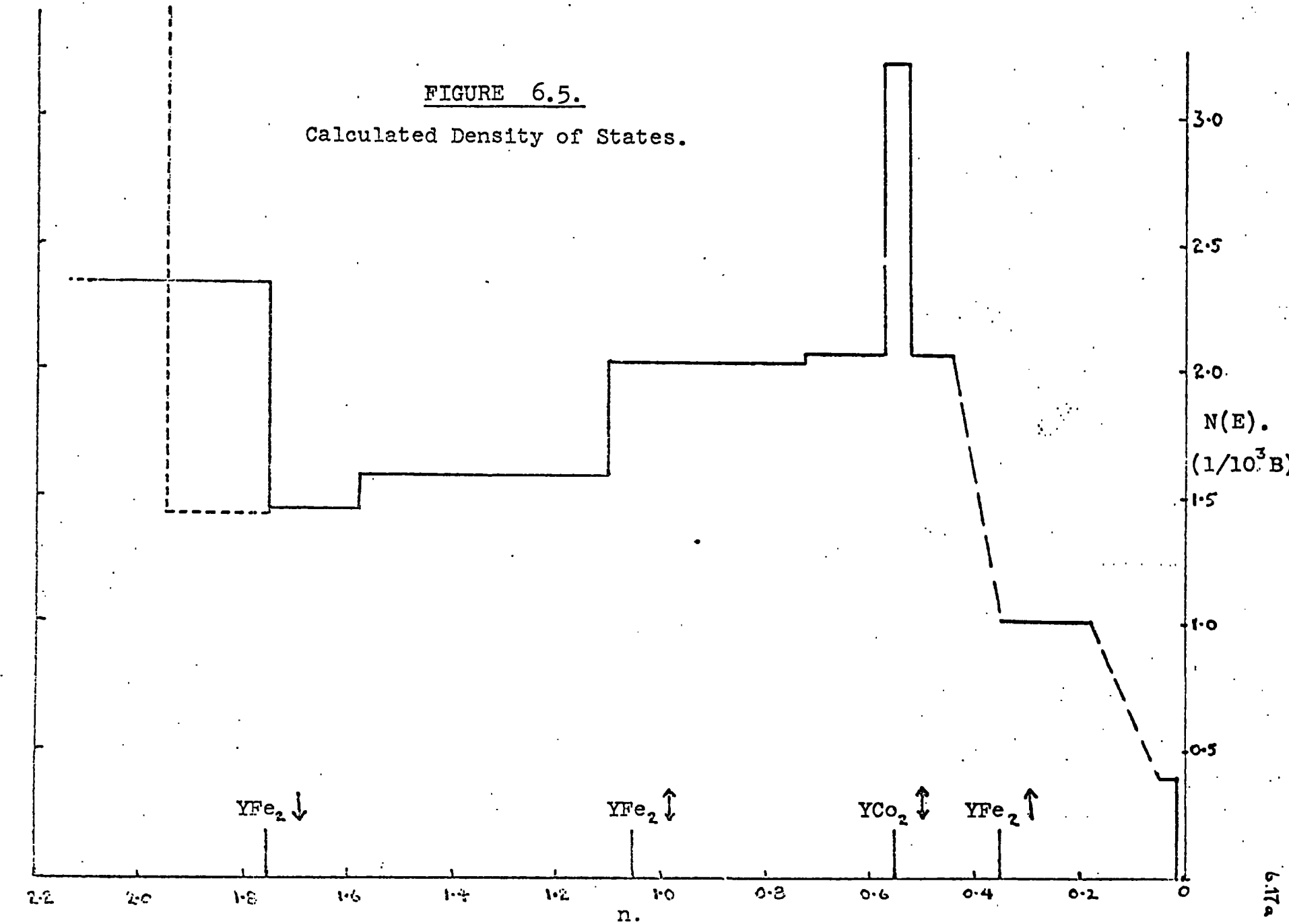

Obviously there is more fine detail in this region but the histogram gives some justification for the previous qualitative discussion.

VI.4. Other Series

The magnetic data presented for the series $R(Fe, Ni)_2$ are perfunctory since, as already explained, these series contain multiphase components. We may note, however, firstly, that the phases appeared to have separate ordering temperatures as there was some ferromagnetic behaviour above the apparent Curie point. Thus the impurity phase appears to have a higher Curie point than the C15 phase. Secondly, the saturation moments for the Dy series are below and, for the Y series, above the values obtained by linear interpolation between the terminal compounds. This behaviour is in qualitative agreement with the previous model.

VI.5. General Considerations on the Model

VI.5 (a) Nature of the Moments and Coupling Mechanisms

The model presented above is not intended to imply that the d electrons are necessarily itinerant in the sense of being uniformly distributed in the material. It should be considered as a method of determining the energetics of the whole system with the possibility of spatial localisation. Indeed it is probable that

the moment carrying electrons are localised on to each atom in the sense of the Anderson model (Section II.5(c)). Relevant facts supporting this view are that neutron diffraction results on these compounds (see references in Chapter III) have been satisfactorily interpreted on the basis of " localised" form factors, and in our discussion (Section VI.3 (a)) of the vec the d electrons were specifically excluded from the calculations of critical values with good results.

The discussion of the deviation of the lattice parameters from Vegards Law (Section VI.1) may be extended in the present context. It is evident in all the series presented that the deviation is greatest for those compositions where the d-band magnetisation is greatest. This suggests that the moment carrying electrons are localised on the atoms and that the magnetic contribution to the binding energy is negative. This latter effect has been noted as an expansion on passing down through the Curie point of Gd Co_2 (Ref. 6.2).

The coupling mechanism for these compounds envisaged in the present model is a combination of the coupling of the Anderson moments by overlap of the " halos" of charge (Section II.5(c)) and the R-K-K-Y interaction (Section II. 6(a)) between the 4f electrons and the conduction electrons. Thus there are three distinguishable interactions;

(i) the R-K-K-Y s-f interaction coupling the R.E. ions.

(ii) the coupling of the Anderson moments on the transition metal ions

and (iii) the coupling between the R.E. and transition metal ions both via the conduction electrons (f-s-d) and by overlap of the Anderson moments and the 4f moments.

In the Ni series obviously only (i) is operative so that the ordering temperatures ($<80^{o}K$) give the magnitude of this effect. In the Fe series on the other hand the interaction (ii) predominates ($YFe_2 \sim 550^{o}K$) while (i) and (iii) appear to be of similar magnitude. In the Co series all three interactions are of comparable magnitude.

VI.5 (b) The RNi_2 Compounds

The absence of a moment on Ni in these compounds (Section III.3(a)) has previously been taken as evidence that it is in the $3d^{10}$ state. On the present model Ni has zero moment because the density of states is low so that the condition for ferromagnetism (Equation 2.5) is not met. With reference to the density of states shown in Figure 6.5, if the ↕ Fermi level for the Ni compounds is in the region 0 - 0.3 holes/atom/sub-band then an exchange interaction $\sim 10^{3o}K$ is required to produce a moment.

VI.5 (c) The R Co_2 Compounds

We wish to show here that some of the anomalies in these compounds (Section III.3(c)) may be understood on the present rigid band model. The basic problem is whether the Curie temperature for YCo_2 reported here, and previously, is correct and, if it is, whether those for the compounds with a magnetic R component are lower than this, as reported.

We assume in the following that the behaviour reported here for YCo_2 is correct. Then the small moment on Co here results from the interaction of type (ii) above (i.e. d-d coupling) and should remain in the other compounds. Where R is magnetic, however, the type (iii) interaction (f-d coupling) should act to increase the Co moment. This behaviour is observed in the pseudo-binary series (Gd, Y) Co_2 (Section III.3(e)) and can account for the variation of the Co moment in the different R Co_2 compounds. Considering the temperature variation of the magnetisation, as the R sublattice uncouples with increasing temperature, the Co moment will be reduced through the f-d coupling. The decreased Co moment will thus effect a reduction in the s polarisation and so in the s-f interaction. This may result in a catastrophic reduction of the magnetisation, as is observed for example in Ho Co_2 (Section III.3 (c)). The temperature of this sharp reduction

has previously been taken as the Curie temperature. However, above this temperature a Co sublattice moment should persist at a value roughly equivalent to that for YCo_2 and thus possibly a moment on the R sublattice through the d-s-f interaction. A moment of the required magnitude occurs in the published results for some of these compounds, above this critical temperature, and the type of R sublattice magnetisation/temperature behaviour envisaged is similar to that found in $TmFe_2$ by Cohen (see Section III.3 (d)) and in $DyFe_2$ by Bowden (Ref. 6.4).

This behaviour would account for the field dependence and temperature hysteresis of this apparent Curie point and the metamagnetism, deviations from Curie-Weiss behaviour, and compensation points observed in some cases above this temperature (Section III.3(c)). Finally these critical temperatures would be proportional to the de Gennes function as observed (Section III.3 (c)).

VI.5 (d) The R Fe_2 Compounds

The model has been developed mainly from the compounds $DyFe_2$ and YFe_2 but should be applicable to all the RFe_2. In particular, assuming that the band structure is similar for all the compounds, the Fe moment in each compound will be determined by the magnitude of the exchange energy. If we again take this, crudely, as

proportional to T_c there should be a universal variation of Fe moment (μ_{Fe}) with Curie temperature (T_c). This is shown in Figure 6.6 where the solid line is obtained from the series (Dy, Y) Fe_2 and the maximum moment is taken again as 2.1 μ_B/atom.

Taking the T_c and Msat. values for several compounds from Table 3.2 the μ_{Fe} values may be obtained from this curve and thus the effective R moment (μ_R) evaluated. These are shown in Table 6.1 together with the gJ values.

Table 6.1

R	Gd	Tb	Ho	Er	Tm	Lu
μ_R	7.6	8.2	8.6;9.3	7.9	6.0;6.5	-0.4
gJ	7	9	10	9	7	0

Considering the variations in the published values the agreement is satisfactory.

As noted already (Section III.3 (d)), Ce Fe_2 is anomalous, having T_c and μ_{Fe} lower than those for YFe_2. However, since in this compound the Ce ion is almost certainly in the 4 + state (see Section III.3), the 3d and conduction bands must contain one electron/atom more than for the other RFe_2 compounds. The measured

FIGURE 6.6

Variation of μ_{Fe} with T_c.

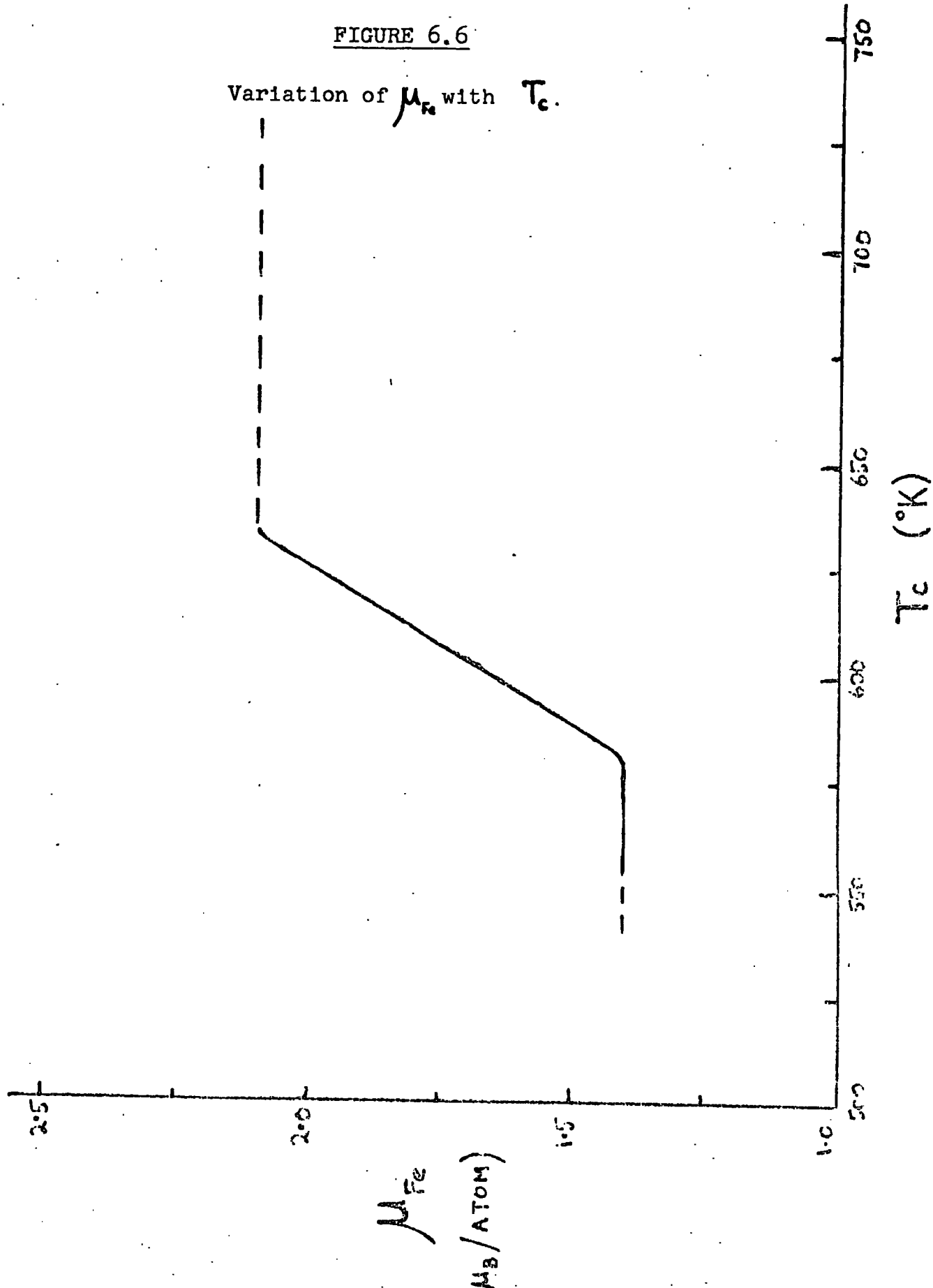

moment can obviously be explained qualitatively on the present model but a quantitative explanation is not possible since the fraction of this one electron/atoms actually entering the d-band, and thus the position of the ↕ Fermi level, is unknown.

Finally we note that the hypothesis of an itinerant rather than strictly localised moment in the RX_2 compounds is supported by the measured paramagnetic moments. Few measurements are available at present but those that are show that the paramagnetic moment is invariably greater than the saturation moment in the ferromagnetic region (Ref. 6.6 and 6.7). This behaviour is expected on the itinerant model (Ref. 6.8).

6.7 Farrell, J., Ph.D Thesis, University of Pittsburgh (1964)

6.8 Rhodes P., and Wohlfarth, E.P., Proc. Phys. Soc.(A) 273, 247,(1963)

CHAPTER VII SUMMARY

This work has presented results for several pseudobinary series of the intermetallic compounds RX_2 which, together with the model proposed, resolve many of the previous difficulties of interpretation of the properties of these materials. The ferrimagnetic nature of the compounds has been clearly demonstrated in the results for the series $(Dy,Y)Fe_2$; several components exhibited compensation points and the saturation moments indicated the presence of an equilibrium concentration. The moments carried by the Fe and Co components could not be reconciled within the existing models but were adequately accounted for on a rigid band model for the 3d electrons. It was on the basis of this model that a unified account of the moments carried by the X components in all the RX_2 compounds was presented. The anomalous temperature - magnetisation behaviour of some compounds was also explained on this model together with the possibility of anisotropy effects. An elementary density of states histogram for the d-band was tentatively presented from the experimental measurements, but it was suggested that these electrons are not necessarily spatially itinerant.

The problem of the variation of the lattice parameters through these series remains unsolved, though a considerable uniformity in

the variation has been demonstrated and a possible connection between the lattice parameter and magnetic moment suggested. Similarly the reason for the existence of multiple phases at some compositions remains essentially obscure.

Acknowledgements

The author wishes to acknowledge his gratitude to his supervisor, Dr. K.N.R. Taylor, for his continual help and encouragement, to Professor G.D. Rochester, the head of the Department where this work was performed, and to his fellow research students and their laboratory technician for ad hoc assistance throughout. The author is additionally indebted to Mr. D. Chatterjee for carrying out the magnetostriction measurements referred to in this work.

Thanks are due also to Mrs. S. Naylor for typing the script.

This work was performed during the tenure of a research scholarship from the Science Research Council.

References

2.1 Weiss, P., J. Phys. 6, 667, (1907)

2.2 Bloch, F., Z. Phys. 61, 206, (1930)

2.3 Phillips, T.G., and Rosenberg, H.M., Repts. Prog. Phys. 24, 285, (1966)

2.4 Weiss, P.R., Phys. Rev., 74, 1493, (1948)

2.5 Neel, L., Ann. Phys. (Paris) 3, 137, (1948)

2.6 Morrish, A.H., " The Physical Principles of Magnetism", Wiley, (1965), Chapter 9

2.7 Lotgering, F.K., Phillips Res. Rept. 11, 190 (1956)

2.8 Herring, C., in " Magnetism", eds. Rado and Suhl, Academic Press, Vol. IIb, Ch. 1,(1966)

2.9 Herring, C., ibid., Vol. IV, (1966)

2.10 Kasuya, T., ibid, Vol. IIb Ch.3, (1966)

2.11 Mott, N.F., Advanc. Phys. 13, 325, (1964)

2.12 " Theory of Magnetism in Transition Metals". Enrico Fermi, Course No. 37, Ed. Marshall, W., Academic Press (New York), 1967.

2.13 (a) Stoner, E.C., Repts, Prog. Phys. 11, 43, (1947)

(b) Wohlfarth, E.P., Proc. Roy. Soc. 195, 434, (1949)

2.14 Mott, N.F., and Jones, H., " Theory of the Properties of Metals and Alloys". Oxford University Press,(1936)

2.15 Friedel, J., Leman, G., and Olszewski, S., J. Appl. Phys. 32, 325 (s), (1961).

2.16 Anderson, P.W., Phys. Rev., 124, 41 (1961)

2.17 Liu, S.H., Phys. Rev., 163, 472 (1967)

2.18 Dimmock, J.O., Freeman, A.J., and Watson, R.E., Proc. Int. Conf. on Optical Prop. of Metals, ed. F. Abeles, (Amsterdam, 1966) p.237.

2.19 de Gennes, P.G., J. Phys. Rad. 23, 510, (1962)

2.20 Elliot, R.J., in "Magnetism" Vol. II.a Ch.7.

2.21 Rudermann, M.A., and Kittel, C., Phys. Rev. 96, 99 (1954)

2.22 Yosida, K., Phys. Rev. 106, 893 (1957)

2.23 Kasuya, T., Progr. Theoret. Phys. (Kyoto) 16, 45,(1956)

2.24 Freeman, A.J., Dimmock, J.O., and Watson, R.E., Phys. Rev. Lettr. 16, 94 (1966)

Loucks, T.L., Phys. Rev. 144, 504 (1966)

Keeton, S.C., and Loucks, T.L., ibid 168, 672 (1968)

Williams, R.W., and Mackintosh, A.R., ibid 168, 679 (1968)

2.25 Roth, L.M., Zeiger, H.J., and Kaplan, T.A., Phys. Rev. 149, 519 (1966)

2.26 Watson, R.E., Koide, S., Peter, M., and Freeman, A.J., Phys. Rev. 139 (A), 167, (1965)

3.1 Bozorth, R.M., and C.D. Graham. I.B.M. Research Report RC-1635 (1966)

3.2 Gibson, J.A., and Harvey, G.S., Technical Report No. AFML-TR-65-430. Air Force Materials Laboratory, Wright-Patterson Air Force Base, Ohio (1966)

3.3 Lemaire, R., Cobalt 32, 132, (1966) and 33, 201, (1966)

3.4 Nevitt, M.V., in P.A. Beck, ed., "Electronic Structure and Alloy Chemistry of the Transition Elements" Interscience, New York (1963)

3.5 Elliot, R.P., and Rostoker, W., Trans. A.S.M. 50, 617, (1958)

3.6 Slick, P.I., et.al., J. Chem. Phys. 43, 2788,(1965) also Wallace, W.E., and Craig, R.S., in " Phase Stability in Metals and Alloys". P.S. Rudman (ed). McGraw-Hill (1967).

3.7 Bleaney, B., Proc. Roy. Soc. A 276, 28,(1963) and in " Rare Earth Research", Vol. 2., K.S. Vorres, ed., Gordon and Breach, (1964).

3.8 Skrabek, E.A., and Wallace, W.E., J. Appl. Phys. 34, 1356, (1963).

3.9 Farrell, J., and Wallace, W.E., Inorg. Chem. 5, 105, (1966)

3.10 Felcher, G.P., Corliss, L.M., and Hastings, J.M., J. Appl. Phys. 36, 1001, (1965).

3.11 Moon, R.M., et.al. J.Appl. Phys. 36 978,(1965)

3.12 Wallace, W.E., and Skrabek, E.A., " Rare Earth Research" Vol. 2. p 431.

3.13 Schweizer, J., Phys. Lettr. 24A, 739, (1967)

3.14 Wallace, W.E., J. Chem. Phys. 41, 3857, (1964)

3.15 Cohen, R.L., Phys. Rev. 134, A94, (1964)

3.16 Gegenwarth, et.al., Phys. Rev. Lettr., 18, 9,(1967)

3.17 Taylor, K.N.R., et.al., Phys. Lettr. 20, 327 (1966)

3.18 Lemaire, R., and Schweizer, J., Phys. Lettr. 21, 366 (1966).

3.19 Oesterreicher, H., and Wallace, W.E., J.Less-Comm. Met., 13, 91,(1967).

3.20 Mansey, R.C., Raynor, G.V., and Harris, I.R., ibid, 14, 337, (1968).

4.1 Ellis, H.D., Ph.D. Thesis, University of Durham (1967)

4.2 Hutchinson, F., Ph.D. Thesis, University of Durham (1958)

4.3 Thompson, D.R., Ph.D. Thesis, University of Durham (to be published)

4.4 Zijlstra, H., " Experimental Methods in Magnetism ", Part 2, North-Holland Publishing Co. (1967)

4.5 " Reference Tables for Copper v. Constanton Thermocouples ". British Standard No. 1828, (1961)

4.6 Weiss, P., and Forrer, R., Ann. Phys.(Paris) 12, 297, (1929)

4.7 See Ref. 2.6, Chapter 6

4.8 Smit, J., and Wijn, H.P.J., " Ferrites ", Philips Technical Library (1959). Meyer, A.J.P., and Asch, G., J. Appl. Phys. 32 (S), 330, (1961)

4.9 Belov, K.P., " Magnetic Transitions ", Consultants Bureau, New York, (1961).

5.1 J.B. Nelson and D.P. Riley, Proc. Phys. Soc. 57, 160 (1945)

6.1 R.L. Mansey, et.al., J. Less-Common Metals 14, 337, (1968)

6.2 R.L. Mansey, et.al., ibid 14, 329, (1968)

6.3 M.V. Nevitt, in P.A. Beck, ed., " Electronic Structure and Alloy Chemistry of the Transition Elements ", Interscience (1963).

6.4 Bowden, G., Ph.D. Thesis, University of Manchester (1968)

6.5 H. Oesterreicher, and W.E. Wallace, J. Less-Comm. Met. 13, 91, (1967).

6.6 S.A. Marei, et.al., ibid, 13, 391, (1967)

6.7 Farrell, J., Ph.D. Thesis, University of Pittsburgh, (1964).

6.8 P. Rhodes, and E.P. Wohlfarth, Proc. Phys. Soc.(A), 273, 247,(1963).